

NONLINEAR MODEL PREDICTIVE CONTROL
OF A REACTIVE DISTILLATION COLUMN

by

ROHIT KAWATHEKAR, B.Ch.E., M.Ch.E.

A DISSERTATION


IN

CHEMICAL ENGINEERING

Submitted to the Graduate Faculty
of Texas Tech University in
Partial Fulfillment of
the Requirements for
the Degree of

DOCTOR OF PHILOSOPHY

Approved

Chairperson of the Committee 

Accepted

Dean of the Graduate School

May, 2004

ACKNOWLEDGEMENTS

I am blessed with all nice people around me through out my life. While working on research project for past four years, many people have influenced my life and my thought processes. It is almost an impossible job to acknowledge them in a couple of pages or for that matter in limited number of words.

I would like to express my sincere thanks to my advisor Dr. James B. Riggs for his financial support, guidance, and patience throughout the project. I would like to express my thanks to Dr. Karlene A. Hoo for her valuable graduate-level courses in the area of process control as well as for her guidance as a graduate advisor. I would also like to thank Dr. Tock, Dr, Leggoe, and Dr. Liman for being a part of my dissertation committee.

My sincere thanks to Mr. Steve Maxner, my employer at the Vietnam Archive, for providing me the financial support during my last years of curriculum. I would like to take this opportunity to thank all the staff members and colleagues at Vietnam Archive for making me a part of their organization.

A person, without her, this accomplishment would have been incomplete, is my wife, Gouri (Maaoo). Her encouragement, her support, care and love at each stage of life helped me in academic as well as non-academic life. I have learned and will continue to learn lots of things from her. Her affection and emotional support during some of my difficult days has provided me an invaluable experience in our life.

Our daughter Anuya is an angel for us. Watching her grow day by day gives me the most enjoyable experience of my life. After long tiring day, when I reach home, her one smile rejuvenates my spirits. She might not have idea how much she has contributed towards our thinking and way of life.

There is no way that this section on acknowledgements could even come close to completion without mentioning all my friends who made my stay in Lubbock memorable. My special thanks for our Rapchick group, Kishor, Rahul, Doc, Ramu, Puru, Vinay, Vamshi, Sachin, Vicky, Robin, Kirti, Vijay, Milind, Pallavi, Sameer, Sangita, Kavita, Anita, Ganesh...list is almost endless. I really wish to express my most sincere thanks to all you guys. I would like to specially thank Raj and Spandana for providing me the laptop in my last phase of the project. It helped me a lot during my writing phase of the dissertation. My sincere thanks for all our 'Marathi Group' in Lubbock. I would like to mention Jatin Bhai and Mili, Dr. Mayank and Ranna for their encouragement throughout all these years.

I would like to thank my fellow graduate students Govind, Satish, Namit, Alpesh, Dale Slaback, Bryan, Eric Vasbinder, Danguang Zheng, Tian, Stifanov, Vikram for making my stay pleasant in the department. I wish to express my thanks to Matthew Hetzel for his help with the computer problems

I would like to express my respect for Mr. Jayesh Daji, Mr. Steve Patel, Mr. Deepak Patel, Mr. and Mrs. Wangipuram for providing me much needed financial support during my last year of curriculum.

In the end, I would like to say that all of this could be possible only because of constant love and encouragement by my parents, my in-laws, my brothers, Gouri's brother and their family and friends back home.

TABLE OF CONTENTS

ACKNOWLEDGEMENTS	ii
ABSTRACT	viii
LIST OF TABLES	ix
LIST OF FIGURES	xi
LIST OF NOMENCLATURE	xiii
CHAPTER	
1. INTRODUCTION	1
2. LITERATURE SURVEY	4
2.1 Modeling of Reactive Distillation Columns	4
2.1.1 Equilibrium (EQ) stage modeling approach	6
2.1.1.1 Review of ethyl acetate reactive distillation system	8
2.1.2 Nonequilibrium (NEQ) stage modeling approach	11
2.1.2.1 Limitations of NEQ stage model	13
2.1.3 Dynamics and control of reactive distillation columns	13
2.1.4 Model Predictive control	17
2.1.5 Nonlinear model predictive control (NLMPC)	18
3. MODEL DEVELOPMENT	22
3.1 Process Description	22
3.2 Modeling Assumptions	24

3.3 Vapor-Liquid Equilibrium and Enthalpy calculations	26
3.4 Reactive Distillation Column Modeling	29
3.4.1 Steady-state simulation development	31
3.4.2 Dynamic Simulation Development	32
3.5 Condenser Heat Transfer Dynamics	33
3.6 PI Level Controllers	35
3.7 Overhead Pressure Dynamics and Control	36
3.8 Inferential Composition Control	38
3.9 Steady state gain analysis of the ethyl acetate reactive distillation system	42
3.10 Summary of design parameters	49
4. DUAL PI COMPOSITION CONTROL	51
4.1 Configuration Selection	51
4.2 Controller tuning methodology	53
4.3 Ethyl acetate reactive distillation PI control results	55
4.3.1 Setpoint Tracking Results	56
4.3.2 Unmeasured feed rate disturbance rejection	62
4.3.3 Unmeasured feed composition disturbance rejection	68
4.4 Discussion of results	74
5. NONLINEAR MODEL PREDICTIVE CONTROL	76
5.1 Solution Algorithm	76
5.1.1 Sequential solution and optimization algorithm	77

5.1.2. Simultaneous solution and optimization algorithm	78
5.1.2.1 Orthogonal Collocation	79
5.1.2.2 Determination of collocation points for a cubic polynomial	81
5.2 Formation of optimization problem	88
5.3 Feedback	90
5.4 Ethyl acetate reactive distillation NLMPC results	92
5.4.1 Selection of Tuning Parameters	92
5.4.2 Setpoint tracking results for NLMPC	102
5.4.3 Unmeasured feed rate disturbance rejection	105
5.4.4 Unmeasured feed composition disturbance rejection	108
5.4.5 Effect of model mismatch on NLMPC performance	111
5.4.5.1 Effect of process / model mismatch on tuning of NLMPC	111
5.5 Discussion of results	120
6. CONCLUSIONS AND RECOMMENDATIONS	123
6.1 Conclusions	123
6.2 Recommendations	125
REFERENCES	128

ABSTRACT

Model Predictive Control (MPC) is an optimal-control based method to select control inputs by minimizing the predicted error from setpoint for the future. Industrially popular MPC algorithms use linear convolution models for predicting controlled variable response in future. For highly nonlinear processes, the linear MPC might not provide satisfactory performance. Nonlinear Model Predictive Control (NLMPC) employs nonlinear models of the process in the control algorithm for controlled variable response in future.

Reactive distillation modeling and control poses a challenging problem because the simultaneous separation and reaction leads to complex interactions between vapor-liquid equilibrium, vapor-liquid mass transfer and chemical kinetics. Hence, reactive distillation processes are highly nonlinear in nature. Application of reactive distillation for the production of ethyl acetate is considered for this dissertation. A detailed steady-state and dynamic mathematical model of reactive distillation is developed. This model is used for control studies of the reactive distillation column. Nonlinear Model Predictive Control algorithm is developed for centralized multivariable control of reactive distillation column. The performance of NLMPC is compared with decentralized PI control structure.

LIST OF TABLES

2.1 Selected Reactive Distillation Systems	5
3.1 Coefficients for modified Margules equation.	28
3.2 Reactive distillation level controller gains and reset times	37
3.3 Tuning parameters for pressure controller	38
3.4 Steady-state gain analysis of the ethyl acetate reactive distillation column	44
3.5 Design specifications and parameters for reactive distillation column	49
4.1 Dual PI composition control MV-CV pairings	53
4.2 Ethyl acetate reactive distillation tuning for dual-ended PI composition control Reset time is in seconds	56
4.3 Ethyl acetate dual PI composition control performance indices for overhead impurity setpoint tracking	61
4.4 Ethyl acetate dual PI composition control performance indices for unmeasured feed rate disturbance	67
4.5 Ethyl acetate dual PI composition control performance indices for unmeasured feed composition disturbance	73
5.1 Tuning parameters for NLMPC with perfect model	101
5.2 Ethyl acetate NLMPC control performance indices for overhead impurity setpoint tracking	102
5.3 Ethyl acetate NLMPC control performance indices for unmeasured feed rate disturbance rejection	105
5.4 Ethyl acetate NLMPC control performance indices for unmeasured feed composition disturbance rejection	108
5.5 Tuning parameters for NLMPC with 25 % process / model mismatch	112

5.6 Effect of model mismatch on NLMPC control performance indices for overhead impurity setpoint tracking	119
5.7 Effect of model mismatch on NLMPC control performance indices for unmeasured feed rate disturbance rejection	119
5.8 Effect of model mismatch on NLMPC control performance indices for unmeasured feed composition disturbance rejection	120

LIST OF FIGURES

3.1 Flow sheet of Ethyl acetate production	25
3.2 Overhead pressure and level and pressure control structure	36
3.3 Steady state temperature profile for the ethyl acetate reactive distillation column.	39
3.4 Plots for developing correlation between top as well as bottom impurity and tray temperature for inferential calculations	41
3.5 Steady-state gain behavior with reflux ratio (RR) and reboiler duty (QR) as manipulated variables	45
3.6 Steady-state gain behavior with reflux ratio (L/D) and boilup ratio (V/B) as manipulated variables	46
3.7 Steady-state gain behavior with reflux flow (L) and reboiler duty (QR) as manipulated variables	47
3.8 Steady-state gain s with reflux flow (L) and boilup ratio (V/B) as manipulated variables	48
4.1 Dual ended composition PI control for overhead impurity setpoint tracking	57
4.2 Dual ended composition PI control for unmeasured feed rate disturbance rejection	63
4.3 Dual ended composition PI control for unmeasured feed composition disturbance rejection	69
5.1 Collocation element	83
5.2: Collocation on finite elements	86
5.3 Effect of the prediction horizon on NLMPC performance	94
5.4 Effect of the control horizon on NLMPC performance	96

5.5: Effect of number of degrees of freedom on computational time for optimization	98
5.6 Effect of equal concern error (ECE) on NLMPC performance	99
5.7 Effect of move suppression factor on NLMPC performance for overhead impurity set point tracking.	100
5.8 Comparison of NLMPC and PI controller for dual ended composition control for overhead impurity setpoint tracking	103
5.9 Comparison between NLMPC and PI controllers for dual ended composition control for unmeasured feed rate disturbance rejection	106
5.10 Comparison between NLMPC and PI controllers for dual ended composition control for unmeasured feed composition disturbance rejection	109
5.11 Effect of model mismatch on the closed loop performance of NLMPC for overhead impurity setpoint tracking	113
5.12 Effect of model mismatch on closed loop performance of NLMPC for unmeasured feed composition disturbance	115
5.13 Effect of model mismatch on closed loop performance of NLMPC for unmeasured feed rate disturbance	117

LIST OF NOMENCLATURE

B	Bottoms flow rate from the reactive column
CV	Controlled variable
D	Distillate flow rate from the column
DMC	Dynamic matrix control
F	Feed flow rate to the column
F_D	Detuning factor for controller gain and reset time
HTC	Hydraulic time constant
$H_{B,j}$	Enthalpy of Vapor flow of component j from reboiler
$H_{i,j}$	Vapor enthalpy of component j on tray I
$h_{B,j}$	Enthalpy of component j in the liquid bottoms
$h_{F,j}$	Enthalpy of component j in the feed
$h_{i,j}$	Liquid enthalpy of component j on tray I
$h_{i,j}^0$	Ideal gas enthalpy of component j on tray I
\dot{K}_B	K value of a pre-chosen reference component
K_j	K value of component j
$K_{i,j}$	K value of component j on tray I
K_c	Gain of the controller based on detuned TL tuning
K_C^{TL}	Gain of the controller based on TL tuning

K_u	Ultimate gain of the controller from ATV method
L	Reflux flow rate
L_i	Liquid flow rate leaving tray I
M_B	Reboiler liquid molar holdup
M_D	Condenser liquid molar holdup
M_i^l	Liquid molar holdup on tray I
MV	Manipulated variable
p	set of model parameters
P_u	Ultimate period of the controller based on ATV method
Q_r	Reboiler duty
T_B	Bubble point temperature of the tray
t	Time
u	manipulated variable vector
V_B	Vapor flow rate from the reboiler to the column
V_i	Vapor flow rate leaving tray i
$x_{D,j}$	Liquid mole fraction of component j in the distillate
$x_{F,j}$	Liquid mole fraction of component j in the feed
$x_{i,j}$	Liquid mole fraction of component j on tray I
y	controlled variable vector
$y_{B,j}$	Vapor mole fraction of component j from the reboiler

$y_{i,j}$ Vapor mole fraction of component j on tray I

Greek symbols

$\Omega_{i,j}^l$ Liquid enthalpy departure function for component j on tray I

$\Omega_{i,j}^v$ Vapor enthalpy departure function for component j on tray I

τ_c^{TL} Reset time of the controller based on TL tuning

τ_I Reset time of the controller based on detuned TL tuning

τ_i Hydraulic time constant for tray i

Φ Objective function

CHAPTER 1

INTRODUCTION

Reactive distillation combines both separation and reaction in one unit. It has been used in a small number of industrial applications for many years. Reactive distillation can offer significant economic advantages in some systems, particularly for reversible reactions which are limited by equilibrium constraints. The last decade has shown an increase in both research and applications of reactive distillation. Doherty and Buzad (1992) reviewed the reactive distillation literature up to 1992. Taylor and Krishna (2000) reviewed the modeling approaches for reactive distillation presented in the literature. Most of the reactive distillation literature is dedicated for steady-state design and simulation approaches.

Only a small number of papers discuss the closed-loop control of reactive distillation columns. Reactive distillation is a challenge to control due to process nonlinearity, complex interactions between vapor-liquid equilibrium, vapor-liquid mass transfer and chemical kinetics. Al-Arfaj and Luyben (2002), Sneesby et al. (1997), Kumar and Daoutidis (1999), discussed the decentralized PI control structures for reactive distillation column. Sneeby et al. (1998), Al-Arfaj and Luyben (2002) discussed the possibility of multiple steady states in many reactive distillation systems. The presence of multiplicities and the highly nonlinear nature of reactive distillation may impose limitations on use of linear controllers. Kumar and Daoutidis (1999) have discussed the superior performance of nonlinear controller compared to linear controller

for reactive distillation systems. Application of advanced process control, which incorporates process model for control algorithm, usually referred as Model Predictive Control (MPC) are used to account for process nonlinearity and non-stationary behavior at a expense of a more complicated and costly control strategy. Industrially popular model predictive control algorithms such as Dynamic Matrix Control (DMC) use a linear convolution model of the process for control algorithm. For highly nonlinear processes the linear MPC might not provide satisfactory performance. Nonlinear Model Predictive Control (NLMPC) can be defined as a MPC algorithm which employs nonlinear models of the process. Reactive distillation processes exhibits highly nonlinear behavior, hence the use of NLMPC for control of reactive distillation process is expected to provide improved performance compared to linear control strategies.

The objective of this study is to assess the performance of NLMPC applied for control of a reactive distillation column. A ethyl acetate reactive distillation column was selected for the modeling and control studies. A FORTRAN simulation of a reactive distillation column was modeled and used for the control studies with following objectives.

1. Determination of optimal control configuration for dual composition control of ethyl acetate reactive distillation column using conventional decentralized PI controllers.

2. Develop an algorithm for Nonlinear Model Predictive Control (NLMPC) and assess the application of NLMPC for dual composition control of ethyl acetate reactive distillation.

3. Compare the closed loop performance of ethyl acetate reactive distillation using conventional PI controller and advanced control strategies of NLMPC.

Chapter 2 covers the previous research on reactive distillation modeling and control. It also covers the literature regarding the development and application of nonlinear and linear model predictive control algorithms. The model used to simulate the ethyl acetate reactive distillation column is detailed in Chapter 3. Chapter 4 covers the application of PI controllers for dual composition control of ethyl acetate reactive distillation column. Development of Nonlinear Model Predictive Control (NLMPC) is described in Chapter 5. This chapter also discusses the comparison of closed loop performance for dual composition control of reactive distillation column using PI controllers and using NLMPC controller. Chapter 6 summarizes the results of this work and makes recommendations for future work.

CHAPTER 2

LITERATURE SURVEY

During recent years there has been an increased interest in reactive distillation. The chemical industry recognizes the favorable economics of carrying out reaction simultaneously with distillation for a certain class of reacting systems. There is also an increasing interest among academic researchers for the development of reactive distillation technology. Systematic design and simulation methods for reactive distillation systems have been reported in recent literature (Kumar and Daoutidis, 1999; Sneesby et. al., 1997a,b; Al-Arfaj and Luyben, 2002). This chapter describes various reactive distillation systems and different modeling approaches proposed. It is followed by the review of the work done on dynamics and control of reactive distillation columns. A brief review of Nonlinear Model Predictive Control (NLMPC) for control of chemical processes is also described.

2.1 Modeling of Reactive Distillation Columns

The design and operation issues of reactive distillation are more complex than those involved for either conventional reactors or conventional distillation columns. The simultaneous separation and reaction leads to complex interactions between vapor-liquid equilibrium, vapor-liquid mass transfer and chemical kinetics. Sharma (1985), and Gaikar and Sharma (1989), have published reviews describing the possibility of reactive distillation as an attractive process alternative for a wide variety of difficult separations.

Doherty and Buzad (1992) reviewed the literature regarding reactive distillation and described several commercial reactive distillation applications. Some selected reactive distillations systems published in the literature are presented in Table 2.1.

Table 2.1 Selected Reactive Distillation Systems

Reactive System	Reference
Acetic Acid + Ethanol \rightarrow Ethyl acetate + water	Suzuki et al.(1971), Komatsu and Holland (1977), Izarraraz et al. (1980), Jing et al. (1985), Alejski and Duprat, (1996), Dudukovic and Lee (1998), Vora and Daoutidis (1998), (2001), Seferlis and Grievink (2001).
Acetic Acid +Methanol \rightarrow Methyl acetate + water	Barbosa and Doherty (1988), (1992) Agreda et al. (1990).
Isobutylene + ethanol \rightarrow ETBE	Sneesby et al. (1997), (1998)
Isobutylene + methanol \rightarrow MTBE	Doherty and Buzad (1992), Isla and Irazoqui (1996), Hauan and Lien (1998), Sneesby (1999), Baur et al. (2000)
Adipic Acid + Hexamethylene diamine \rightarrow Nylon 6,6	Jacobs and Zimmerman (1977), Grosser et al. (1987), Doherty and Buzad (1992).

The complete list of all reactive distillation systems is not attempted here but the systems described in Table 2.1 show the application of the reactive distillation technology in the chemical industry, petroleum refining and polymer processing

Reactive distillation modeling literature can be broadly classified into two different approaches used for modeling reactive distillation process. These modeling approaches are as follows:

1. Equilibrium (EQ) stage modeling approach
2. Non-equilibrium (NEQ) stage modeling approach

2.1.1: Equilibrium (EQ) stage modeling approach

The development and application of the EQ stage model for conventional (i.e. non-reactive) distillation has been discussed in several textbooks and review articles. (See for example Holland, 1981; Kister, 1992). In developing EQ stage model for reactive distillation, the kinetics terms representing the rate of the reactions are added to the material balance equations. Similarly, the energy balance equations are modified by the inclusion of heat of reaction terms.

Much of the early literature on reactive distillation modeling is concerned primarily with the development of methods for solving the steady-state EQ stage model. Review of these methods reveal that these methods are by and large extensions of the methods that have been developed for solving conventional distillation problems. Suzuki et al. (1971) extended the bubble point method of Wang and Henke (1966) to solve the distillation problem. Nelson (1971) has modified Newton-Raphson method for solving

reactive distillation equations. Komatsu and Holland (1977) have modified the θ method (Holland, 1981), developed for solving conventional distillation problems, to solve the reactive distillation system for esterification reaction. Another article from this group is Izarraez et al. (1980). Mommessin and Holland (1983) discussed the computational problems associated with multiple columns. Relaxation methods involve writing the material and energy balance equations in unsteady state form and integrating numerically until the steady-state solution is found. Komatsu (1977) compares the EQ stage model calculations based on relaxation methods with experimental data, showing that the EQ model composition profiles are qualitatively correct. Chang and Seader (1988) applied the homotopy-continuation method for reactive distillation for the esterification reaction. Lee and Dudukovic (1998) have also used homotopy continuation method to solve reactive distillation problems. Venkatraman et al. (1990) describe the use of the inside-out algorithm used in Aspen Plus commercial software package (RADFRAC). Sneesby et al. (1997) used two different commercial simulators: Pro/II (Simulation Sciences, 1994) and SpeedUp (Aspen Technology, 1993) for solving reactive distillation problem for ethyl tert butyl ether (ETBE) synthesis.

Bock et al. (1997) reported a detailed analysis of a reactive distillation system using the esterification of acetic acid as an example. The slow reaction rate of the system results in less conversion for the reactive distillation column and hence the use of a recovery column along with reactive column has been proposed for obtaining high purity ethyl acetate. Seferlis and Grievink (2001) discussed the optimal design and sensitivity analysis of reactive distillation units using collocation models. The ethyl acetate process,

which consists of a reactive column along with a recovery column, has been considered for this study. The optimal design of ethyl acetate process flowsheet was used as a basis for our study.

2.1.1.1 Review of ethyl acetate reactive distillation system

Suzuki et al. (1971) described the design and simulation of an ethyl acetate reactive distillation column. A reactive column with thirteen equilibrium stages, made up of eleven trays, one total condenser and one reboiler, was simulated in the study. Ethyl acetate was withdrawn from the top in the distillate stream, and the feed consisting of the reactants acetic acid and ethyl alcohol was introduced on stage six. This single feed configuration for ethyl acetate reactive distillation has become a prototype configuration and many researchers have developed/applied several numerical algorithms to solve the nonlinear steady-state model for the above prototype configuration. The objective of above research was to establish the convergence characteristics and the robustness of the numerical algorithms, rather than to analyze the column behavior in detail.

The ethyl acetate conversion ($\approx 30\%$) and the ethyl acetate purity ($\approx 50\%$) reported in the literature (Suzuki et. al., 1971) for the single feed configuration. This ethyl acetate composition is lower than the azeotropic composition (54%). In practice, it would be desirable for the column at least attain product purity greater than the azeotropic composition to justify the use of a reactive distillation instead of a conventional configuration of a reactor followed by a distillation column.

The composition as well as reaction rate profiles for the single feed composition shows that majority of the reaction takes place in the reboiler and the bottom part of the column, and the upper half of the column acts essentially as a distillation column instead of reactive distillation column. This happens because the acetic acid, which is the heaviest of the four components, moves down the column and is present in negligible amount in the upper half of the column, resulting in negligible reaction in the upper half of the column. The absence of the reaction in the upper part of the column hinders achieving a composition higher than the azeotropic composition with this configuration. Furthermore, it can be observed that ethanol is present in significant amounts in the upper half of the column, which retards the separation (and hence achievable purity) due to closeness of boiling points between the ethyl acetate and ethyl alcohol. These observations suggest that the countercurrent flow of the reactants ethyl alcohol and acetic acid in the column could enhance the forward reaction on several trays, thus improving the overall conversion. Alejski et al. (1996) studied the multiple feed configuration for an experimental setup for ethyl acetate column. The experimental results show an improvement in the conversion of ethyl acetate.

Bock et al. (1997) reported a detailed analysis of ethyl acetate reactive distillation column. The slow reaction rate of the ethyl acetate system results into less conversion for the reactive distillation column. The use of a recovery column along with reactive column has been proposed for obtaining high purity ethyl acetate. The reactive column with countercurrent flow of reactants was used. Pure ethanol and acetic acid are fed separately into the column that operates at atmospheric pressure. Under these conditions, acetic acid

is the heaviest of the components and moves toward the bottom of the column. Ethyl acetate is the lightest and moves toward the top of the column. It is expected that the middle portion of the distillation column is the chief reaction zone. The rectifying section fractionates the ethyl acetate out of acetic acid, and the stripping section removes alcohol from water. Ideally, the ethyl acetate is the distillate and water is the bottoms product for this system. The quaternary system consisting of ethanol, acetic acid, water and ethyl acetate is highly nonideal. It can form four binary azeotrope mixtures and one ternary azeotrope. Over the wide range of composition, ethanol and water do not differ greatly in volatility, making it difficult to strip only water as bottom product. The reactant ethanol has a relatively high volatility and prefers the vapor phase rather than liquid phase where the reaction takes place. This leads to a low composition of ethanol in the liquid phase, reducing the production rate of ethyl acetate.

The rate of the esterification reaction between acetic acid and ethanol is generally low, which implies that it is favored by long residence times in each stage. It is evident from all the previous studies on ethyl acetate reactive distillation columns that an unfavorable physical equilibrium makes the production of high-purity ethyl acetate impossible from a single distillation column. However, the use of a second recovery column operating at a higher pressure or a feed with a large excess of acetic would lead to the production of ethyl acetate of the desired purity. The first option of using a recovery column at a higher pressure is selected for the study.

A distillation column operating at higher pressure (350 kPa) to break the azeotrope and produce high purity ethyl acetate was considered as a recovery column.

The distillate stream from the reactive column is fed to the recovery column. At the increased pressure, ethyl acetate becomes heavier than ethanol and water so that it appears as the bottoms product. The target purity level of the ethyl acetate is set at 99.5%. The effect of reaction is considered negligible because the column operates without any sulfuric acid catalyst and stages have small liquid phase holdups. Acetic acid appears as the bottom product of the recovery column and therefore directly affects the purity of final ethyl acetate product. Hence, a specification is imposed on the maximum allowable concentration of acetic acid in the distillate of the reactive column. The control of the concentration of the acetic acid in the distillate of reactive column can be achieved through the reduction of the liquid phase holdup in the upper section of the reactive column to suppress the reverse reaction.

2.1.2: Non-equilibrium (NEQ) stage modeling approach

The NEQ stage model for reactive distillation follows the methodology of rate-based models for conventional distillation (Krishnamurthy and Taylor (1985); Taylor and Krishna, 1993). The NEQ stage model assumes the interface between vapor and liquid on each stage is in thermodynamic equilibrium. The component molar balances for vapor and liquid phase consist of an interfacial mass transfer rate term, which is the product of the molar flux and the net interfacial area. The interphase energy transfer rates have conductive and convective contributions. Building an NEQ model for reactive distillation problem involves the detailed consideration of mechanism of reaction, namely whether the system is homogenous or heterogeneous. The theoretical knowledge of mass transfer

and heat transfer with chemical reactions is applied while determining the interfacial transfer rates.

Sawistowski and Pilavakis (1979, 1988) reported a model of a packed reactive distillation column for the esterification of methanol and acetic acid to methyl acetate based on NEQ stage approach. In 1990, Aspen Technology Inc. introduced the RATEFRAC model for rate-based multicomponent separation modeling (Sivasubramanian and Boston, 1990). RATEFRAC is based on the NEQ stage model of Krishnamurthy and Taylor (1985) with the addition of the equations to account for the effect of reaction on mass transfer. Zheng and Xu (1992) have used an NEQ stage model to simulate catalytic distillation operations in a packed column. Kreul et al. (1999) used an NEQ stage model for homogeneous reactive distillation. They demonstrated that EQ and NEQ models can lead to significantly larger differences in calculated concentration profiles for reactive separation units than for non-reactive operations. Hence, the additional efforts of the more complicated NEQ approach are justified. Baur et al. (1999) compared the EQ and NEQ stage models for MTBE process. They also have demonstrated the differences in the predictions of conversions and composition profiles using these modeling approaches. Lee and Dudukovic (1998) described an NEQ stage model for homogeneous reactive distillation for esterification of ethanol and acetic acid to ethyl acetate. A close agreement between predictions of EQ and NEQ stage models was found only when the tray efficiency could be correctly predicted for the EQ stage model.

2.1.2.1 Limitations of NEQ stage model

The NEQ stage model requires hardware design specifications to calculate mass transfer coefficients, interfacial areas, and liquid holdups. The NEQ stage model requires thermodynamic properties, not only for the calculation of phase equilibrium but also for the calculation of the driving forces for mass transfer accompanied by chemical reactions. In addition, physical properties such as surface tension, diffusion coefficients, viscosities, etc. for the calculation of mass and heat transfer coefficients and interfacial areas are required. The necessity of accurate predictions of interfacial transfer coefficients based on predicted thermophysical properties of the system may increase the complexity of the model and may limit the usage of this approach for control purposes.

2.1.3. Dynamics and Control of Reactive Distillation.

The majority of literature available on reactive distillation studies is concerned with the development of steady-state profiles for the system under consideration. Very few articles deal with the dynamics of reactive distillation. Some of these articles deal with the control of reactive distillation column. However, there is abundant literature available on the general subject of control of conventional distillation columns. Several authors have written entire books on control of distillation columns (Shinsky, 1984; Deshpande, 1985; Luyben, 1992). However, the available literature dealing with reactive distillation control is quite limited.

Sorensen and Skogestad (1994) discussed control strategies for reactive batch distillation for the esterification reaction. Control of both reactor temperature and distillate composition (two point control) is found to be difficult due to large interactions

in the column. Controlling the temperature on the tray in the column (one point control) was found to give good performance for a given process with no loss of reactant and higher reactor temperature.

Ruiz et al. (1995) described a software package called READSYS (Reactive distillation dynamic simulator) for which an EQ stage model was used. The authors state that their program can be used to study unstable column operations such as start-up, shut down. Scenna et al. (1998) employ READSYS to study the start-up of reactive distillation columns. They show that the start-up policy can have strong influence on the ultimate steady state behavior of the reactive distillation column. Abufares and Douglas (1995) used an EQ stage model for steady-state and dynamic modeling of reactive distillation column for production of MTBE. The steady-state model was RADFRAC from Aspen Plus and dynamic model was SpeedUp, a commercial dynamic process simulator. The focus of this study was the transient response of the system.

Alejski and Drupat (1996) described a dynamic model of reactive distillation for esterification of ethanol and acetic acid to ethyl acetate. The model is based on EQ stage approach with conventional assumptions of negligible vapor phase holdups. Departures from the phase equilibrium could be handled by specification of vaporization efficiency. The corrections of the conversion due to imperfect mixing were accounted for using 'conversion efficiency' which was calculated by eddy diffusion model in terms of the Peclet number. The model was compared with a pilot-scale column. Column start-up operation was investigated.

Sneesby et al. (1997a) developed an EQ stage model for synthesis of ETBE using SpeedUp. Sneesby (1997b) developed a dynamic model for the same process. The dynamic model assumed that reaction equilibrium was attained on all stages and hence reaction kinetics term was neglected in the material and energy balances. Linear control studies using decentralized PI controllers were performed on the reactive distillation column. The product purity as well as limiting reactant conversion was assumed to be the control objectives. An inferential control scheme that uses temperature of a suitable tray was developed. Several control configurations namely, (L, V), (L, B), (L/D, V), (L/D, V/B) were studied. These control configurations were set up for single composition control using the first variable in the bracket as primary manipulated variable and the second variable in the bracket as secondary manipulated variable. The control scheme performance was compared statistically by means of Integral Absolute Error (IAE) and Integral Time Absolute Error (ITAE). The (L, V) and (L, B) configurations, both set up for single composition control, were recommended.

Daoutidis and Kumar (1995) developed a detailed dynamic model incorporating vapor dynamics for reactive distillation column for the generalized esterification reaction. An output feedback controller was developed on the basis of a (Differential Algebraic Equation) DAE model and its superior performance over an analogous controller derived on the basis of the ODE model was demonstrated. Daoutidis and Vora (1999, 2001) developed a nonlinear input-output linearizing controller for reactive distillation column for production of ethyl acetate. The superior performance of nonlinear controller over the linear PI controller was demonstrated.

Chen et al. (2000) presented the design and the performance of a hybrid model based control of an industrial reactive distillation column. The model structure was the combination of first principles with standard black-box techniques. They demonstrated that this model structure could be successfully used in Internal Model Control (IMC) scheme for the on-line control of the process.

Al-Arfaj and Luyben (2002 a,b,c) presented the control of reactive distillation systems with single input single output PI control schemes. The results are provided for a methyl acetate reactive distillation system and a ETBE reactive distillation systems. Overall three types of control structures are evaluated for the reactive distillation systems under consideration. In the first control structure, the top and bottom purities are controlled by adjusting reflux and reboiler heat duty, respectively. The composition inside the reactive zone of the column is measured and controlled by manipulating one of the fresh feeds. In the second control structure only the column internal composition is controlled and a temperature is controlled in the stripping section in order to maintain bottom purity at a specified value. Distillate purity is not controlled but the reflux ratio is held constant. The third control structure uses two temperatures that manipulate the two fresh feeds. Reboiler heat input is flow controlled and serves as a production rate handle while the reflux ratio is held constant. It was found that a control structure with one internal composition controller and one temperature controller provide effective control. It was shown that direct control of the product purity for the high conversion/high-purity methyl acetate system is difficult because of system nonlinearity. It was also shown that the tray temperature control avoids the nonlinearity

2.1.4: Model Predictive Control

Model Predictive Control (MPC) is an optimal-control based method to select control inputs by minimizing the predicted error from setpoint for the future. The objective function is defined in terms of both present and predicted system variables and is evaluated using an explicit model to predict future process outputs. MPC is normally applied to multivariable process control, where its real benefits can be realized.

Cutler and Ramaker (1979) developed the most popular form of MPC, which is called Dynamic Matrix Control (DMC). The DMC algorithm uses linear step-response convolution models for predicting controlled variable responses in future. The general topic of model identification is covered extensively by Box et al. (1994). Many researchers have reported applications of DMC on distillation column control. McDonald and McAvoy (1987) applied DMC to simulations of a benzene-toluene column and an isobutene-n-butane column. For moderate and high purity columns they have reported difficulties in obtaining step response process models. They developed a nonlinear DMC approach by updating the process model with online gain and time scheduling.

Gokhale et al (1995) applied DMC to a propylene propane splitter (C3 splitter) and compared its performance to that of PI control. They did not observe a significant difference in the performance between PI control and DMC for servo and regulatory control. Cutler and Finlayson (1988a, 1988b) reported the application of DMC on industrial hydrocracker C₃-C₄ splitter and a hydrocracker preflash column. Huang and Riggs (2000) reported the application of DMC to a gas recovery unit.

Though there are many applications of DMC reported for conventional distillation column, very few MPC applications are reported for reactive distillation control. Ruiz et al. (1997) have reported application of DMC for control of reactive distillation for ethyl acetate synthesis.

2.1.5 Nonlinear Model Predictive Control (NLMPC)

MPC, which is industrially popular, employs linear models in the control algorithms. For highly nonlinear processes as well as processes involving changes in operating condition over a wide range (e.g., polymerization process, pH control, etc.), the linear MPC might not provide satisfactory performance. Nonlinear Model Predictive Control (NLMPC) can be defined as a MPC algorithm, which employs nonlinear models of the process. Instead of using linear convolution models, NLMPC can be applied to processes described by a wide variety of model equations such as nonlinear ordinary differential/algebraic equations, partial differential equations, etc.

The solution procedure for NLMPC involves setting up the control problem as a nonlinear programming (NLP) problem and solving it over some prediction horizon. There are two ways of implementing model predictive control. The first method employs separate algorithms to solve model equations and to carry out optimization. This method is called sequential solution and optimization approach. The detail discussion of this approach is provided in Chapter 5. The various versions of this strategy have been reported by Hicks and Ray (1971), Sargent and Sullivan (1978), and Morshedi (1986). The algorithm requires solution of the model dynamic equations at each iteration. Jones

and Finch (1984) reported that such methods spend about 85% of the time integrating the model equations in order to obtain gradient information. This can make the sequential solution and optimization approach prohibitive in terms of computation time, and unattractive for use in a large-scale real-time application.

An attractive alternative to solve the NLP problem is to use a simultaneous solution and optimization strategy. Tsang et al. (1975) used the collocation method to discretize the model differential equations in conjunction with a constrained optimization problem. The discretized model differential equations are included as constraints in NLP problem to optimize the objective function such that the (discretized) model differential equations are satisfied and other constraints (if any) on the states and manipulated variables are met. Hertzberg and Asbjorsen (1977) suggested using orthogonal collocation to discretize the differential equations in order to keep the dimensionality of the NLP problem low.

A powerful method for solving NLP problems is Successive Quadratic Programming (SQP) (Edgar and Himmelblau, 1988). It doesn't require that constraints be satisfied (the model equations to be solved) at each iteration but finds the optimum and satisfies the constraints simultaneously. Biegler (1984), Renfro et al. (1987) and Cuthrell and Biegler (1987) have reported the application of simultaneous solution and optimization strategy to determine open-loop optimal manipulated variable trajectories. Cuthrell and Biegler (1987) recommended using orthogonal collocation on finite elements to discretize the model differential equations to provide more robustness for the strategy. Renfro et al. (1987) reported that when the manipulated variable is piecewise

constant, as in digital control, the simultaneous solution and optimization strategy can only be implemented within a finite element framework of discretized equations.

Patwardhan et al. (1990) extended the application of simultaneous solution and optimization strategy by incorporating feedback, which effectively increases the robustness of the nonlinear control scheme to modeling errors and disturbances. They demonstrated the use of NLMPC algorithm for efficient start-up of a non-isothermal, non-adiabatic CSTR case study. Patwardhan and Edgar (1991) described the use of NLMPC algorithm for control of a packed distillation column. The NLMPC formulation was based on a steady-state model of the system with dynamic models of the reboiler and the accumulator. The NLP problem was solved to obtain optimized values of manipulated variables, which act as setpoints for lower-level controllers.

Ganguly and Saraf (1993) described the startup of a distillation column using nonlinear analytical model predictive control. The NLP problem was formulated by discretizing the nonlinear dynamic model of the system by means of orthogonal collocation. The NLP problem was solved using SOCOLL with SQP optimization algorithm. Meadows and Rawlings (1997) demonstrated the application of NLMPC for the control of a fluidized bed reactor. They demonstrated the effect of tuning parameters, such as prediction horizon, control horizon, move suppression factor, on the performance of the NLMPC controller.

Badgwell and Quin (2001) provided a review of NLMPC applications in industry. They focused primarily on recent applications reported by NLMPC vendors. Zheng and Zhang, (2001) demonstrated computationally efficient nonlinear model predictive

algorithm for control of constrained nonlinear systems. A method is suggested to exactly calculate the first control move, which is implemented, and approximating the further control moves, which are not implemented. They claimed a significant reduction in computational burden by means of the proposed algorithm. The feasibility for a practical implementation of proposed algorithm was demonstrated for distillation control and the Tennessee-Eastman challenge problem.

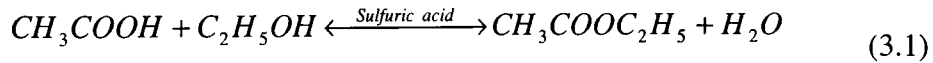
CHAPTER 3

MODEL DEVELOPMENT

An ethyl acetate reactive distillation column was considered for the modeling and control studies. This chapter discusses the process description, modeling assumptions, the vapor/liquid equilibrium model, the design parameters for the ethyl acetate reactive distillation, and the steady-state and dynamic model development.

3.1 Process Description.

Ethyl acetate is produced in an esterification reaction between acetic acid and ethanol. The achievable conversion in this reversible reaction is limited by the equilibrium conversion. The reaction is slightly endothermic and takes place in the liquid phase. Though the esterification reaction is self-catalyzed, sulfuric acid can act as external catalyst to enhance the reaction rate.



The kinetics of this reaction have been studied for both uncatalyzed reaction and catalyzed reaction in the literature. The uncatalyzed rate expression provided by Arnikaar et. al., 1970 has been used for a number of simulation studies (Suzuki et. al., 1971; Komatsu et.al., 1977; Chang and Seader, 1988). This expression is given as follows:

$$r = k_1[CH_3COOH][C_2H_5OH] - k_2[CH_3COOC_2H_5][H_2O] \quad (3.2)$$

$$k_1 = 4.85 \times 10^4 \exp\left(\frac{-7150}{T}\right)$$

$$k_2 = 1.23 \times 10^4 \exp\left(\frac{-7150}{T}\right)$$

where, r is the reaction rate in mole s^{-1} , k_1 is the forward reaction rate constant in moles $m^3 s^{-1}$ and k_2 is the backward reaction rate constant in moles $m^3 s^{-1}$.

Alejski et al. (1989) proposed a kinetic expression for acid catalyzed esterification reaction as,

$$r = k_1 [CH_3COOH][C_2H_5OH] - \frac{k_2}{K_c} [CH_3COOC_2H_5][H_2O] \quad (3.3)$$

$$k_1 = (4.195 C_k + 0.08815) \exp\left(\frac{-6500.1}{T}\right)$$

$$K_c = 7.558 - 0.012T$$

where,

r is the reaction rate in mole s^{-1} , k_1 is forward reaction rate constant in moles $m^3 s^{-1}$, K_c is the equilibrium constant, and C_k is the concentration of the catalyst in vol%.

Seferlis and Grievink (2001) have studied the optimal design of the ethyl acetate reactive distillation system. The details of the process consisting of the reactive column and the recovery column are discussed in the Section 2.1.1.1. We used the same process parameters for our study as Seferlis and Grievink (2001). The design of the recovery column was not considered for the current study. The recycle stream from the recovery column was considered with constant flow and composition for the reactive column. The flow sheet for the ethyl acetate production is shown in Figure 3.1.

3.2 Modeling Assumptions

1. Pure acetic acid feed is introduced in between the top and the middle portion of the column. Ethanol feed is introduced in between the middle and the bottom portion of the column. Recycle feed is introduced near the bottoms of the column.
2. The tray efficiency is assumed to be 100%..
3. The condenser is considered as a partial condenser
4. The column is operated at constant pressure of 1 atm.
5. The vapor holdup in the column is negligible.
6. Vapor and liquid phases are uniformly mixed.
7. Non-equal molar overflow is assumed.
8. Vapor/liquid equilibrium is calculated using the empirical correlation developed for calculation of liquid activity coefficient (Suzuki et al., 1970)

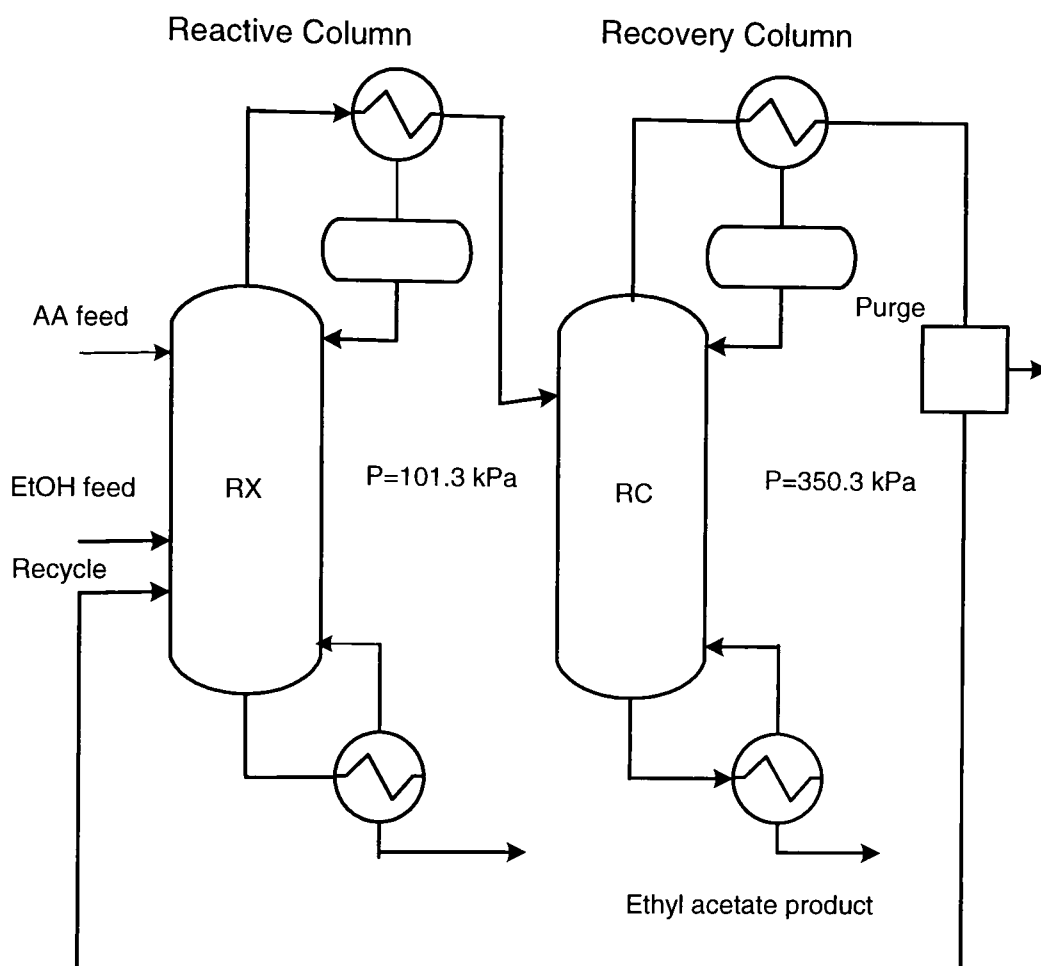


Figure 3.1 Flow sheet of Ethyl acetate production

9. Enthalpy departure functions using Soave-Redlich-Kwong (SRK) equation of state are used to correct the ideal enthalpy calculations for each phase
10. The Modified Margules equation developed by Suzuki et al (1970) for the ethyl acetate system is used for the calculation of the activity coefficients of the liquid phase.
11. Tray liquid dynamics use the Hydraulic Time Constant method (Franks 1972) for both the stripping and rectifying section.
12. The heat transfer dynamics in the condenser are considered.
13. The volumetric holdup on each tray is considered constant. Molar holdup on the tray is function of liquid phase compositions on the tray.
14. Tray temperatures are used to infer overhead and bottom compositions for control.
15. PI controllers are used to control the levels in the partial condenser, the reflux accumulator and the reboiler. A PI controller was also used to control the overhead pressure.

3.3 Vapor-Liquid Equilibrium and Enthalpy calculations

The component property data was obtained from Reid and Prausnitz (1987) for each component. K-values were computed from the following equation:

$$K_j = \frac{\gamma_j P_j^v}{P} \quad (3.4)$$

where,

P_j^v = the vapor pressure of component

γ_j = activity coefficient of component j

P = total pressure

The vapor pressure of liquid is calculated by using the Antoine equation:

$$\log P_j^v = A_j - \frac{B_j}{T + C_j} \quad (3.5)$$

where A_j , B_j , C_j are the constants for the Antoine equations, and are given by Suzuki et al. (1970). T is the temperature in Kelvin.

The activity coefficient was calculated from a modified Margules equation developed by Suzuki et al.(1970) for the ethyl acetate quaternary system. The Margules equation is rearranged as a polynomial series in mole fractions of the components in the mixture as follows:

$$\begin{aligned} \log_{10}(\gamma_A) = & a_1 x_B^2 + a_2 x_C^2 + a_3 x_D^2 + a_4 x_B x_C + a_5 x_B x_D \\ & + a_6 x_C x_D + a_7 x_A x_B^2 + a_8 x_A x_C^2 + a_9 x_A x_D^2 + a_{10} x_A x_B x_C \\ & + a_{11} x_B x_C x_D + a_{12} x_C x_D x_A + a_{13} x_D x_A x_B + a_{14} x_B x_C \\ & + a_{15} x_B x_D^2 + a_{16} x_C x_D^2 \end{aligned} \quad (3.6)$$

x_j is liquid mole fraction of components j . γ represents the activity coefficient and a_1 - a_{16} are constants determined from quaternary equilibrium data. The expression for the activity coefficient of the remaining components can be obtained by rotating the subscripts: A-B-C-D-A. This 16-coefficient modified Margules equation is the most

widely used relation in predicting non-ideal phase equilibrium of the above system, and the constants, a_j , of modified Margules equation are given in Table 3.1

Table 3.1: Coefficients for modified Margules equation.

Constant	Acetic Acid	Ethanol	Water	Ethyl Acetate
a_1	-0.554296	0.581778	0.688636	-0.0601361
a_2	-0.324357	0.209245	0.0243031	0.229571
a_3	-0.103685	-0.257329	0.375534	1.86575
a_4	-0.705455	-0.562636	1.27548	0.355191
a_5	-2.01335	-0.314853	1.77863	0.468416
a_6	-2.25362	0.451732	0.696259	1.51110
a_7	0.837926	-0.115411	0.936722	-0.0599682
a_8	0.52376	0.069531	0.449357	0.0673994
a_9	0.434061	0.0740529	0.717790	-3.15997
a_{10}	-0.534056	0.18701	1.44979	0.941858
a_{11}	-3.25231	-0.3699985	-2.11099	-1.92225
a_{12}	5.90329	-0.082339	0.746905	-0.755731
a_{13}	3.3540	-0.409472	1.12914	1.03791
a_{14}	0.197296	1.09247	0.120436	0.365254
a_{15}	-0.45266	0.192416	-1.64268	-1.36587
a_{16}	0.014715	-0.172565	0.330018	-2.13818

Enthalpy for multicomponent system was calculated by following equations

$$h_{i,j} = h_{i,j}^0 + \Omega_{i,j}^l \quad (3.7)$$

and

$$H_{i,j} = h_{i,j}^0 + \Omega_{i,j}^v \quad (3.8)$$

The SRK equation of state was used to calculate the enthalpy departure function for the liquid phase as well as the vapor phase. The enthalpy departure function is a function of temperature, pressure and composition (via the solution compressibility factor z).

3.4 Reactive distillation column modeling

To properly develop steady-state and dynamic models to simulate the multicomponent ethyl acetate reactive distillation column, tray-to-tray material and energy balances were developed.

For a standard reactive distillation tray where vapor holdup is considered negligible and reaction taking place in liquid phase, the modeling equations can be written as follows:

$$\frac{d(M_i^l)}{dt} = F_i + L_{i+1} + V_{i-1} - L_i - V_i + Vol_i \sum_{j=1}^{nc} \mu_j r_i \quad (3.9)$$

$$\frac{d(M_i^l x_{i,j})}{dt} = F_i x_{f,i,j} + L_{i+1} x_{i+1,j} + V_{i-1} y_{i-1,j} - L_i x_{i,j} - V_i y_{i,j} + Vol_i \mu_j r_i \quad (3.10)$$

$$\frac{d(M_i^l h_i)}{dt} = F_i h_{f,i} + L_{i+1} h_{i+1} + V_{i-1} H_{i-1} - L_i h_i - V_i H_i \quad (3.11)$$

$$\frac{dh_i^l}{dt} \approx 0 \quad (3.12)$$

$$r_i = \rho_i^2 k_{fi} (x_{A,i} x_{B,i} - \frac{1}{k_i} x_{C,i} x_{D,i}) \quad (3.13)$$

$$y_{i,j} P_i = \gamma_{i,j} x_{i,j} P_{i,j}^s \quad (3.14)$$

For the partial condenser, the material balance and energy balance equations are as follows:

$$\frac{d(M_c^l)}{dt} = V_n - L_c - V_D + Vol_c \sum_{j=1}^{nc} \mu_j r_c \quad (3.15)$$

$$\frac{d(M_c^l x_{c,j})}{dt} = V_n y_{n,j} - L_c x_{c,j} - V_D y_{D,j} + Vol_c \mu_j r_c \quad (3.16)$$

$$\frac{d(M_c^l h_c)}{dt} = V_n H_n - L_c h_c - V_D H_D - Q_c \quad (3.17)$$

$$\frac{dh_c^l}{dt} \approx 0 \quad (3.18)$$

$$r_i = \rho_i^2 k_{fi} (x_{A,i} x_{B,i} - \frac{1}{k_i} x_{C,i} x_{D,i}) \quad (3.19)$$

$$y_{i,j} P_i = \gamma_{i,j} x_{i,j} P_{i,j}^s \quad (3.20)$$

where subscript c represents condenser stage, subscript n represents the top tray of the column and subscript D represents the distillate. V_D represents the vapor distillate from the partial condenser stage.

The reflux accumulator stage is modeled as a liquid holdup tank. The terms relating to the vapor phase, i.e., vapor flow, vapor composition, vapor enthalpy corresponding to reflux accumulator are absent in the material and energy balances.

The material and energy balance equations for the reboiler are written as follows:

$$\frac{d(M_B^l)}{dt} = L_i - B - V_B + Vol_B \sum_{j=1}^{nc} \mu_j r_B \quad (3.21)$$

$$\frac{d(M_B^l x_{B,j})}{dt} = L_i x_{i,j} - B x_{B,j} - V_B y_{B,j} + Vol_B \mu_j r_B \quad (3.22)$$

$$\frac{d(M_B^l h_B)}{dt} = L_i h_i - B h_B - V_B H_B + Q_R \quad (3.23)$$

$$\frac{dh_B^l}{dt} \approx 0 \quad (3.24)$$

$$r_i = \rho_i^2 k_{fi} (x_{A,i} x_{B,i} - \frac{1}{k_i} x_{C,i} x_{D,i}) \quad (3.25)$$

$$y_{i,j} P_i = \gamma_{i,j} x_{i,j} P_{i,j}^s \quad (3.26)$$

3.4.1 Steady-state simulation development

For steady-state design of a multi-component reactive distillation column, The material and energy balance equations developed in the section 3.4 were set equal to zero for steady state. Holland (1981) describes how to use the Theta Method to improve convergence of a steady state distillation simulation. The basic procedure described by Holland and used in this study for solving the steady state ethyl acetate reactive distillation simulation was as follows:

1. Initial guesses for the required reboiler duty, tray temperature, and vapor flow rates were made.
2. On the basis of the most recent sets of temperature and vapor flow rates, the values of n_j 's, i.e. number of moles of components reacted per unit time on stage j , were calculated.

3. Material balances and VLE calculations were used to update the component flow rates on each tray.
4. The Theta Method was used to converge the component mole fractions on each tray
5. Tray temperatures were updated using VLE and the Kb method.
(Holland, 1982)

Vapor flow rates on each tray were updated using energy balance equations. The above steps were repeated until the tray-to-tray material and energy balances were converged to a desired tolerance.

3.4.2 Dynamic Simulation Development

A dynamic simulation was developed using a FORTRAN 77 code. The differential equations developed in section 3.4 were integrated numerically using the explicit Euler integration (Riggs, 1994) with a fixed step size of 0.5 seconds. The small step size was required because the overall system of equations was stiff. The small step size assured numerical stability over long integration times. Rigorous VLE combined with a small integration step size settled in relatively large computational time. To speed up the simulation, the inside-out algorithm (Boston and Sullivan, 1974) was applied for VLE calculations.

The inside-out algorithm is a modified version of the Kb method (Holland, 1982). A linear approximation for K values as a function of tray temperature was used for each component.

$$\ln(K_B) = A - \frac{B}{T_B} \quad (3.27)$$

Using basic rules for vapor/liquid equilibrium for a given tray and j components,

$$\ln(K_B) = \sum_j y_j \ln(K_j) \quad (3.28)$$

Using rigorous VLE calculations, the K values and compositions were calculated for use in Equation 3.27 at two different temperatures, T and T+ΔT, where ΔT is small. Then by combining Equations 3.27 and 3.28 with the data at two temperatures, A and B are updated.

$$B = \frac{\sum_j y_j \ln(K_{j,T+\Delta T}) - \sum_j y_j \ln(K_{j,T})}{\frac{1}{T} - \frac{1}{T + \Delta T}} \quad (3.29)$$

$$A = \sum_j y_j \ln(K_{j,T}) + \frac{B}{T} \quad (3.30)$$

During an integration step if any temperature did not change by more than 1⁰ C , the inside-out algorithm was used to calculate K values for each component on each tray. However after every composition control action or when tray temperatures changed by more than 1⁰ C, the rigorous VLE calculations were used to reparameterize A and B for the Kb model for each component on each tray.

3.5 Condenser Heat Transfer Dynamics

The cooling duty of the condenser can be manipulated freely by adjusting the coolant flow rate, when refrigeration is used, or by adjusting a hot vapor bypass around

the condenser. In some distillation studies the pressure control is assumed perfect and the cooling duty is not calculated (Duvall, 1999). Heat transfer dynamics of the condenser was not modeled in this case.

For the reactive distillation column under consideration, the partial condenser is modeled as a flooded condenser. In this case the heat transfer area decreases as more cooling water tubes are covered by the condensate (i.e. UA is not a constant). To simplify the model, the heat transfer area is assumed to be proportional to the available vapor volume is the shell side of the condenser:

$$UA(t) = K_1 (V_{total} - V_{liq}(t)) \quad (3.31)$$

where $V_{liq}(t)$ = volume occupied by liquid in the shell side of the condenser at time t ,

V_{tot} = total volume of condenser shell side,

K_1 = constant.

At each time step, the liquid volume can be calculated from the liquid material balance, and the $UA(t)$ term is calculated from Equation 3.31. Then the cooling duty can be calculated by using the value of $UA(t)$ and ΔT . The condenser duty calculated at each time step is used in energy balance equation of partial condenser (Equation 3.17). It should be noted that the condenser heat transfer model presented here is just an approximation. However, it is reasonable enough to represent the control relevant process behavior.

3.6 PI Level Controllers

The level controllers were not considered part of the composition control problem for the reactive distillation problem. The level controllers were tuned prior to composition controllers for all control configurations and controllers (i.e., PI, NLMPC, or DMC). PI level control was used to maintain the holdups in the condenser and the reboiler at 50 % capacity. Tuning was critically damped for a 5% change in the level setpoint (Marlin, 1995).

The condenser for the reactive distillation was assumed to be a partial condenser. The overall system was modeled as a shell and tube heat exchanger and a reflux accumulator tank. The overhead vapor acts as the tube side fluid and cooling water as shell side fluid. The heat transfer rate for condensation of vapor was assumed to be proportional to the area of tube bundle exposed to the vapor in the condenser. Hence the level in the heat exchanger determines the condenser duty (QC). The level in the heat exchanger is manipulated with the condensed liquid flow from the heat exchanger. The level controller on the reflux accumulator is cascaded to the level controller on the heat exchanger as shown in Figure 3.2. Table 3.2 summarizes the values for gains and reset values for the condenser level, the accumulator level and the reboiler level for each configuration. Gains for L, D, and B are in lbmol/sec while gains for V (reboiler duty controlled) are in btu/sec. Units for reset times are in seconds.

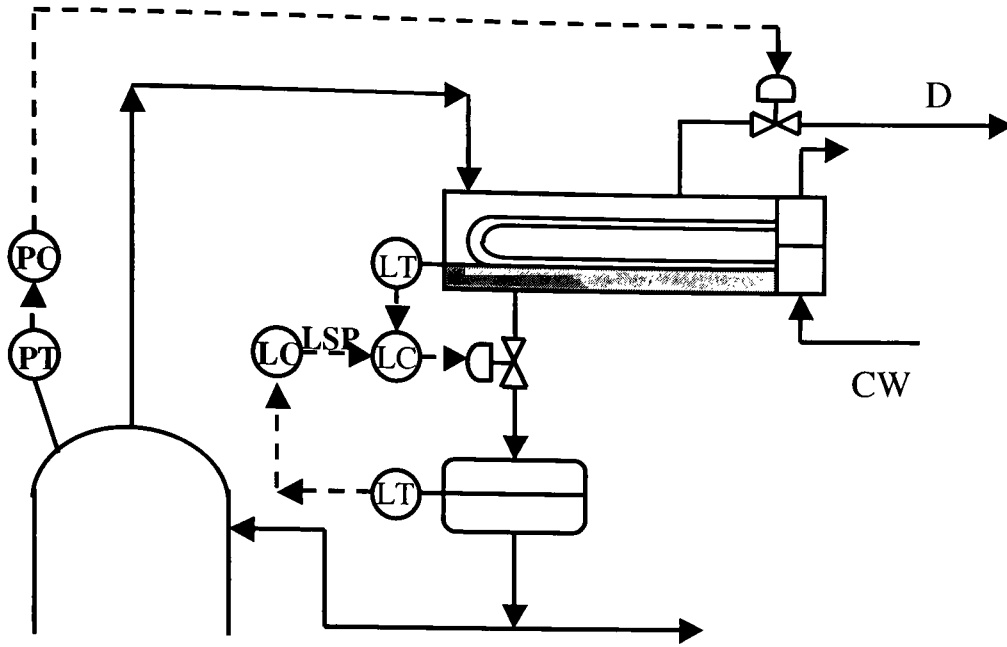


Figure 3.2 Overhead level and pressure control structure

Table 3.2: Reactive distillation level controller gains and reset times.

3.7.Overhead Pressure Dynamics and Control

The relative changes in the pressure for the reactive distillation column are small, and have very small or negligible effect on phase equilibrium and enthalpy calculations. Hence, mass and energy balances and phase equilibrium models are solved first by assuming constant tray pressures. To account the pressure changes in partial condenser, a total molar balance is written for the entire vapor volume in the column, reflux drum, the overhead piping vapor mass balance is applied to the pressure condenser (Luyben, 1987).

$$\frac{dM_v}{dt} = \frac{V_{total}}{RT_{top}} \frac{dP}{dt} = V_T - V - L_c \quad (3.32)$$

where M_v = moles of vapor in the partial condenser

Table 3.2: Reactive distillation level controller gains and reset times.

Configuration	Level Controller	Gains	Reset Time
[L,V]	Condenser level	-2×10^{-2}	3×10^3
	Accumulator level	1×10^{-1}	1×10^2
	Reboiler level	2×10^{-4}	8×10^3
[L,B]	Condenser level	-2×10^{-2}	3×10^3
	Accumulator level	1×10^{-1}	1×10^2
	Reboiler level	0.9×10^1	4×10^3
[L/D,V/B]	Condenser level	-2×10^{-2}	3×10^3
	Accumulator level	1×10^{-1}	5×10^1
	Reboiler level	4×10^{-3}	1×10^4
[L/D,V]	Condenser level	-2×10^{-2}	3×10^3
	Accumulator level	1×10^{-1}	5×10^1
	Reboiler level	4×10^{-3}	1×10^4
[L/D,B]	Condenser level	-2×10^{-2}	3×10^3
	Accumulator level	1×10^{-1}	5×10^1
	Reboiler level	0.9×10^1	4×10^3
[L,V/B]	Condenser level	-2×10^{-2}	3×10^3
	Accumulator level	1×10^{-1}	1×10^2
	Reboiler level	4×10^{-3}	1×10^4

V = vapor distillate molar flowrate

V_T = molar vapor flow rate leaving the top tray in the column entering partial condenser

L_c = molar flowrate of vapor being condensed to liquid in the condenser

V_{total} = Total vapor volume in the column, partial condenser and overhead piping

R = universal gas constant

T_{top}= temperature of the top tray.

Overhead pressure of the column is controlled by the vapor distillate flow from the partial condenser for all the control configurations. The PI pressure controller was tuned using a field tuning procedure (Riggs, 2001). The response of pressure controller to pressure setpoint change was tuned for critically damped or slightly overdamped response. The tuning parameters for the pressure controller used in this study are given in Table 3.3.

Table 3.3 Tuning parameters for pressure controller

	Gain	Reset Time
Pressure controller	-3×10^{-2}	3×10^3

The units of gain are atm/(lbmol s⁻¹) and units of reset time are seconds.

3.8. Inferential Composition Control

For ethyl acetate reactive column, composition of acetic acid in the overheads and ethyl acetate in the bottoms was inferred from the temperature using a linear correlation of

$$\ln(x) = A + \frac{B}{T} \quad (3.33)$$

where x is product impurity (mole fraction), and T is tray temperature. Riggs, 2001 describes a simple technique to locate the proper tray temperature to infer product

composition. Marlin (1995) also has given guidelines and a procedure to develop inferential control for distillation columns.

Figure 3.3 shows the steady state temperature profile for the ethyl acetate reactive distillation column. The trays are numbered from bottom to top. The temperature within the reactive (middle) section of the reactive column decreases because of the endothermic nature of the esterification reaction.

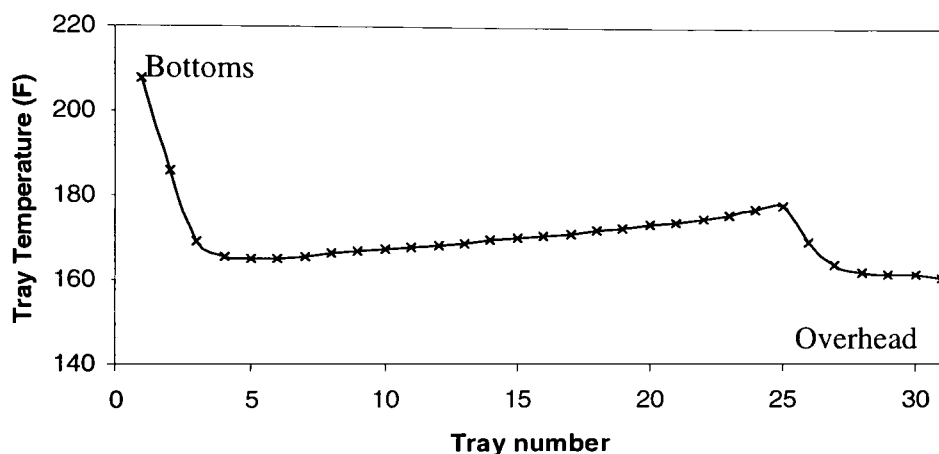


Figure 3.3 Steady state temperature profile for ethyl acetate reactive distillation column

The guidelines provided by Riggs (2001) and Moore (1992) were followed to locate the proper tray location for inferential calculation. Tray 26 was selected for overhead inferential composition calculation and Tray 2 was selected for bottom inferential composition control calculations.

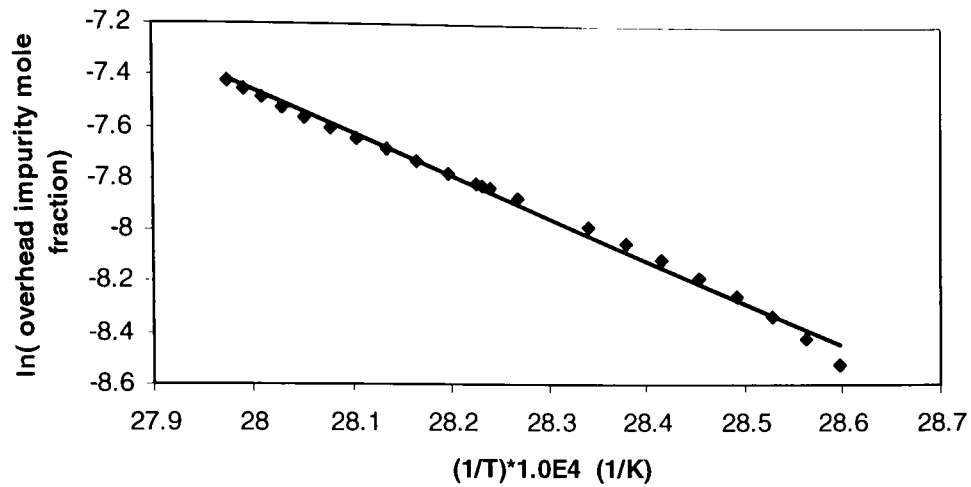
For multi-component distillation systems, setting temperature and pressure does not specify composition. On-line analyzers were required to update the B parameter at

each analyzer sampling period of 5 minutes. The parameter B was updated for top inferential calculations as well as bottom inferential calculations. Based on these updated B parameter, one past temperature and inferred composition, and Equation 3.33, the new inferred compositions for control were calculated as follows for both top and bottom inferential calculations

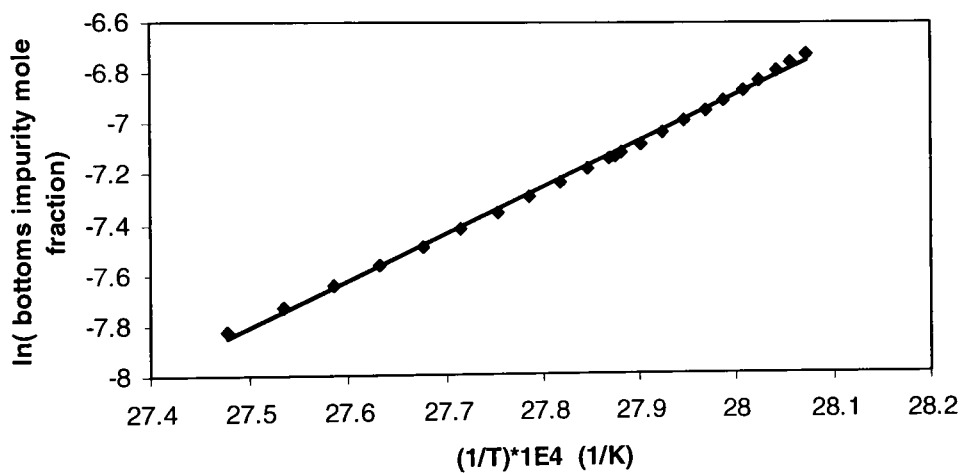
$$\Delta x = x_{old} \left[e^{B \left(\frac{1}{T} - \frac{1}{T_{old}} \right)} - 1 \right] \quad (3.34)$$

$$x = x_{old} + \Delta x \quad (3.35)$$

Here T_{old} and x_{old} are the old temperature and composition, respectively. Exactly similar equations can be written for Δy with corresponding terms related to overhead inferential calculations.



(a) Top inferential calculation based on temperature on Tray 26



(b) Bottom inferential calculation based on temperature on Tray 2

Figure 3.4 Plots for developing correlation between top as well as bottom impurity and tray temperature for inferential calculations.

3.9. Steady state gain analysis of the ethyl acetate reactive distillation system

Reactive distillation columns are highly nonlinear, and many researchers have reported multiple steady-state solutions for reactive distillation systems, e.g., Al-Arfaj and Luyben (2002). Such phenomena have impact on design and control of reactive distillation systems. For the ethyl acetate reactive distillation system the desired control objectives are to control the acetic acid impurity in the overhead and the ethyl acetate impurity in the bottoms of the column. The available manipulated variables are the reflux rate, bottoms flowrate, reboiler heat duty, reflux ratio and boilup ratio. The steady-state gain analysis of ethyl acetate reactive distillation was performed to analyze the effect of different manipulated variables on the control variables of the system.

The sensitivity of the steady-state gain of overhead acetic acid impurity to the reflux ratio (L/D) when the reboiler duty (QR) was kept constant shows significant nonlinear behavior [Figure 3.4 (a)]. As the reflux ratio is changed by around 5%, the process gain changes by over a factor of two. Figure 3.4 (d) shows that the sensitivity of the steady-state gain of bottom ethyl acetate impurity to the reboiler duty (QR) at constant reflux ratio (L/D). As the reboiler duty is changed by 10%, the process gain changes by factor over two. At constant reflux ratio, the gain of overhead acetic acid impurity to the reboiler duty changes sign for varying reboiler duty values as shown in Figure 3.4 (c). This indicates that at constant reflux ratio, the same value of overhead acetic acid impurity is obtained for two different values of reboiler duty. Hence, ethyl acetate reactive distillation system shows input multiplicity.

Figure 3.5 (a) shows the sensitivity of the steady state gain of overhead acetic acid impurity to the reflux ratio (L/D) at constant boilup ratio (V/B). The sensitivity of the steady state gains of bottom ethyl acetate impurity to the boilup ratio (V/B) at constant reflux ratio (RR) exhibits significant nonlinearity of the system [Figure 3.5 (d)]. As the boilup ratio was changed by about 10%, the process gain changes by over a factor of two. At constant reflux ratio, gains of overhead acetic acid impurity to the boilup ratio (V/B) changes sign as shown in the Figure 3.5 (b).

Figure 3.6 (a) shows the sensitivity of the steady state gain of overhead acetic acid impurity to the reflux flowrate (L) at constant reboiler duty (QR). As reflux flow changes by about 10%, the gain value changes by a factor of two. At constant reflux rate, as the value of reboiler duty was changed by 10% , the gain of the bottom ethyl acetate impurity to the reboiler duty changes by a factor over four [Figure 3.6 (d)]. This shows highly nonlinear behavior of the system.

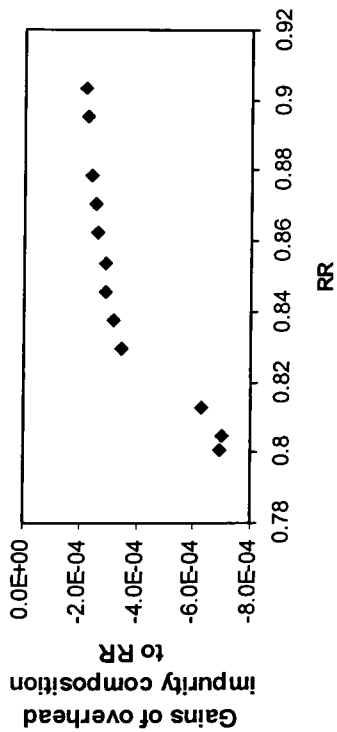
Figure 3.7 (a) shows that at constant value of boilup ratio (V/B) the gain of overhead acetic acid impurity to the reflux flowrate (L) increases with value of reflux flowrate. Figure 3.7 (d) shows that at constant reflux flowrate, as the boilup ratio changes by 10%, the gain of bottom ethyl acetate impurity to the boilup ratio (V/B) changes by a factor over eight.

Table 3.1 summarizes the steady-state gain analysis for the ethyl acetate reactive distillation system. The table shows the % change in steady-state process gain corresponding to a specified % change in the manipulated variable. The figures in the table are not exact values but represents a approximate values.

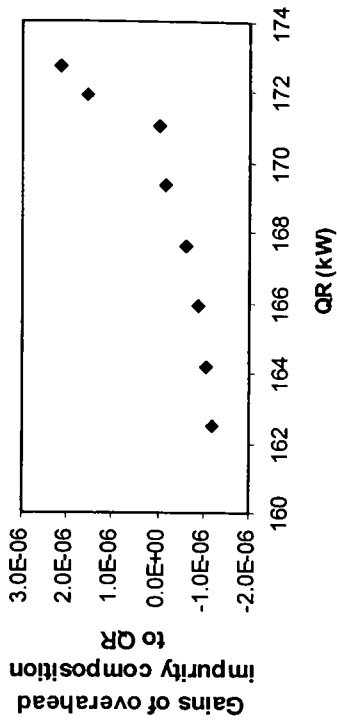
Table 3.4 Steady-state gain analysis of the ethyl acetate reactive distillation column

Configuration	% change in manipulated variable for overhead loop	% change in process gain for overhead loop	% change in manipulated variable for bottoms loop	% change in process gain for bottoms loop
[L/D,V]	10	200	11	300
[L/D,V/B]	12.5	150	10	300
[L,V]	12	150	10	600
[L,V/B]	12	33	12	300

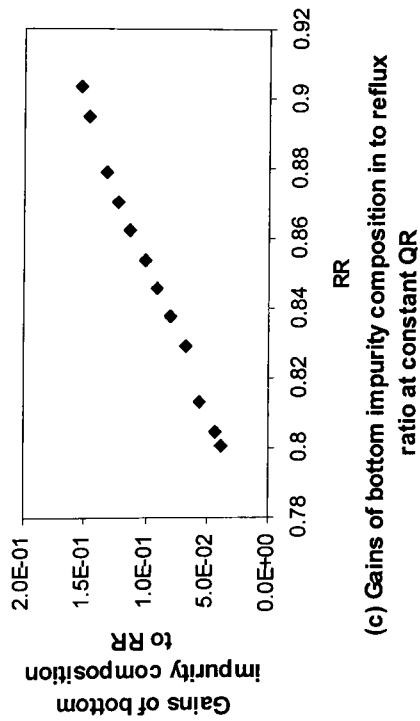
Overall the steady-state gain analysis of the ethyl acetate reactive distillation system shows highly nonlinear behavior.



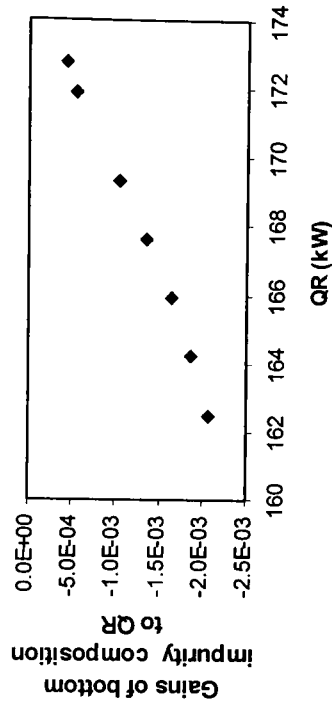
(a) Gains of overhead impurity composition to Reflux ratio at constant QR



(b) Gains of overhead impurity composition to QR at constant reflux ratio



(c) Gains of bottom impurity composition in to reflux ratio at constant QR



(d) Gains of bottom impurity composition in QR at constant reflux ratio

Figure 3.5 Steady-state gain behavior with reflux ratio (RR) and reboiler duty (QR) as manipulated variables.

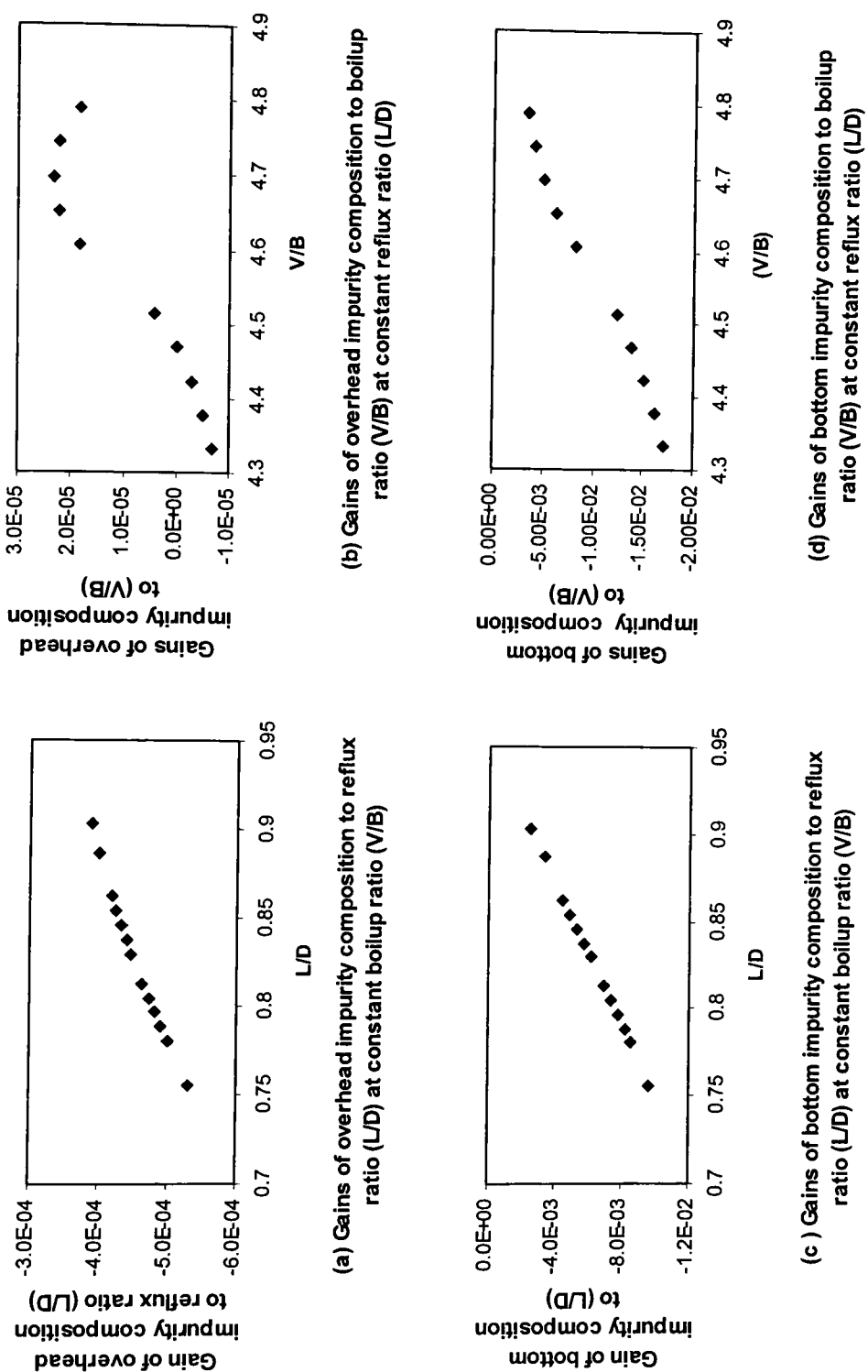


Figure 3.6 Steady-state gain behavior with reflux ratio (L/D) and boilup ratio (V/B) as manipulated variables.

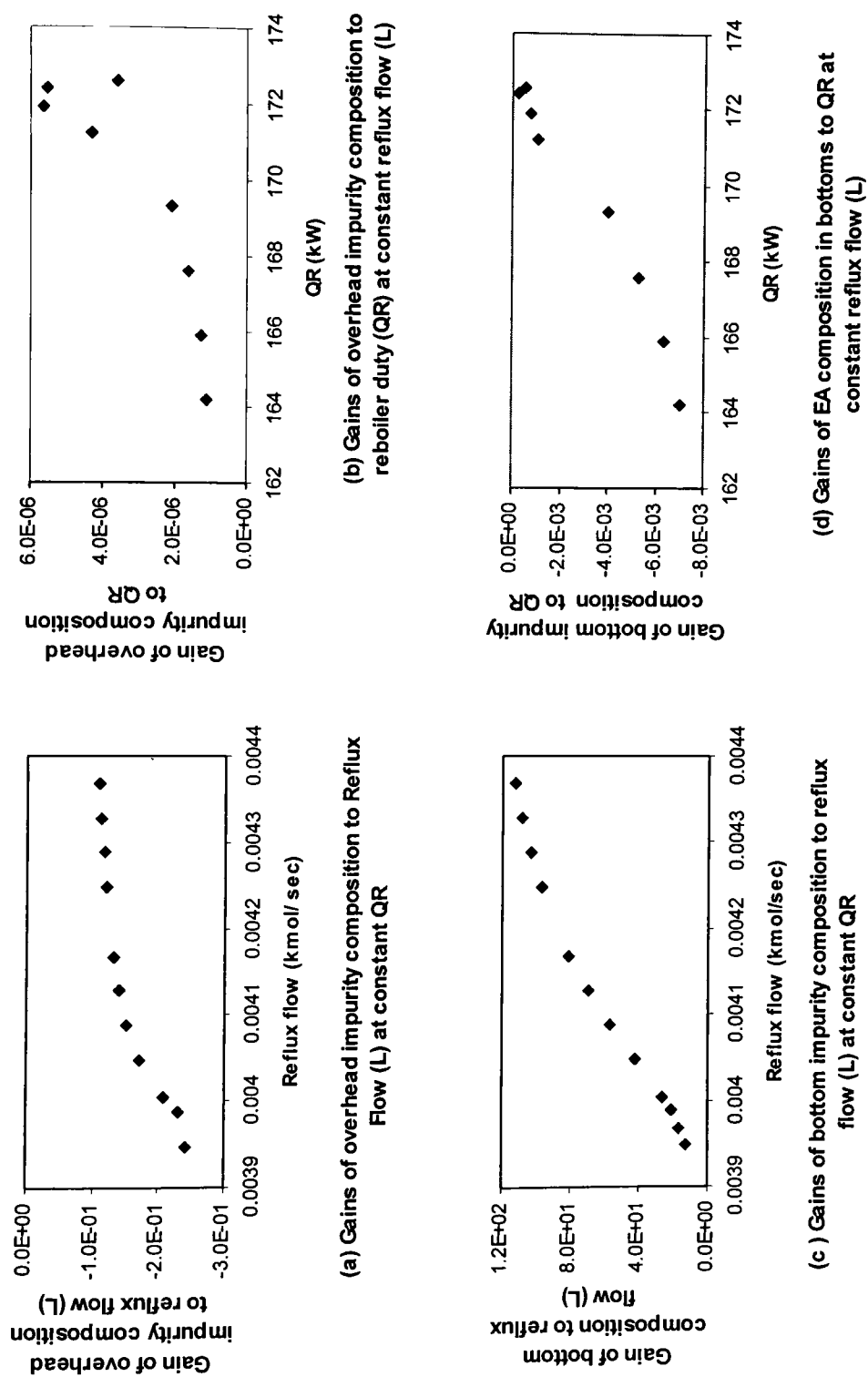


Figure 3.7 Steady-state gain behavior with reflux flow (L) and reboiler duty (QR) as manipulated variables

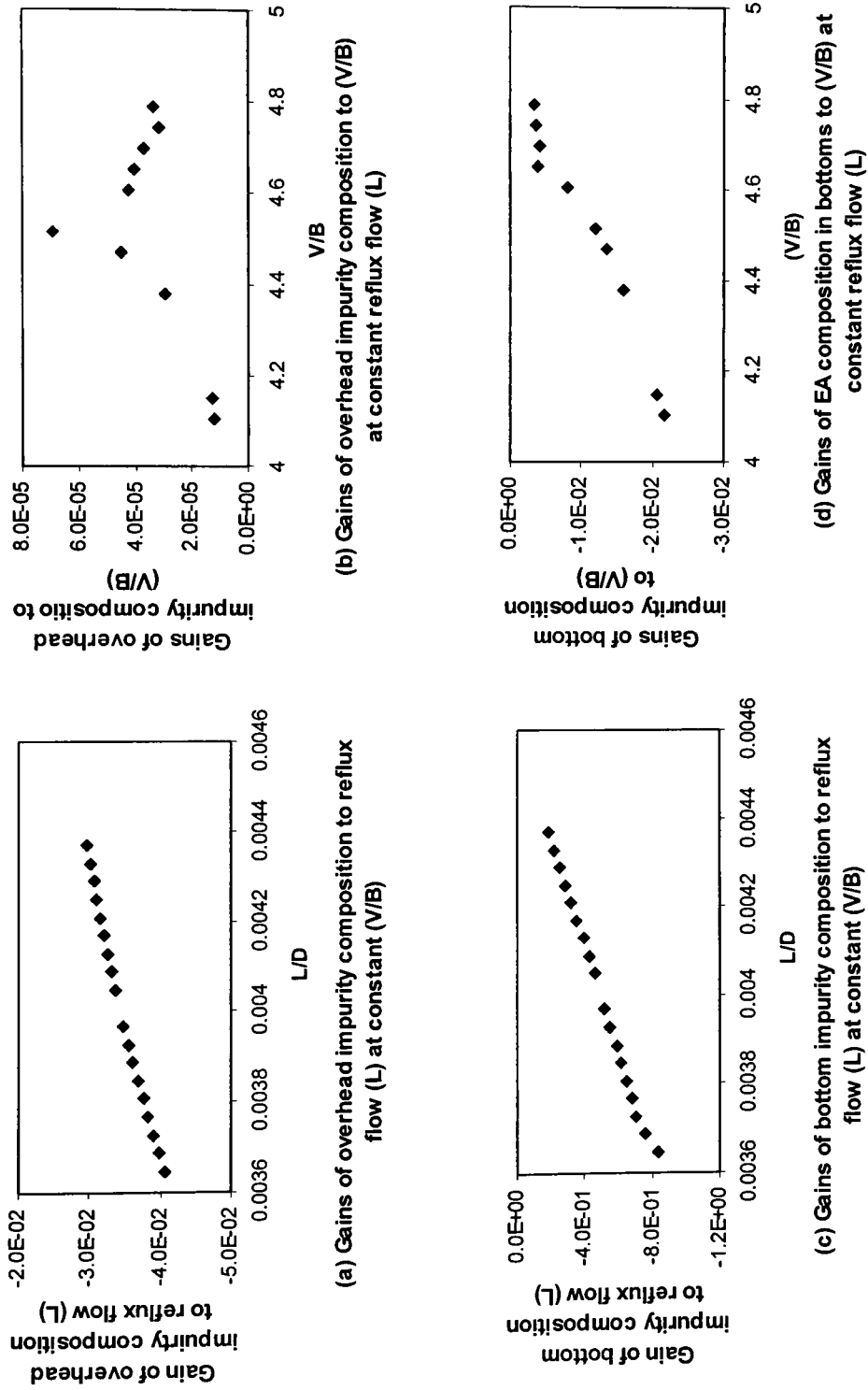


Figure 3.8 Steady-state gains with reflux flow (L) and boilup ratio (V/B) as manipulated variables

3.10. Summary of design parameters

Table 3.5: Design specifications and parameters for reactive distillation column

Number of stages	31
Rectifying section	25-31
Reactive section	7-24
Stripping section	1-6
Stage holdups	
Rectifying section (m ³)	0.15 ¹
Reactive section (m ³)	1.75
Stripping section (m ³)	1.65
Distillate flow (kmol/sec)	4.881×10^{-3}
Bottoms flow (kmol/sec)	9.094×10^{-4}
Reflux ratio	0.8211
Feed flowrate	
Acetic acid feed (kmol/sec)	8.916×10^{-4}
Ethanol feed (kmol/sec)	8.736×10^{-4}
Recycle feed (kmol/sec)	4.025×10^{-3}
Distillate product composition (mol fraction)	
Ethanol	0.2383
Acetic acid	0.0004
Water	0.2093
Ethyl acetate	0.5520
Bottoms product composition (mole fraction)	
Ethanol	0.0249
Acetic acid	0.0876
Water	0.8867
Ethyl acetate	0.0008
Reboiler duty (kW)	171.035

Condenser duty (kW)	137.736
Recycle feed composition (mole fraction)	
Ethanol	0.2856
Acetic acid	0.0
Water	0.2514
Ethyl acetate	0.4630
Tray number for overhead inferential composition calculations	26
Tray number for bottoms inferential composition calculations	2

1 The liquid holdup in the rectifying section is reduced to suppress the reverse reaction and control the concentration of acetic acid in distillate. (refer Section 2.1.1).

CHAPTER 4

DUAL PI COMPOSITION CONTROL

This chapter considers the application of dual PI composition controllers applied to the ethyl acetate reactive distillation column. The issue of configuration selection is discussed in Section 4.1. The approach used to tune the composition controllers is discussed in Section 4.2. The dual composition control results are presented in Section 4.3. The overall discussion of the control results is presented in the end of this chapter.

4.1 Configuration Selection

The application of PI control to a distillation column is essentially a 5×5 control problem. The five variables to be controlled are the overhead column pressure, the accumulator and reboiler levels, and the overhead and bottoms product compositions. The five variables that can be manipulated in order to meet the control objectives are the reflux (L), distillate (D), bottoms (B), and vapor boilup (reboiler duty) flow rates (QR), and the condenser duty (QC). Additionally, the reflux ratio (L/D) and boilup ratios (V/B) may also be considered as manipulated variables. In ethyl acetate reactive distillation, the overhead pressure is controlled by means of vapor distillate flow (D) from the partial condenser, as discussed in Section 3. Hence, the vapor distillate flow is not available as a manipulated variable for level or composition control of the column.

For the ethyl acetate reactive distillation column, the ethyl acetate composition in the bottoms, referred as bottom impurity, acts as controlled variable for bottom

composition loop. Acetic acid composition in the distillate, referred as overhead impurity, acts as controlled variable for overhead composition control loop. Acetic acid present in the vapor distillate of reactive distillation appears as the bottom product of the recovery stream and therefore directly affects the purity of the final ethyl acetate product. Hence, the control of overhead impurity is primary control objective for this system.

Once the two manipulated variables that will be used to control the product compositions are determined, the remaining manipulated variables are used to control the levels in the accumulator and reboiler. Section 3.6 describes the overhead level control scheme for the ethyl acetate reactive distillation column. The level in the partial condenser heat exchanger is adjusted by means of condensed liquid and level in the reflux accumulator is cascaded with level in the partial condenser. This cascade level control scheme is used for all the configurations. The following different configurations can be considered for dual PI composition control scheme for ethyl acetate reactive distillation column.

Table 4.1 Dual PI composition control MV-CV pairings.

Configuration	Manipulated Variables			
	Overhead Composition Loop	Bottoms Composition Loop	Reboiler Level	Accumulator Level
(L, V)	L	V	B	Cascade Loop
(L, B)	L	B	V	Cascade Loop
(L, V/B)	L	V/B	V+B	Cascade loop
(L/D, V)	L/D	V	B	Cascade loop
(L/D, B)	L/D	B	QR	Cascade loop
(L/D, V/B)	L/D	V/B	V+B	Cascade loop

4.2 Controller tuning methodology

Tuning of PI controller require the values of gain and reset time. For the ethyl acetate reactive distillation column, ratio of dead time (θ_p) to time constant (τ_p) is less than 0.5. Hence, PI controllers can be used and no derivative action is necessary. While an open-loop test can be used to calculate a controller gain and reset time, open-loop test requires a large amount of time to complete. Open-loop tuning results are significantly affected by process disturbances and nonlinear behavior which makes this tuning method unacceptable. Luyben (1986) suggested using the Biggest Log modulus Tuning (BLT) method for tuning the PI control loops. However, the BLT method requires the use of transfer functions which are time consuming to develop and often lead to significant errors.

The tuning approach used in this work uses the Autotune Variation (ATV) method (Astrom and Hagglund, 1984) to determine the ultimate gain and ultimate period

of the controller. Then, the Tyreus and Luyben (1992) controller gain and reset time were determined as follows,

$$K_c^{TL} = \frac{K_u}{3.22}$$

$$\tau_c^{TL} = 2.2P_u.$$

Distillation control exhibits significant coupling. Since the TL tuning parameters were developed for non-coupled controllers, the TL tuning parameters usually resulted in non-optimal control, which required further tuning. A detuning factor was used to tune the composition controller. A detuning factor value above 1.0 made the control action less aggressive. A detuning factor value below 1.0 resulted in more aggressive control action.

$$K_c = \frac{K_c^{TL}}{F_D}$$

$$\tau_I = \tau_c^{TL} \times F_D$$

The control of overhead impurity is the primary control objective for the ethyl acetate reactive distillation system. Hence, the bottom composition loop is tuned sluggishly for the system. An ATV test is performed for bottom composition loop to determine the ultimate gain and ultimate period. Then the detuning factor was used to tune the bottom composition loop for overdamped behavior.

After tuning the bottom composition loop for sluggish dynamic behavior, an ATV test is performed for top composition loop to determine the ultimate gain and ultimate period. Integral of the Absolute Value of Error (IAE) for a composition setpoint change

was used as a criteria for determining the optimal detuning factor. It was observed that improved performance in terms of IAE could be obtained by adjusting the values of gain and reset times independently once the optimal detuning factor value was determined. The following series of step tests in the overhead composition setpoint were used to calculate the IAE used for controller tuning,

1. At a time of 10 minutes, the overhead impurity was increased by 25% over the nominal impurity in mole fraction (4.0×10^{-4}).
2. At a time of 2000 minutes, the overhead impurity setpoint was decreased by 25 % below the nominal impurity in mole fraction (4.0×10^{-4}).
3. At a time of 4010 minutes, the simulation was ended.

IAE on composition setpoint was recorded for each configuration. Once the composition controllers were tuned, feed flow and feed composition disturbances were used to test the performance of the controller for unmeasured disturbances.

4.3 Ethyl acetate reactive distillation PI control results

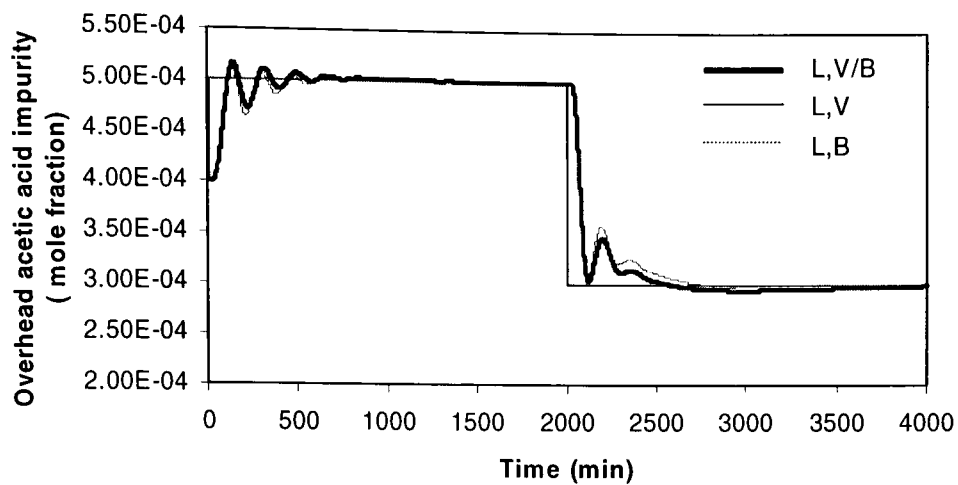
The Dual-ended composition control tuning methodology, described earlier, was implemented on six control configurations. Table 4.2 lists the gain, reset times used for all configurations.

Table 4.2. Ethyl acetate reactive distillation tuning results for dual-ended PI composition control. Reset time is in seconds.

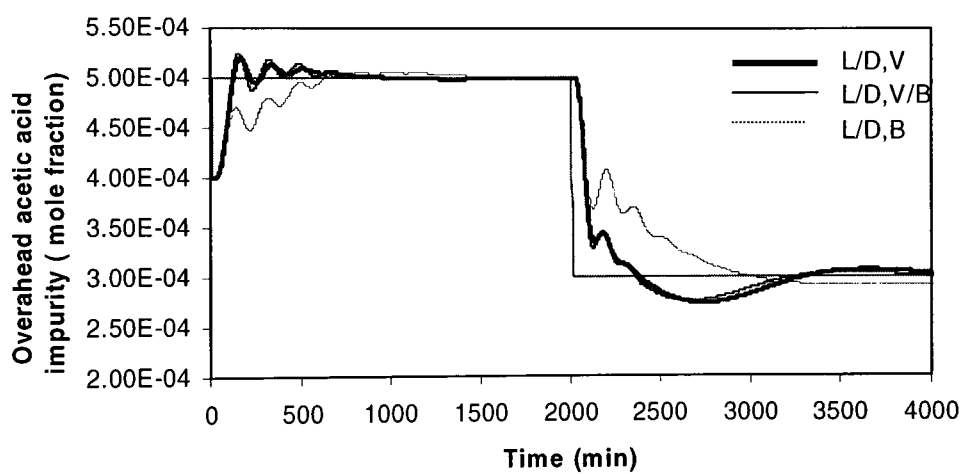
Configuration	Overhead Loop		Bottom Loop	
	Gain	Reset Time	Gain	Reset Time
[L,V]	22.5	7700.0	9.58×10^4	6667.7
[L,B]	23.5	10600.0	7.275	18667.0
[L/D,V/B]	1475.0	2500.0	10.5×10^3	9000.0
[L/D,V]	1210.0	2000.0	9.98×10^4	6400.0
[L/D,B]	1651.3	14933.0	4.81	27000.0
[L,V/B]	21.11	7200.0	9800.0	9600.0

4.3.1 Setpoint Tracking Results

To assess the performance of the PI controller for setpoint tracking, the test described in the section 4.2 was conducted using simulator. The dynamic responses for controlled variables as well as manipulated variables for selected configurations are shown in Figure 4.1 (a) to 4.1 (f). The IAE control performance indices for the ethyl acetate reactive column overhead impurity setpoint change are given in Table 4.3.

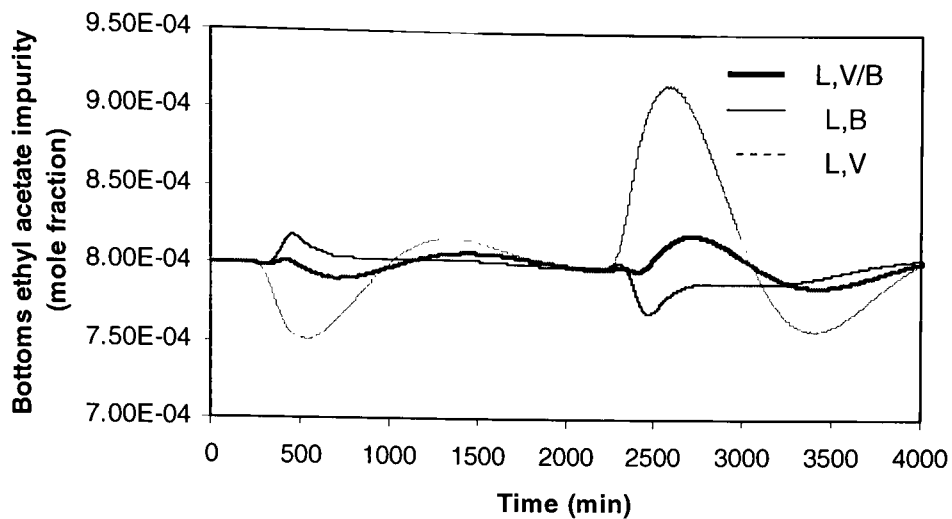


(a) Overhead acetic acid impurity

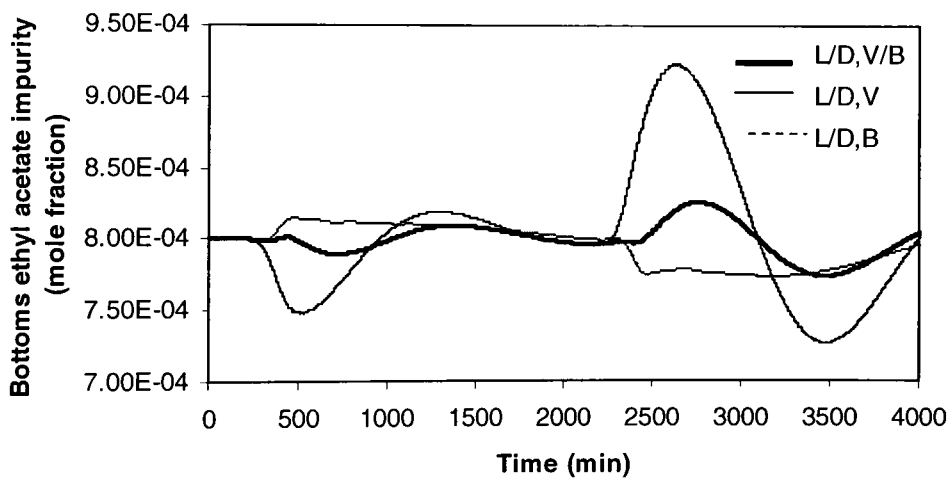


(b) Overhead acetic acid impurity

Figure 4.1 Dual ended composition PI control for overhead impurity setpoint tracking

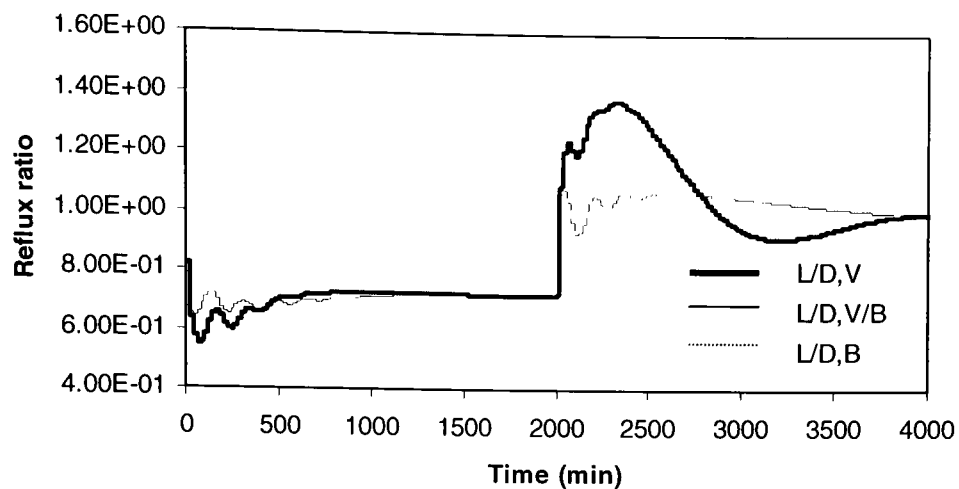


(c) Bottoms ethyl acetate impurity

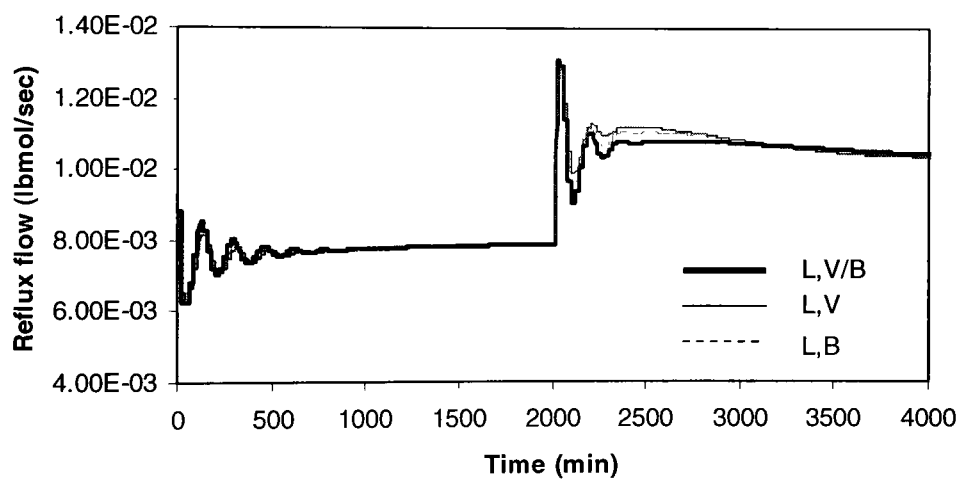


(d) Bottoms ethyl acetate impurity

Figure 4.1 Dual-ended composition PI control for overhead impurity setpoint tracking

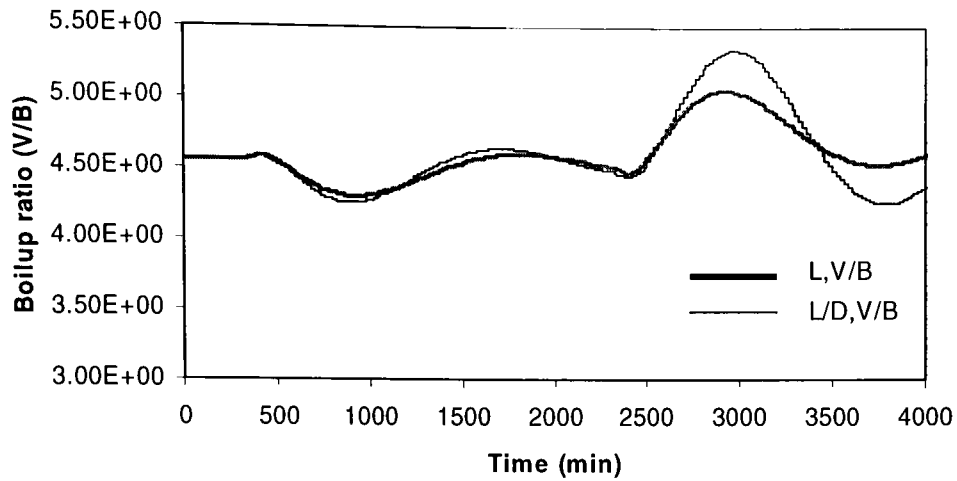


(e) Manipulated variables for overhead composition loop.

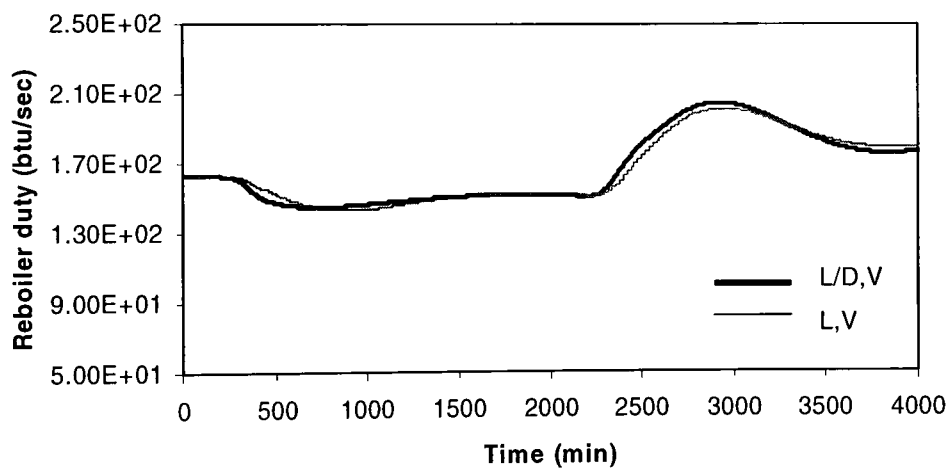


(f) Manipulated variables for overhead composition loop

Figure 4.1-Dual ended composition PI control for overhead impurity setpoint tracking

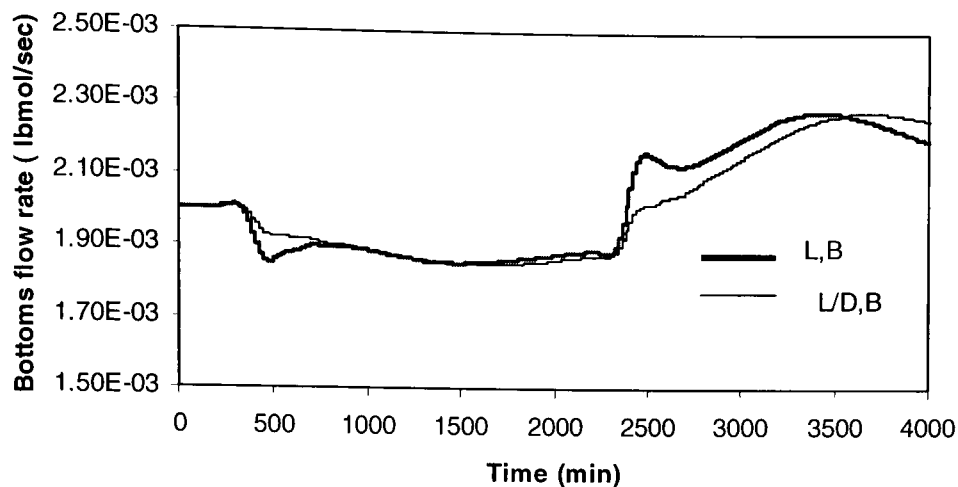


(g) Manipulated variable for bottom composition loop



(h) Manipulated variable for bottom composition loop.

Figure 4.1 Dual ended composition PI control for overhead impurity setpoint tracking



(i) Manipulated variable for bottom composition loop

Figure 4.1 Dual-ended composition PI control for overhead impurity setpoint tracking

Table 4.3 Ethyl acetate dual PI composition control performance indices for overhead impurity setpoint tracking.

Configuration	Overhead Loop IAE	Bottoms Loop IAE
[L,V]	2.28	6.67
[L,B]	2.39	1.43
[L,V/B]	2.68	1.26
[L/D,V]	2.41	6.84
[L/D,B]	4.81	2.90
[L/D,V/B]	2.72	2.14

Figures 4.1 (a), (b) as well as IAE performance indices from Table 4.3 show that almost all the configurations show comparable control performance for the overhead acetic acid impurity. [L, V] and [L/D, V] configurations show comparatively sluggish performance for the bottoms ethyl acetate impurity. However, as discussed earlier the primary control objective for the ethyl acetate column is controlling the overhead acetic acid impurity. Hence, from the setpoint tracking results it is difficult to conclude that one control configuration is superior in the control performance to other configurations.

4.3.2 Unmeasured feed rate disturbance rejection

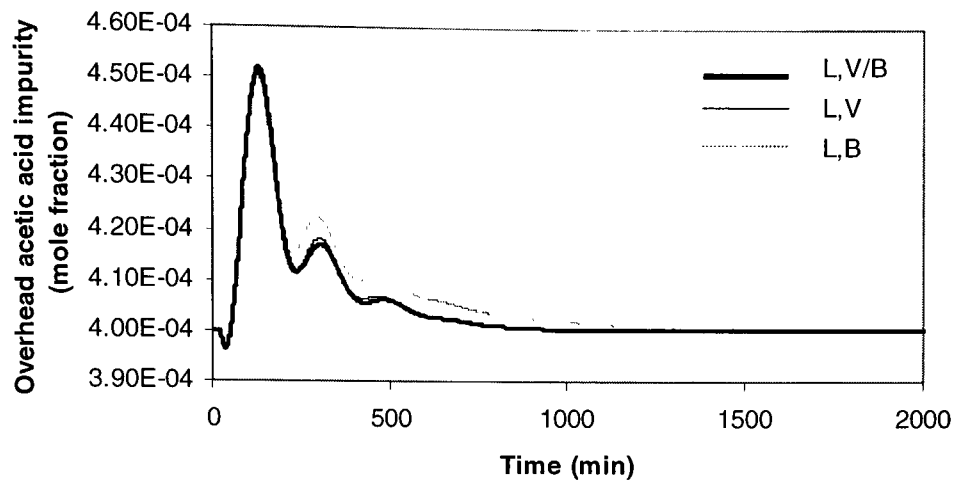
The ability of each control configuration to reject an unmeasured load disturbance was tested by introducing a 25% step change in the recycle feed flow. For dual-ended composition control, the feed flow step test was initiated as follows

1. At time of 10 minutes, a step change decrease of 25% in the feed rate of recycle feed was introduced.
2. At 6010 minutes, the simulation was ended.

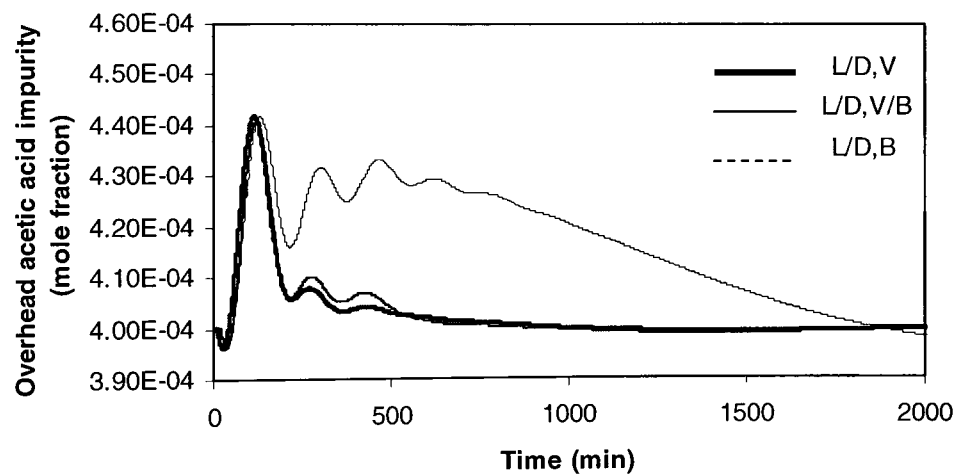
Riggs (2000) has discussed the application of ratio control to reduce the effect of feed rate disturbance on the distillation process. For distillation, all the liquid and vapor flow rates within the column are directly proportional to the feed rate if the product purities are maintained and the tray efficiency is constant. Hence, when a feed rate change is measured, the manipulated variable is proportionally adjusted by means of ratio control.

The IAE control performance indices for ethyl acetate reactive column unmeasured disturbance rejection test are given in the Table 4.4. Figure 4.2 (a) to (f)

shows selected responses for controlled variables and manipulated variables for different control configurations.

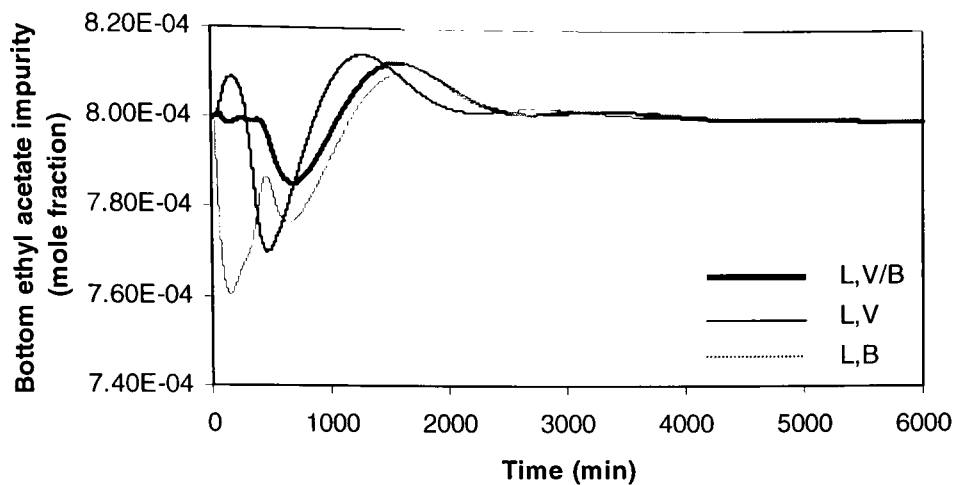


(a) Overhead acetic acid impurity

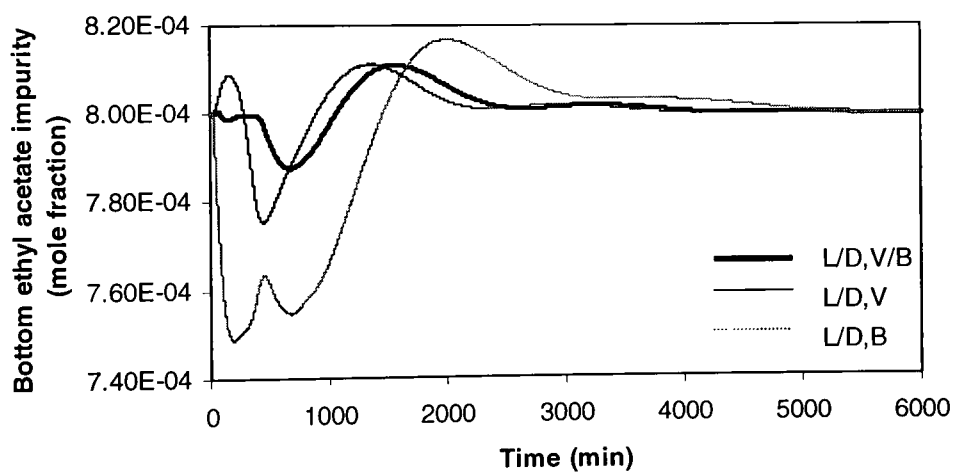


(b) Overhead acetic acid impurity

Figure 4.2 Dual-ended composition PI control for unmeasured feed rate disturbance rejection

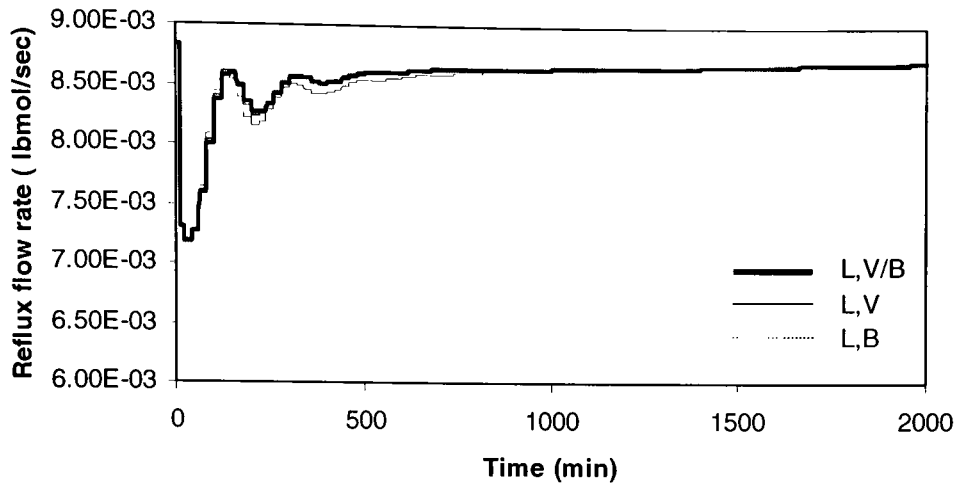


(c) Bottoms ethyl acetate impurity

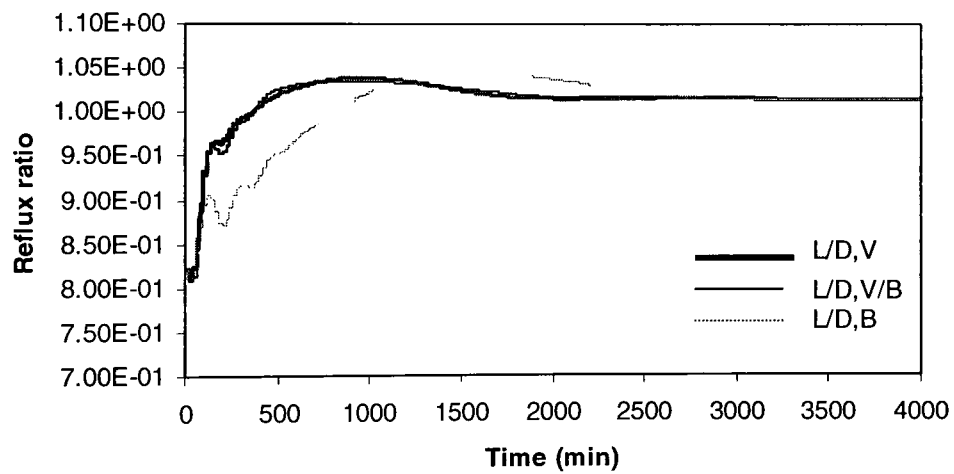


(c) Bottoms ethyl acetate impurity

Figure 4.2 Dual-ended composition PI control for unmeasured feed rate disturbance rejection

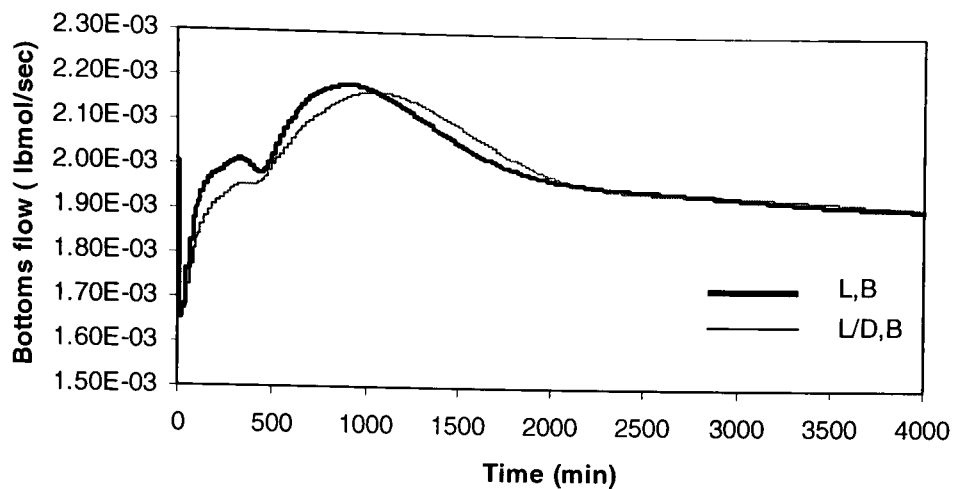


(d) Manipulated variables for overhead composition loop

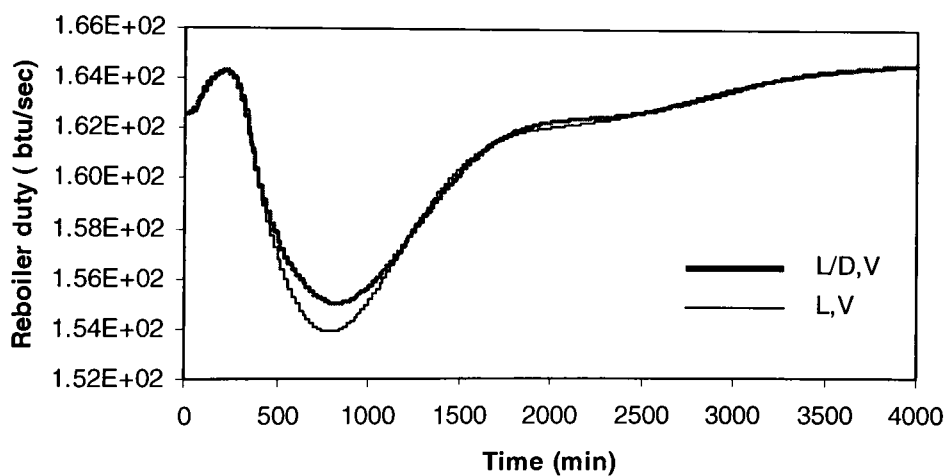


(d) Manipulated variables for overhead composition loop

Figure 4.2 Dual-ended composition PI control for unmeasured feed rate disturbance rejection

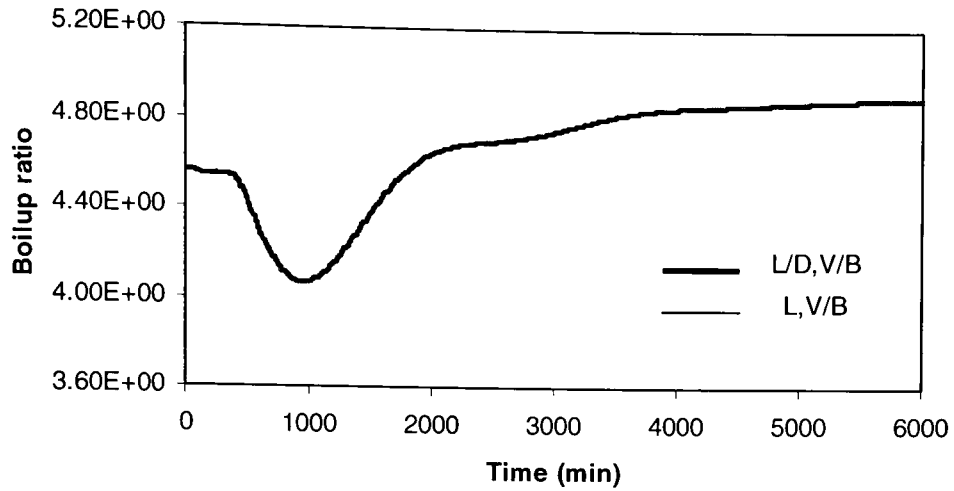


(e) Manipulated variables for bottom composition loop



(f) Manipulated variable for bottom composition loop

Figure 4.2 Dual-ended composition PI control for unmeasured feed rate disturbance rejection



(g) Manipulated variable for bottom composition loop

Figure 4.2 Dual-ended composition PI control for unmeasured feed rate disturbance rejection

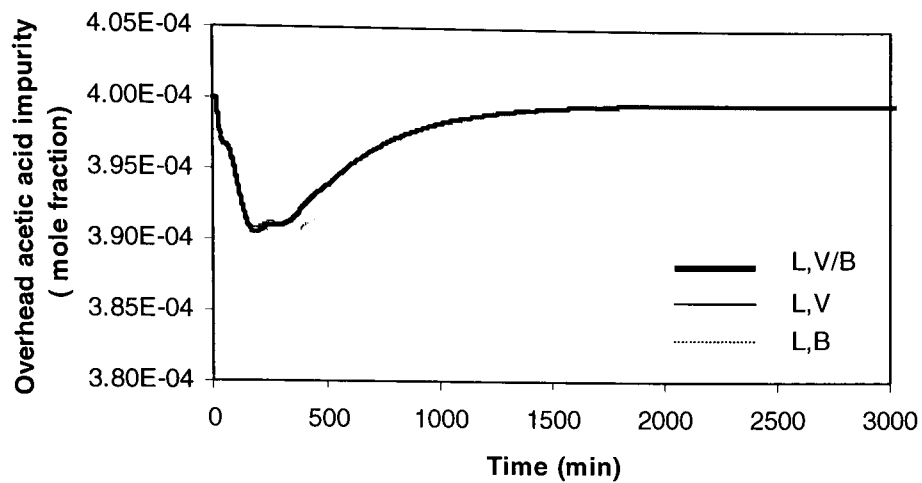
Table 4.4 Ethyl acetate dual PI composition control performance indices for unmeasured feed rate disturbance.

Configuration	Overhead Loop IAE	Bottoms Loop IAE
[L,V]	0.6215	1.5132
[L,B]	0.8119	2.1823
[L,V/B]	0.6194	1.2389
[L/D,V]	0.4216	1.2712
[L/D,B]	1.9708	1.4112
[L/D,V/B]	0.4239	1.0778

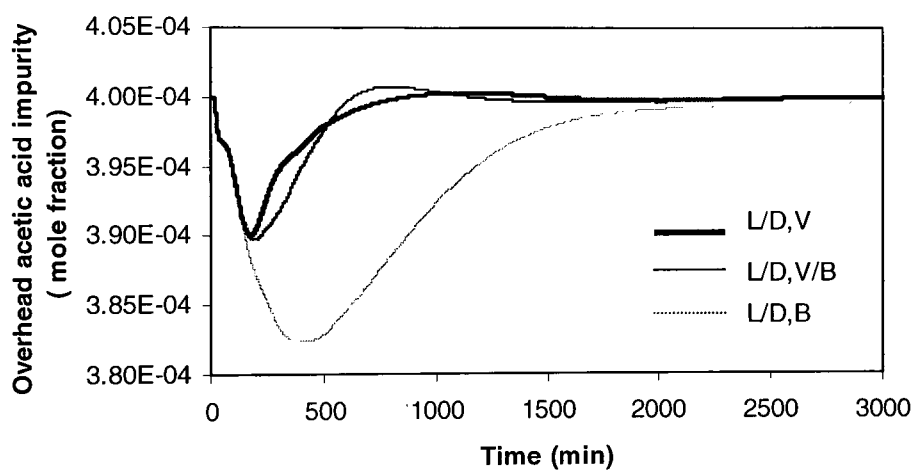
For an unmeasured feed rate disturbance rejection, [L/D, V] and [L/D, V/B] configurations resulted in better control performances than other configurations. [L, V] and [L, V/B] configurations resulted into similar control performances in terms of overhead composition loop. [L/D,B] configuration resulted into the worse overhead control performance for an unmeasured feed rate disturbance.

4.3.3 Unmeasured feed composition disturbance rejection

The ability of each control configuration to maintain composition control during an unmeasured disturbance was tested by using a composition step change of -10% in the acetic acid feed at $t=10$ minutes. The IAE control performance indices for the ethyl acetate reactive column unmeasured disturbance rejection test are given in Table 4.5. The control responses for controlled variables and manipulated variables for different configurations are shown in Figure 4.3 (a) to (f).

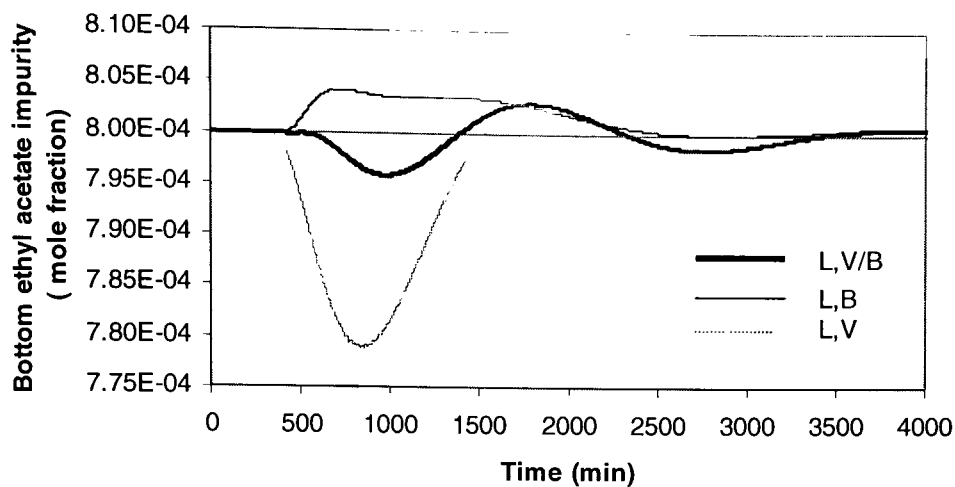


(a) Overhead acetic acid impurity

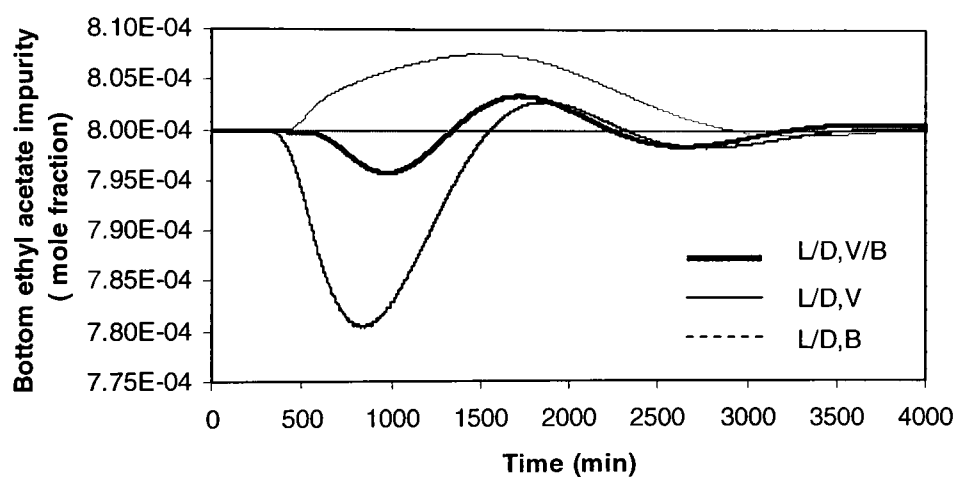


(b) Overhead acetic acid impurity

Figure 4.3 Dual-ended composition PI control for unmeasured feed composition disturbance rejection

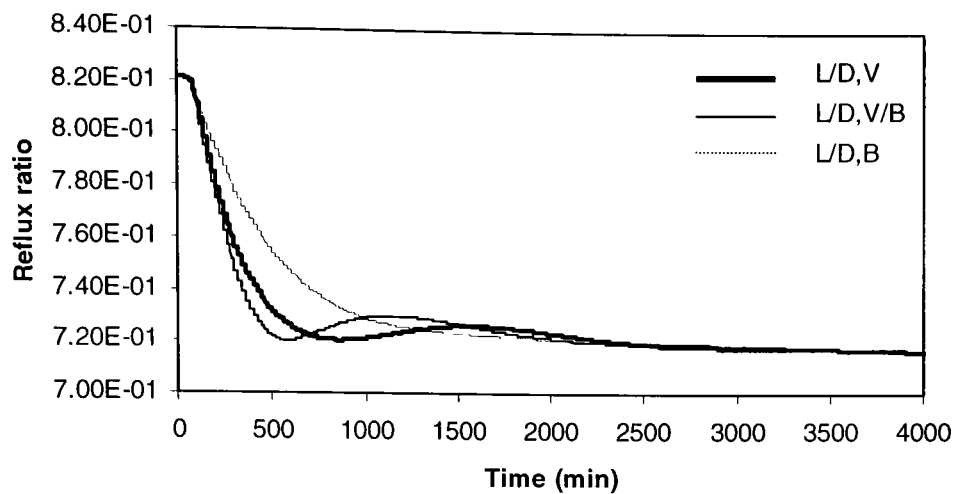


(c) Bottom ethyl acetate impurity

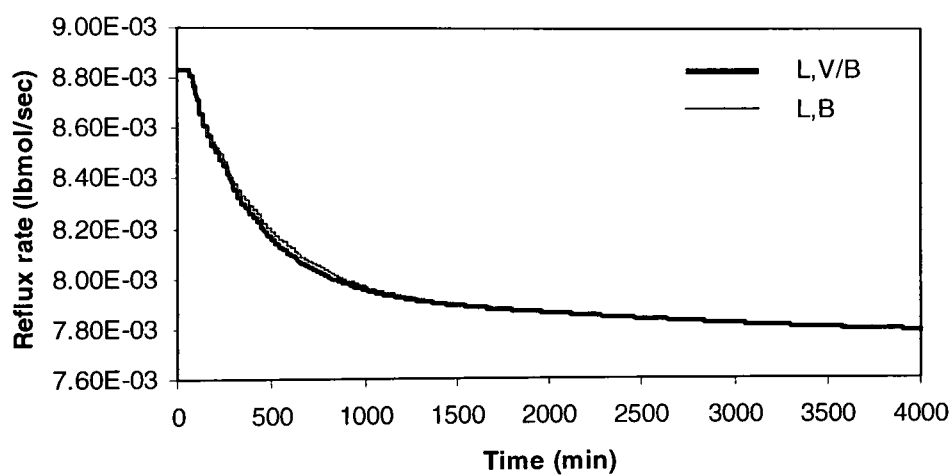


(d) Bottom ethyl acetate impurity

Figure 4.3 Dual-ended composition PI control for unmeasured feed composition disturbance rejection

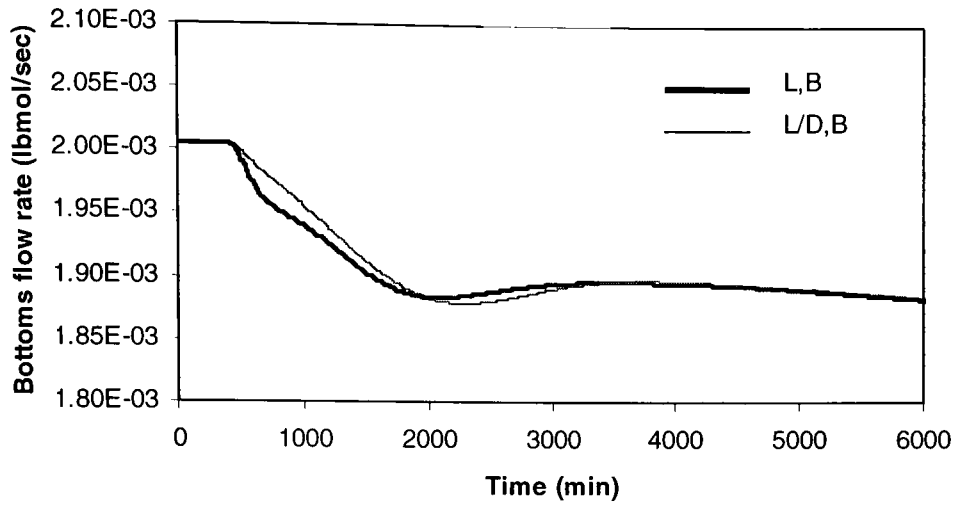


(e) Manipulated variable for overhead composition loop

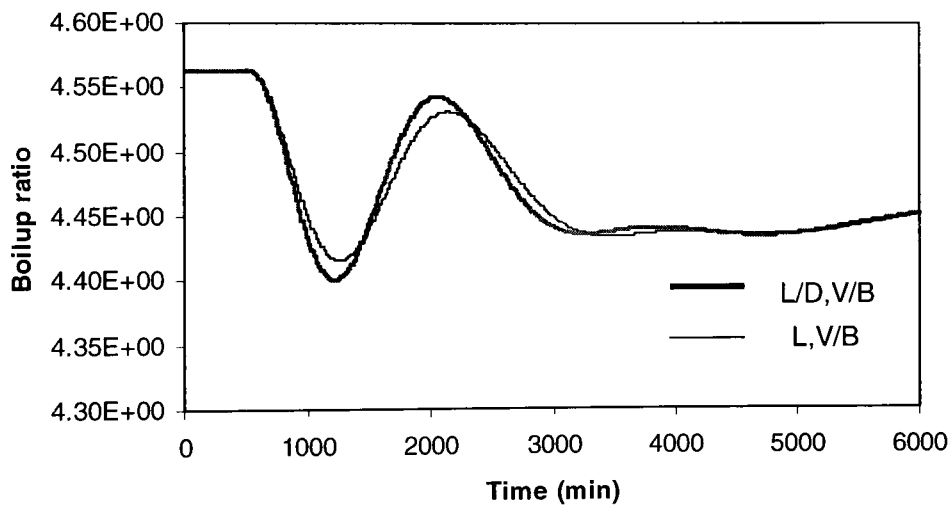


(f) Manipulated variable for overhead composition loop

Figure 4.3 Dual-ended composition PI control for unmeasured feed composition disturbance rejection

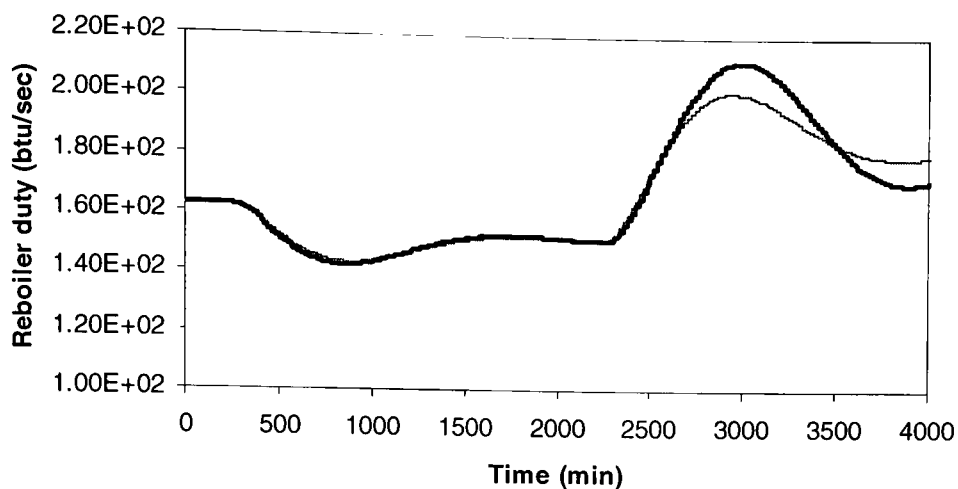


(g) Manipulate variable for bottom composition loop



(h) Manipulated variable for bottom composition loop

Figure 4.3 Dual-ended composition PI control for unmeasured feed composition disturbance rejection



(i) Manipulated variable for bottom composition loop

Figure 4.3 Dual-ended composition PI control for unmeasured feed composition disturbance rejection

Table 4.5 Ethyl acetate dual PI composition control performance indices for unmeasured feed composition disturbance.

Configuration	Overhead Loop IAE	Bottoms Loop IAE
[L,V]	0.1433	1.2781
[L,B]	0.1771	0.8295
[L,V/B]	0.1418	1.2389
[L/D,V]	0.1153	1.2703
[L/D,B]	0.3928	1.2145
[L/D,V/B]	0.1138	0.9878

For feed composition upsets, [L/D, V] and [L/D, V/B] configurations provided better control performance than other configurations. These configurations provided similar control performance for overhead composition loop, however, [L/D, V/B] provided better control performance for bottom composition loop. [L/D, B] configuration showed larger deviation from the setpoint for an unmeasured feed composition disturbance.

4.4 Discussion of results

The primary control objective for the ethyl acetate reactive distillation column was to control the overhead acetic acid impurity. Hence, the for tuning of dual-PI controller structures, the bottom loop was detuned. This provides dynamic decoupling between the overhead composition loop and bottoms composition loop. Hence, the decentralized dual-PI controller gives satisfactory performance for overhead setpoint tracking as well as an unmeasured disturbance rejection. The IAE results for overhead composition loop indicates that almost all the configurations except [L/D,B] exhibit satisfactory control performances. Figure 4.1 shows that the dynamic responses for these different configurations for overhead setpoint tracking are also similar in nature.

The dynamic responses for overhead impurity setpoint tracking exhibit an aggressive nature of controller for positive step change in setpoint for overhead impurity. However, for negative step change in the setpoint for overhead impurity the dynamic responses are sluggish in nature. This behavior can be attributed to the nonlinear nature of the system.

Based on all results for dual PI composition control of the ethyl acetate reactive distillation, use of the [L/D,V] and [L/D,V/B] configurations provided best overall performance for overhead impurity setpoint tracking and for unmeasured disturbances in feed composition and feed rate.

CHAPTER 5

NONLINEAR MODEL PREDICTIVE CONTROL

Model Predictive Control (MPC) is an optimal control based algorithm which selects manipulated variable levels to minimize the performance objective function by utilizing a process model. The objective function is defined as a combination of the sum of the square of the error from the setpoint and the change in the manipulated variables over a future time horizon and is evaluated using an explicit process model to predict future process behavior. Although chemical processes are inherently nonlinear, the most common approach in controller design is to express the model equations in a linear form using linearization about some nominal point. For highly nonlinear processes, the linear MPC might not provide satisfactory performance. Nonlinear Model Predictive Control (NLMPC) can be defined as a MPC algorithm, which employs nonlinear process model in the controller algorithm. This chapter discusses the NLMPC algorithm development for dual composition control of an ethyl acetate reactive distillation column.

5.1 Solution Algorithm

The Solution procedure for NLMPC involves setting up the control problem as a nonlinear programming (NLP) problem and solving it over the prediction horizon. It is necessary to simultaneously solve an optimization problem and the system model equations. These two procedures may be implemented either sequentially or simultaneously.

5.1.1 Sequential solution and optimization algorithm

The sequential algorithm employs separate algorithms to solve the differential equations and to carry out the optimization. First, the manipulated variable profile is selected and the differential equations are solved numerically to obtain the controlled variable profile. The objective function is then determined. The gradient of the objective function with respect to the manipulated variable can be found either by numerical perturbation or by solving sensitivity equations. The control profile is then updated using an optimization algorithm. The process is repeated until the optimal profiles are obtained. This is referred to as a sequential solution and optimization algorithm.

The availability of accurate and efficient integration and optimization packages can permit implementation of the sequential solution and optimization algorithm with little programming effort. However, there are some drawbacks associated with this approach. The sequential solution and optimization requires the solution of differential equations at each iteration of the optimization. Jones and Finch (1984) found that such methods spend about 85% of the time integrating the model equations in order to obtain gradient information. This can make the implementation of this algorithm computationally expensive for cases involving a large number of model equations. The gradient information required for the optimization procedure is often obtained through numerical differentiation, as the analytical derivatives are not available for the highly nonlinear model equations involving complicated thermodynamic relations. To obtain the gradients using finite difference typically involves differencing the output of an integration routine with adaptive step size. Gill et al. (1981) pointed out that the

integration error is unpredictable and hence differencing output of an integration routine greatly degrades the quality of the finite difference derivatives. It is also difficult to incorporate the constraints on state variables with the use of the sequential solution and optimization approach. (Rawlings and Meadows, 1997).

5.1.2. Simultaneous solution and optimization algorithm

A simultaneous solution and optimization algorithm involves the model equations appended to the optimization problem as equality constraints. Then the NLP problem is posed to optimize the objective function such that

- (a) the (discretized) model differential equations are satisfied, and
- (b) the constraints on states and manipulated variables are met.

This can greatly increase the size of optimization problem, leading to a tradeoff between the two approaches. Rawlings and Meadows (1997) reported that for small problems with few states and a short prediction horizon, the sequential solution and optimization algorithm is probably a better approach. For larger problems, the simultaneous solution and optimization approach is more reliable.

The simultaneous solution and optimization approach involves discretization of the model differential equations and their approximation by a set of algebraic equations. This can be achieved using orthogonal collocation on finite elements. The details of orthogonal collocation on finite elements are discussed in the next section. The simultaneous solution and optimization is presented in the following discussion.

5.1.2.1 Orthogonal Collocation

The model differential equations in the time domain are converted into an approximating set of algebraic equations by orthogonal collocation (Finlayson, 1980). A cubic polynomial (i.e., three internal collocation points) is used for the algebraic equation approximation.

In orthogonal collocation, the trial function is taken as a series of orthogonal polynomials and the collocation points are taken as the roots to one of those polynomials. In many of these problems the solution is not a symmetric function of t , (where t is the time coordinate of dynamic model), i.e., it is a function of odd and even powers of t . To do this we construct orthogonal polynomials that are functions of t^n , where $n = 1, 2, 3, \dots, N$, N – order of polynomial. One choice is

$$y = t + t(1-t) \sum_{i=1}^N a_i P_{i-1}(t). \quad (5.1)$$

an equivalent choice for Eq. (5.1) is

$$y = \sum_{i=1}^{N+2} b_i P_{i-1}(t). \quad (5.2)$$

Eq. (5.2) can be simplified as follows:

$$y = \sum_{i=1}^{N+1} d_i t^{i-1}. \quad (5.3)$$

We define the polynomials to be orthogonal with the condition

$$\int_0^1 W(t) P_k(t) P_m(t) dt = 0 \quad k \leq m-1. \quad (5.4)$$

Again, we take the first coefficient of the polynomial as one, so that the choice of the weighting function $W(t)$ completely determines the polynomial, and hence the trial function and the collocation points.

We take the collocation points as the N roots of the polynomial $P_N(t) = 0$. These roots are between zero and one. The collocation points are then $t_1 = 0$, t_2, t_3, \dots, t_{N+1} and $t_{N+1} = 1$, where, $t_1 = 0$ and $t_{N+1} = 1$ are the boundary collocation points and t_2, t_3, \dots, t_N are interior collocation points. Eq. (5.3) can be written at a collocation point j ,

$$y(t_j) = \sum_{i=1}^{N+1} d_i t_j^{i-1}. \quad (5.5)$$

Differentiating Eq (5.5) with respect to t , we get

$$\frac{dy}{dt}(t_j) = \sum_{i=1}^{N+1} (i-1) d_i t_j^{i-2}. \quad (5.6)$$

Now differentiating Eq. (5.6) with respect to t , we get

$$\frac{d^2 y(t_j)}{dt^2} = \sum_{i=1}^{N+1} (i-1)(i-2) d_i t_j^{i-3}. \quad (5.7)$$

We can write Eqs (5.5), (5.6) and (5.7) in matrix form as follows:

$$y = Qd \quad \frac{dy}{dt} = Cd \quad \frac{d^2 y}{dt^2} = Dd, \quad (5.8)$$

where

$$Q_{ji} = t_j^{i-1} \quad C_{ji} = (i-1)t_j^{i-2} \quad D_{ji} = (i-1)(i-2)t_j^{i-3} \quad (5.9)$$

where

$$i = 1, 2, 3, \dots, N+2$$

$$j = 1, 2, 3, \dots, N+2$$

Solving for d gives,

$$\frac{dy}{dt} = CQ^{-1}y = Ay \quad \frac{d^2y}{dt^2} = DQ^{-1}y = By. \quad (5.10)$$

Thus, the orthogonal collocation method can be used to convert the differential equations into algebraic equations. Stiff problems are solved by using multiple subintervals along the axial direction, i.e., time axis in the present discussion. Dependent variables values are equated at the first and last collocation points of consecutive intervals. Low order polynomials (e.g., quadratic or cubic) are used for the approximation resulting in a set of algebraic equations. This is because higher order polynomial tends to oscillate in the intervals between the collocation points. Therefore in discretization of model differential equations, a cubic polynomial is used for algebraic approximation.

5.1.2.2 Determination of collocation points for a cubic polynomial.

Let $W(t) = 1$, and the polynomials be

$$P_0 = 1, \quad P_1 = 1 + bt, \quad P_2 = 1 + ct + dt^2, \quad P_3 = 1 + et + ft^2 + gt^3. \quad (5.11)$$

P_1 is found by requiring the orthogonality condition,

$$\int_0^1 W(t) P_0 P_1 dt = 0 \quad \text{or} \quad \int_0^1 (1 + bt) dt = 0, \quad (5.12)$$

which makes $b = -2$. Then P_2 is found from

$$\int_0^1 W(t) P_0 P_2 dt = 0 \quad \int_0^1 W(t) P_1 P_2 dt = 0, \quad (5.13)$$

i.e.,

$$\int_0^1 (1 + ct + dt^2) dt = 0 \quad \int_0^1 (1 - 2t)(1 + ct + dt^2) dt = 0 \quad (5.14)$$

which makes $c = -6, d = 6$.

Then P_3 is found by requiring the orthogonality condition,

$$\int_0^1 W(t) P_0 P_3 dt = 0 \quad \int_0^1 W(t) P_1 P_3 dt = 0 \quad \int_0^1 W(t) P_2 P_3 dt = 0, \quad (5.15)$$

i.e.,

$$\begin{aligned} \int_0^1 (1 + et + ft^2 + gt^3) dt &= 0 \\ \int_0^1 (1 - 2t)(1 + et + ft^2 + gt^3) dt &= 0 \\ \int_0^1 (1 - 6t + 6t^2)(1 + et + ft^2 + gt^3) dt &= 0 \end{aligned} \quad (5.16)$$

which makes $e = -12, f = 30, g = -20$.

The polynomials are $P_0 = 1, P_1 = 1 - 2t, P_2 = 1 - 5t + 5t^2, P_3 = 1 - 12t + 30t^2 - 20t^3$

The roots of the cubic polynomial $P_3(t) = 0$ are 0.1127, 0.5, 0.8873, so these are the internal collocation points along with $t = 0$ and $t = 1$ as the boundary collocation points.

In this study, all the differential equations are approximated as a set of algebraic equations using three internal collocation points and one on the boundaries of each finite element. Three internal collocation points are illustrated in Figure 5.1. If the element is scaled so that $t_1 = 0$ and $t_5 = 1$, then the node points are given by $\{t_1, t_2, t_3, t_4, t_5\} = \{0, 0.1127, 0.5, 0.8873, 1.0\}$, which are the roots of the third-order

Lengendre polynomial, augmented by element endpoints. If $t_1 \neq 0$ and $t_5 \neq 1$, then a linear change of variable is necessary to transform the time interval to $[0, 1]$. When the dynamic model is time invariant, the only correction necessary is to scale the right hand side of equation $\dot{x} = f(x, u, t)$ by $t_5 - t_1$.

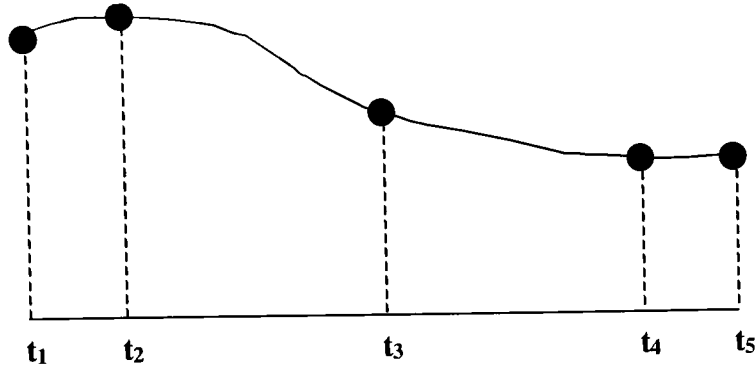


Figure 5.1 Collocation element

Refer to Equation (5.16),

$$Q = \begin{bmatrix} 1 & t_1 & t_1^2 & t_1^3 & t_1^4 \\ 1 & t_2 & t_2^2 & t_2^3 & t_2^4 \\ 1 & t_3 & t_3^2 & t_3^3 & t_3^4 \\ 1 & t_4 & t_4^2 & t_4^3 & t_4^4 \\ 1 & t_5 & t_5^2 & t_5^3 & t_5^4 \end{bmatrix}. \quad (5.17)$$

Therefore,

$$C = \begin{bmatrix} 0 & 1 & 2t_1 & 3t_1^2 & 4t_1^3 \\ 0 & 1 & 2t_2 & 3t_2^2 & 4t_2^3 \\ 0 & 1 & 2t_3 & 3t_3^2 & 4t_3^3 \\ 0 & 1 & 2t_4 & 3t_4^2 & 4t_4^3 \\ 0 & 1 & 2t_5 & 3t_5^2 & 4t_5^3 \end{bmatrix} \quad (5.18)$$

$$D = \begin{bmatrix} 0 & 0 & 2 & 6t_1 & 12t_1^2 \\ 0 & 0 & 2 & 6t_2 & 12t_2^2 \\ 0 & 0 & 2 & 6t_3 & 12t_3^2 \\ 0 & 0 & 2 & 6t_4 & 12t_4^2 \\ 0 & 0 & 2 & 6t_5 & 12t_5^2 \end{bmatrix}. \quad (5.19)$$

This gives

$$A = \begin{bmatrix} -13 & 14.7883 & -2.6667 & 1.8784 & -1 \\ -5.3238 & 3.8730 & 2.0656 & -1.2910 & 0.6762 \\ 1.5 & -3.2275 & 0.0 & 3.2275 & -1.5 \\ -0.6762 & 1.2910 & -2.0656 & -3.8730 & 5.3238 \\ 1 & -1.8784 & 2.6667 & -14.7883 & 13 \end{bmatrix}. \quad (5.20)$$

Thus, using the matrix A , we can approximate the dynamic equation of state x balance as follows:

$$\frac{dx_j}{dt} = \sum_{i=1}^5 A_{ji} x_i \quad (5.21)$$

where

x_j - state variable at j^{th} collocation point ($j = 1$ to 5),

e.g., at 2nd collocation point ($j = 2$), the above equation becomes

$$\frac{dx_2}{dt} = A_{21}x_1 + A_{22}x_2 + A_{23}x_3 + A_{24}x_4 + A_{25}x_5. \quad (5.22)$$

Let the i^{th} state at node j be represented by x_{ji} . Let the notation $x_{j,*}^T$ represents the entire state vector at node j . With constant control, an approximate solution to the differential equation can be obtained by solving the following nonlinear equation:

$$AX = F(X, u) \quad (5.23)$$

where,

$$X = \begin{bmatrix} x_{1,1} & x_{1,2} & \cdots & x_{1,nn} \\ x_{2,1} & x_{2,2} & \cdots & x_{2,nn} \\ x_{3,1} & x_{3,2} & \cdots & x_{3,nn} \\ x_{4,1} & x_{4,2} & \cdots & x_{4,nn} \\ x_{5,1} & x_{5,2} & \cdots & x_{5,nn} \end{bmatrix} \quad (5.24)$$

$$F(X, u) = \begin{bmatrix} x_{init}^T \\ f^T(x_{2,*}^T, u, t_2) \\ f^T(x_{2,*}^T, u, t_3) \\ f^T(x_{2,*}^T, u, t_4) \\ f^T(x_{2,*}^T, u, t_5) \end{bmatrix} \quad (5.25)$$

Since we cannot use only three internal collocation points to calculate the state profiles for the entire time domain, we extend the orthogonal collocation method to a set of finite elements in time direction, with time derivative approximated by cubic polynomials defined on each element. This situation is illustrated in Figure 5.2.

The use of orthogonal collocation on finite elements requires incorporating an indexing scheme to provide the information on the states and location of state in a finite element.

Orthogonal collocation on finite element applies orthogonal collocation at M interior points in each subinterval. This method is more desirable than the standard orthogonal collocation because better results are obtained with a set of low order

polynomials than with a single higher order polynomial. Also, this approach addresses the stiffness issue for the differential/algebraic equations, since the integration process can be custom designed if so desired. In orthogonal collocation on finite elements the process equations are integrated independently on each sub interval, each having its own constant set of independent variables. These integrations are joined by connection equations. These connection equation specify that the value of each of the dependent variables at the first and last collocation points of each subinterval are equal.

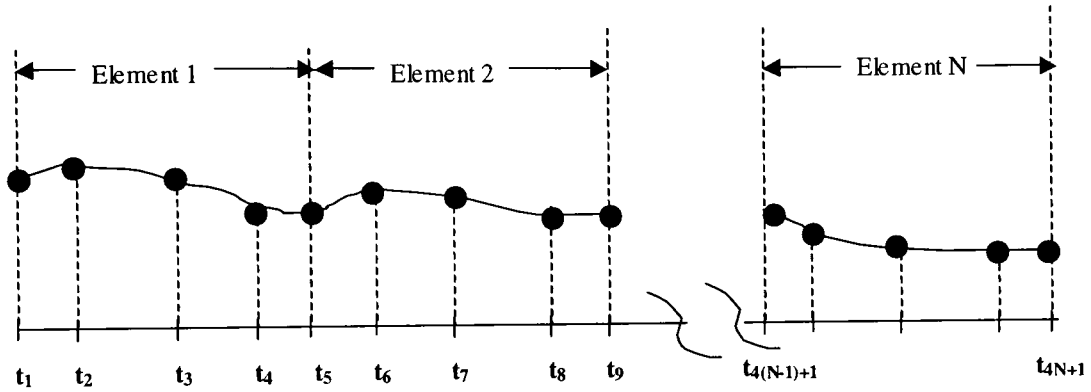


Figure 5.2: Collocation on finite elements

In the matrix form, the orthogonal collocation on finite element can be represented as

$$\tilde{A} \tilde{X} = \tilde{F}(\tilde{X}, U) \quad (5.26)$$

$$\tilde{X} = \begin{bmatrix} x_{1,1} & x_{1,2} & \cdots & x_{1,nn} \\ x_{2,1} & x_{2,2} & \cdots & x_{2,nn} \\ x_{3,1} & x_{3,2} & \cdots & x_{3,nn} \\ x_{4,1} & x_{4,2} & \cdots & x_{4,nn} \\ x_{5,1} & x_{5,2} & \cdots & x_{5,nn} \\ \vdots & \vdots & & \vdots \\ x_{5n-2,1} & x_{5n-2,2} & \cdots & x_{5n-2,nn} \\ x_{5n,1} & x_{5n,2} & \cdots & x_{5n,nn} \end{bmatrix} \quad (5.27)$$

$$\tilde{A} = \begin{bmatrix} A & & & \\ & A & & \\ & & \ddots & \\ & & & A \\ & & & & A \end{bmatrix} \quad (5.28)$$

$$\tilde{F}(\tilde{X}, u_1, u_2, \dots, u_{n-1}) = \begin{bmatrix} x_{init}^T \\ f^T(x_{2,*}^T, u_0, t_2) \\ f^T(x_{3,*}^T, u_0, t_3) \\ \vdots \\ f^T(x_{5,*}^T, u_0, t_5) \\ f^T(x_{6,*}^T, u_1, t_6) \\ \vdots \\ f^T(x_{10,*}^T, u_1, t_{10}) \\ f^T(x_{11,*}^T, u_2, t_{11}) \\ \vdots \\ f^T(x_{5n-1,*}^T, u_{n-1}, t_{5n-1}) \\ f^T(x_{5n,*}^T, u_n, t_{5n}) \end{bmatrix} \quad (5.29)$$

$$U = [u_1^T, \quad u_2^T, \quad \cdots, \quad u_n^T] \quad (5.30)$$

5.2 Formation of optimization problem

The simultaneous solution and optimization algorithm is applied to the following nonlinear optimization problem:

$$\min \phi(x, u). \quad (5.31)$$

Here, the objective function is defined symbolically, the formulation of objective function is described in the Section 5.3.

The process is described by the following differential/algebraic equations:

$$\begin{aligned} \frac{dx}{dt} &= f(x, u; p) \\ y &= g(x, u; p) \end{aligned} \quad (5.32)$$

where, y and u are controlled and manipulated variable vectors, respectively. x is the state variable vector and p is the set of model parameters, which may include disturbances. The orthogonal collocation on finite elements is used to convert the differential equations into an approximating set of algebraic equations. For simplicity of explanation; consider that the prediction horizon of n sampling periods corresponds to n finite elements –one element for each sampling period, as shown in the Figure 4.1. The Control horizon is p sampling periods. x_{ij} is the state vector at the j^{th} collocation point on the i^{th} finite element and u_i is the manipulated variable on the i^{th} finite element. If M collocation points (including two end points) are used on each finite element, the NLP problem can be formulated as shown below:

$$\min_u \sum_{i=1}^n \sum_{j=1}^M w_j \phi \quad (5.33)$$

subject to:

- (i) Model differential equations(A contains the first-derivative weights at the collocation points)

$$A \begin{bmatrix} x_{i1} \\ x_{i2} \\ \vdots \\ x_{iM} \end{bmatrix} = \begin{bmatrix} f(x_{i1}, u_i; p) \\ f(x_{i2}, u_i; p) \\ \vdots \\ f(x_{iM}, u_i; p) \end{bmatrix} \quad i = 1, \dots, n \quad (5.34)$$

Since x_{i1} is known from the estimator or the previous element, the first equation in Eq.(5.34) is redundant and not used as a constraint.

- (ii) Model algebraic equations

$$y_{ij} = g(x_{ij}, u_i; p) \quad i = 1, \dots, n; \quad j = 1, \dots, M \quad (5.35)$$

- (iii) Initial condition and continuity of the state variables

$$\begin{aligned} x_{11} &= \text{initial condition} \\ x_{21} &= x_{1M} \\ &\vdots \\ x_{n1} &= x_{n-1, M} \end{aligned} \quad (5.36)$$

- (iv) Definition of control horizon

$$u_i = u_{i+1} \quad i = p, \dots, n-1 \quad \text{for } n > p \quad (5.37)$$

- (v) Bounds on state variables

$$x_l \leq x_{ij} \leq x_u \quad i = 1, \dots, n; \quad j = 1, \dots, M \quad (5.38)$$

- (vi) Bounds on the outputs

$$y_l \leq y_{ij} \leq y_u \quad i = 1, \dots, n; \quad j = 1, \dots, M \quad (5.39)$$

- (vii) Bounds on manipulated variables

$$u_l \leq u_i \leq u_u \quad i = 1, \dots, n \quad (5.40)$$

(viii) Bounds on changes in the manipulated variables

$$|u_i - u_{i+1}| \leq \Delta u_{\max} \quad i = 1, \dots, p-1 \quad (5.41)$$

The constrained NLP problem is solved using SQP, and the first manipulated move is implemented. This process is repeated at every control interval.

5.3 Feedback

The most common feedback method in MPC is to compare the measured output of the process to the model prediction at time k to generate a disturbance estimate $\hat{d} = y_k - y_k^m$, in which y_k and y_k^m represent the process measurement and model prediction, respectively. The formation of MPC objective function will involve the disturbance term, which is added to the output prediction over the entire prediction horizon. Hence, the modified objective function can be given as:

$$\phi = \sum_{j=0}^{N-1} [y_{ref} - (y_{k+j|k} - \hat{d}_k)]^2 + \sum_{j=0}^{N-1} \mathcal{Q} [\Delta u_{k+j|k}]^2 \quad (5.42)$$

This procedure assumes that the differences observed between the process output and the model prediction are due to additive step disturbances in the output. These disturbance terms are assumed to remain constant over the prediction horizon. This choice of disturbance model offers several practical advantages (Medows and Rawlings, 1997):

- a. It accurately models setpoint changes, which often enter feedback loops as step disturbances.
- b. It approximates slowly varying disturbances. Since errors in the model can appear as slowly varying output disturbances, it provides robustness to model error.
- c. It provides zero offset for step changes in setpoint.

Feedback through the estimation of a step disturbance, coupled with a linear step response model, has been extensively applied in industrial applications. Garcia and Morari (1982) have analyzed the stability and robustness for linear unconstrained systems.

Feedback through differencing model prediction and measurement does not require a state-space description. Linear MPC methods used in the industry do not use state-space model and incorporate the disturbance directly into the MPC objective function. Using a state-space model, conventional MPC feedback can be shown to be a particular form of a state observer for the resulting system:

$$\begin{aligned} x_{k+1} &= f(x_k, u_k) \\ d_{k+1} &= d_k \\ y_k &= g(x_k) + d_k \end{aligned} \quad (5.43)$$

A design of state observer is not considered in the scope of present studies. Inferential calculations are used to obtain the information of the outputs of the system, i.e., top and bottom impurity of the column. The details of inferential calculations of top and bottom impurities as function of states of the system (i.e., tray temperature) are provided in the Section 3.8.

5.4 Ethyl acetate reactive distillation NLMPC results

The NLMPC control algorithm described in previous sections was applied for dual-ended composition control of ethyl acetate reactive distillation column. The previous PI dual-ended composition control results indicated that [L/D, V] configuration provided satisfactory control performance for setpoint tracking as well as unmeasured disturbance rejection. NLMPC was applied using [L/D, V] configuration to determine the benefits in control performance considering the increased complexity of control algorithm using NLMPC. The model development for an ethyl acetate reactive distillation is described in Chapter 3. This model was discretized by means of the orthogonal collocation on finite elements, as described in the Section 5.1.2. This discretized model was used in NLMPC control algorithm. For application of NLMPC to the ethyl acetate reactive distillation column, level controls are not included in the NLMPC controller. PI level controls as discussed in the Section 3.6 are used for the implementation of NLMPC.

5.4.1 Selection of Tuning Parameters

The tuning parameters that have a significant effect on MPC performance are the prediction horizon, control horizon, sampling interval and penalty weight matrices. A set of heuristics based on the linear systems, numerical simulations are normally used to select the final tuning parameters.

- a. Sampling Interval: For stable, minimum phase systems, stability does not depend on sampling interval. To ensure good closed-loop performance, the sampling

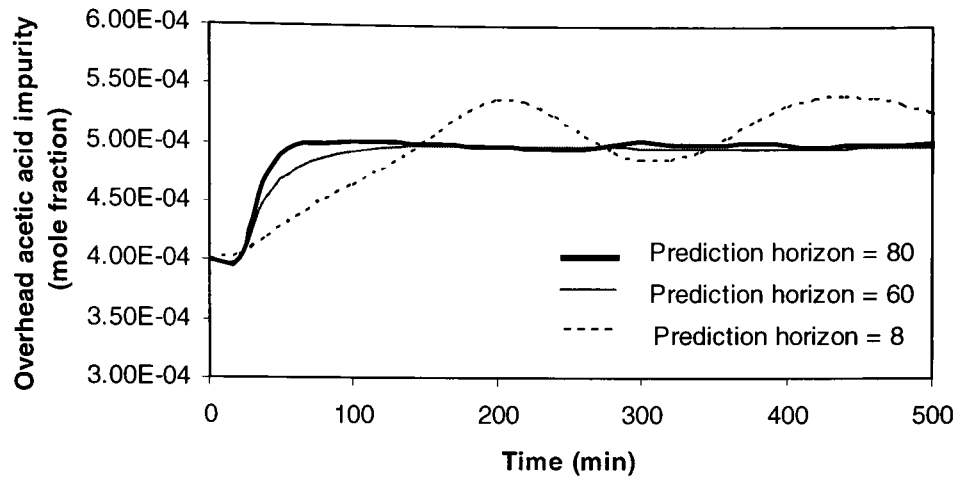
interval should be small enough to capture adequately dynamics of the process, yet large enough to permit the online computations necessary for implementation.. Marlin (1995) has provided a general rule that the control interval should be selected such that

$$\Delta t \leq 0.05(\theta_p + \tau_p) \quad (5.44)$$

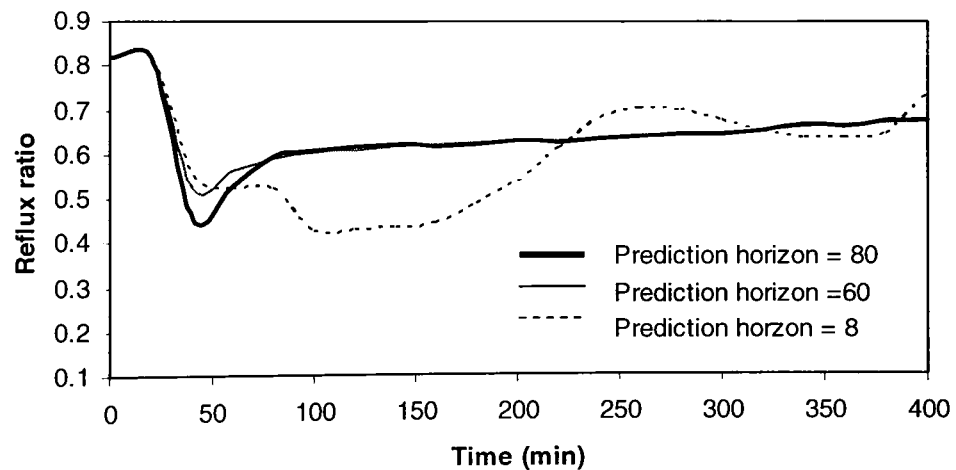
to obtain control performance approaching that of continuous control for which θ_p and τ_p are the first order plus deadtime (FOPDT) model parameters of the process. An ethyl acetate reactive distillation column under consideration exhibits a very large open loop time constant over 500 minutes. Hence, the sampling interval or control interval was chosen as 20 minutes, which satisfies the criteria described in the Equation (5.44). The same control interval was used for dual-ended PI controller results.

- b. Prediction Horizon: For linear systems, the choice of prediction horizon is normally decided by the time for steady state. The literature provides selection criteria for prediction horizon that assures the closed-loop stability. For nonlinear systems, there is no definite selection criteria provided. Hence, the simulation results are normally used for determination of prediction horizon for NLMPC. With simultaneous solution and optimization approach, the increase in size of prediction horizon increases the size of constrained nonlinear optimization problem. Hence, the advantages of longer horizons are outweighed by the increase in computations required.

In order to select the appropriate value for the prediction horizon, closed loop simulations were carried out for setpoint change in overhead impurity. The



(a) Overhead acetic acid impurity



(b) Manipulated variable for overhead composition loop

Figure 5.3 Effect of the prediction horizon on NLMPC performance

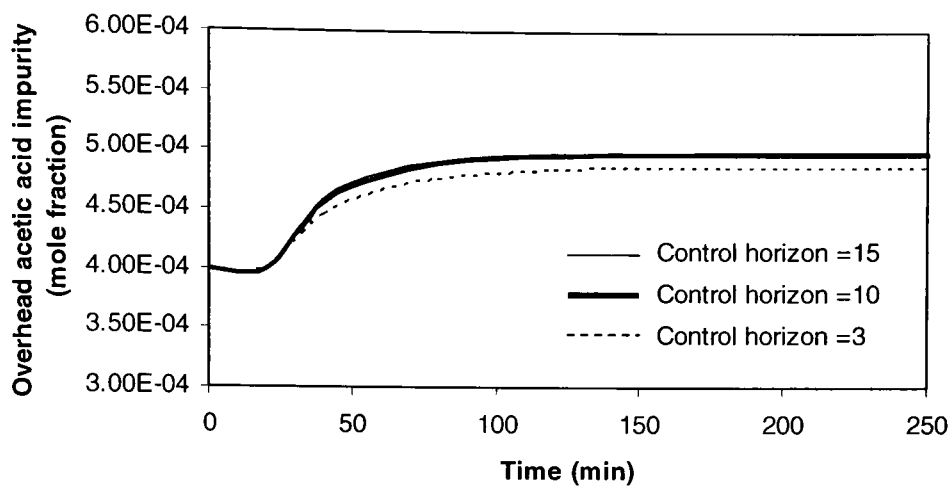
performance of primary controlled variable i.e. overhead acetic acid impurity was observed to determine the value of the prediction horizon. It was observed that small values of prediction horizon show oscillatory or unstable responses. Figure 5.3 shows that the prediction horizon of 80 sample interval provide satisfactory control performance.

- c. Control Horizon: Linear systems results indicate that shortening the control horizon relative to the prediction horizon tends to produce less aggressive control actions, less sensitivity to disturbances (Garcia and Morari, 1982). For nonlinear systems, the selection of control horizon issue has not been discussed in the literature. Hence, simulation results are used for determination of control horizon.

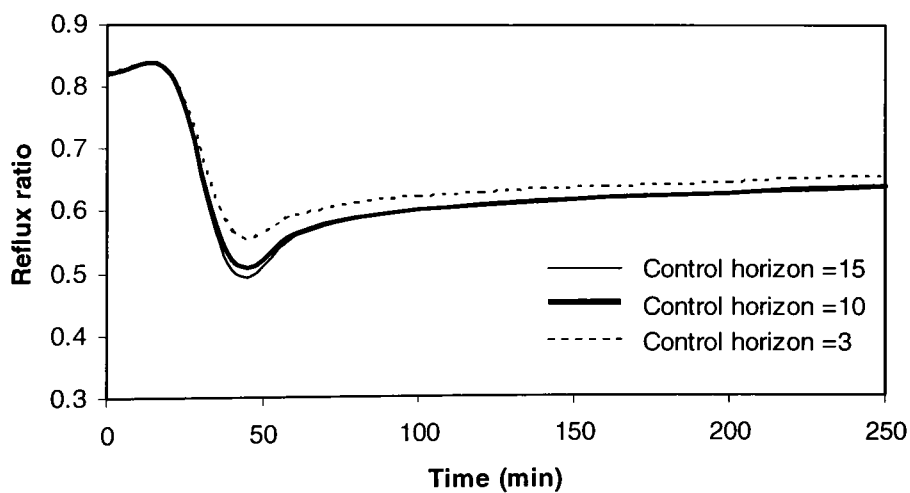
Figure 5.4 shows the effect of varying control horizon length on the closed loop performance of NLMPC for overhead impurity setpoint change. The prediction horizon was selected as 80 sample intervals. Shorter control horizon provide sluggish control response for overhead impurity setpoint tracking. It was observed that after certain value of control horizon length, the improvement in control performance was not significant to justify the additional computational efforts required for higher value of control horizon. Hence, the control horizon value of 10 sample intervals was selected.

Secondly, the value of control horizon normally decides the number of degrees of freedom for the optimization problem that is solved at each sample interval. The computational effort for the optimization problem increases with number of degrees of

freedom, hence computational effort might provide some limitations for selection of control horizon. The generalized algorithm described



(a) Overhead acetic acid impurity



(b) Manipulated variable for overhead composition loop

Figure 5.4 Effect of control horizon on NLMPC performance

in the Section 5.2 shows that value of control inputs are taken as piece wise constant functions. In such case, if the value of the control horizon was chosen as 'm' sample interval, then optimization problem will have ' $m \times$ number of manipulated variables' as degrees of freedom. However, instead of considering each sample time as a equally spaced node for manipulated or input variable, one can chose fewer number of unequally spaced nodes for manipulated variables over the control horizon. The optimization problem is solved to determine the values of input variables at these fewer number of nodes. Then the values of input variables at each sample interval can be determined by interpolation. This approach is expected to improve the computational efficiency to some extent. The simulation results were used to assess the benefits of above approach.

Figure 5.5 shows the computational time versus number of nodes considered for optimization. The computational time on the y-axis is normalized with respect to the computational time while considering all equally spaced nodes for each sample interval. The figure shows the results for the case for which the control horizon was chosen as 12 sample interval. The control input profile over the 12 sample interval was discretized by means of unequally spaced fewer number of nodes for control input. The optimization was carried out for determining the values of input variables at those node values. It was observed that around 20% improvement in the computational requirement can be achieved by considering a smaller number of unequally spaced nodes for optimization.

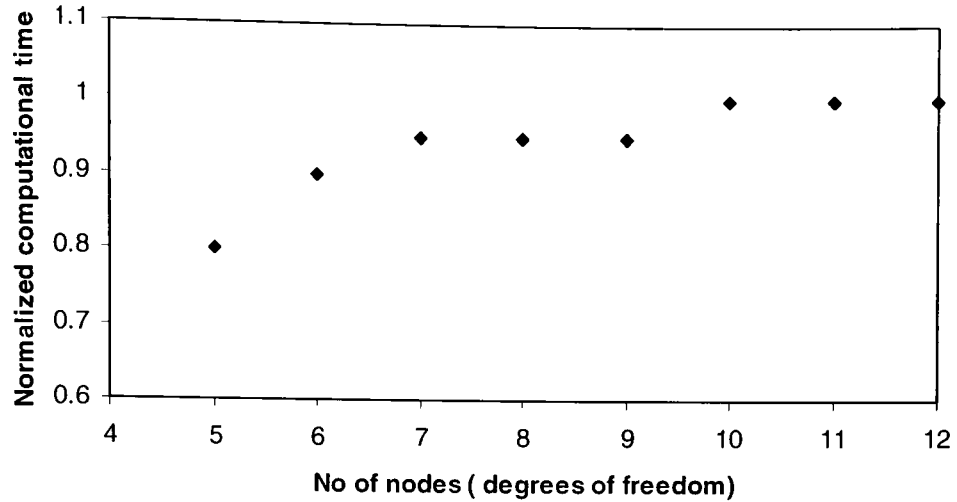
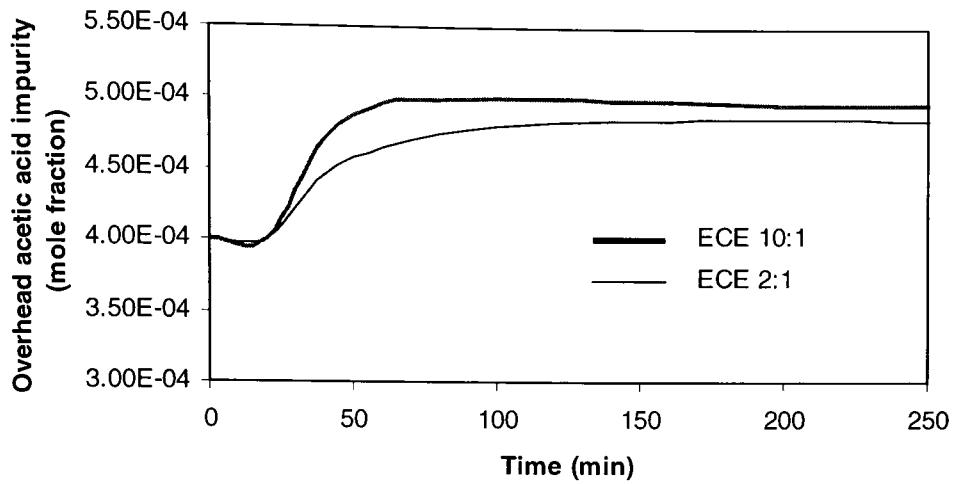


Figure 5.5: Effect of number of degrees of freedom on computational time for optimization

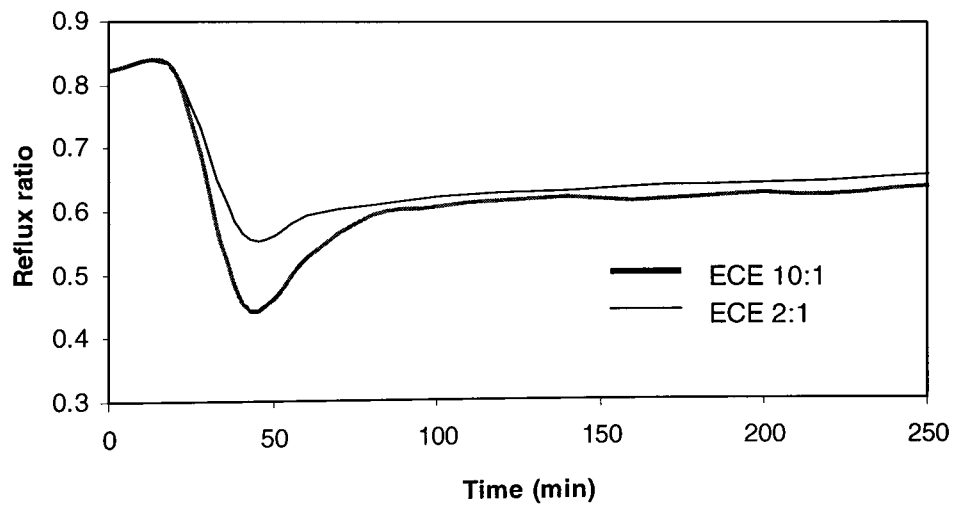
- d. Equal concern error: For MIMO control, the controlled variables may have different magnitudes as well as different engineering units. Moreover, from a control point of view, some variables have more priority than the others. The equal concerned errors are used to normalize the engineering unit values and prioritize the controlled variables.

In ethyl acetate reactive distillation the primary control objective was to control the overhead acetic acid impurity. Hence, in objective function for nonlinear optimization appropriate weights need to be provided for overhead and bottom impurities. To determine the appropriate value of equal concerned errors, closed loop simulations were performed for overhead impurity setpoint change. The prediction horizon of 80 and the control horizon of 10 sample interval was

chosen for these simulations. Equal concerned error ratio of 10:1 corresponding to normalized values of controlled variables showed satisfactory performance.



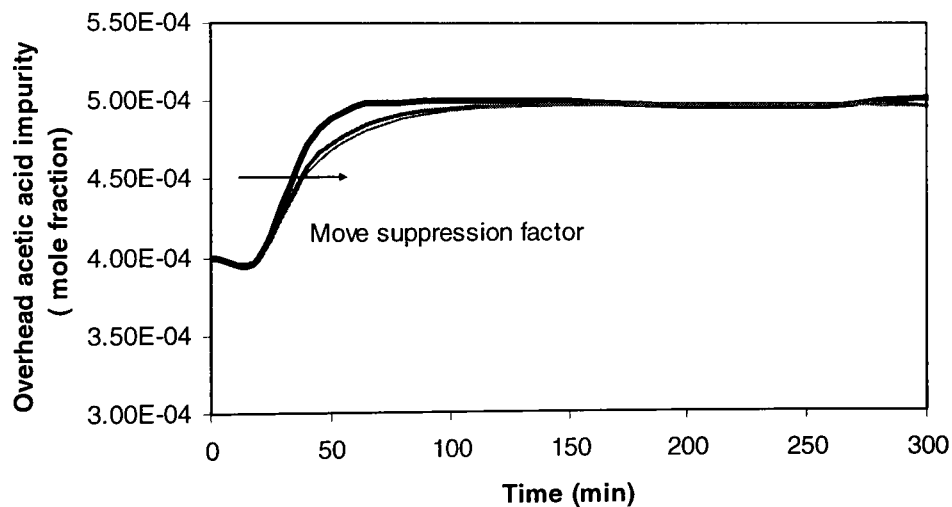
(a) Overhead acetic acid impurity



(b) Manipulated variable for overhead composition loop

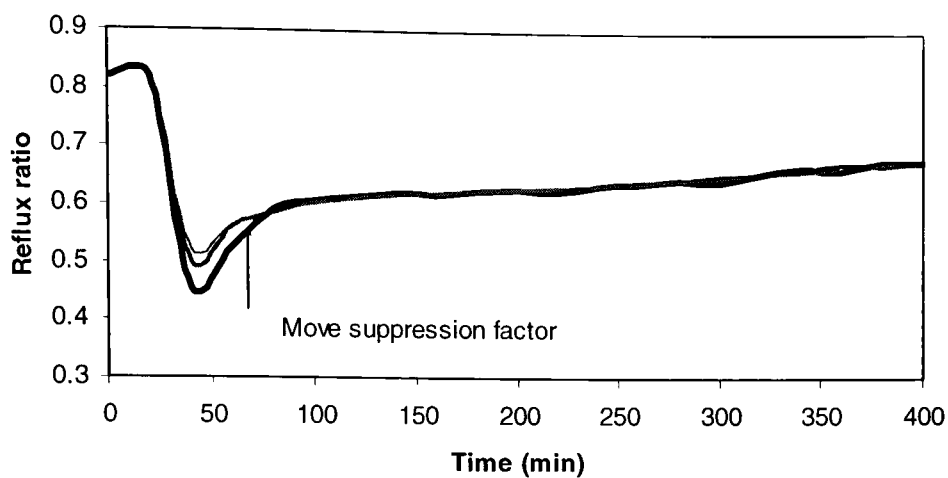
Figure 5.6 Effect of equal concern error (ECE) on NLMPC performance

- e. Move suppression factor: Move suppression factors are used to adjust the aggressiveness of the MPC controller with respect to each manipulated variable. Move suppression factors are analogous to the detuning factor used in PI control. After weighting is set based on product importance, move suppression factors are adjusted to select the aggressiveness of the controller tuning. Minimum IAE for setpoint changes described for tuning PI control was used as the criteria for determining the optimal move suppression factors for NLMPC. Figure 5.4 shows the effect of move suppression factor for the setpoint change for overhead composition loop.



(a) Controlled variable for overhead composition loop

Figure 5.7 Effect of move suppression factor on NLMPC performance for overhead impurity set point tracking.



(b) Manipulated variable for overhead composition loop

Figure 5.7 Effect of move suppression factor on NLMPC performance for overhead impurity set point tracking.

Table 5.1 Tuning parameters for NLMPC with perfect model

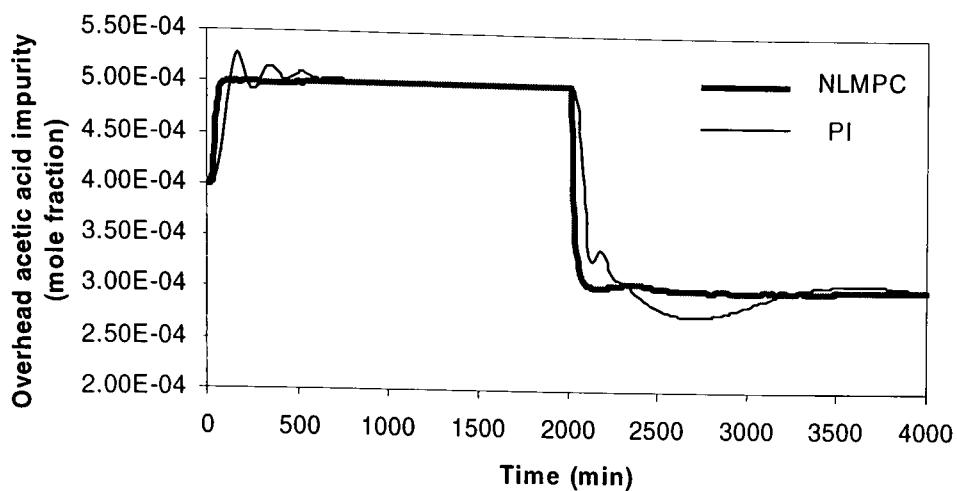
Prediction Horizon	80
Control Horizon	10
Equal concern error (Overhead Impurity: Bottom impurity)	10:1
Move suppression factor	
Overhead manipulated variable	0.03
Bottom manipulated variable	0.05

5.4.2 Setpoint tracking results for NLMPC

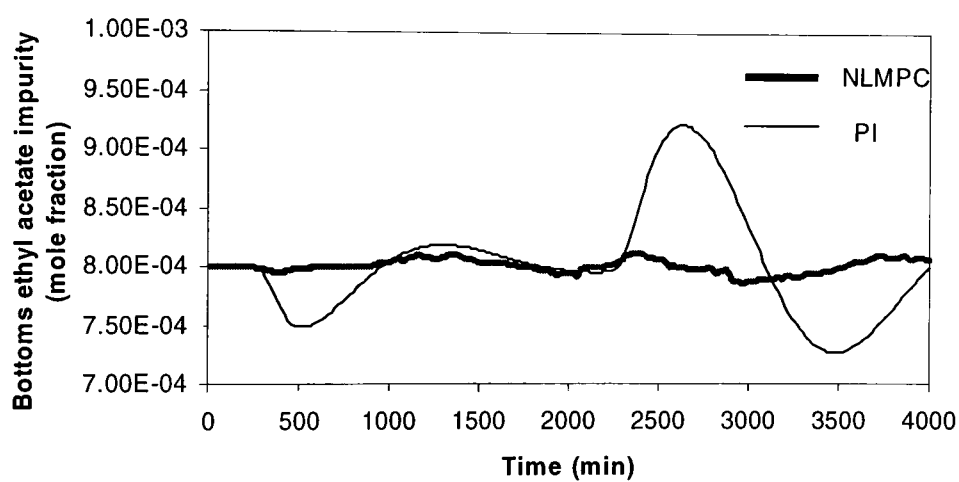
Step changes in setpoints (see chapter 4) were used to determine move suppression factors which minimized the IAE. Table 5.2 shows the IAE for NLMPC and PI for an overhead impurity setpoint change. Figure 5.8 (a) to (d) shows the dynamic responses of the controlled variables and manipulated variables for the setpoint tracking test.

Table 5.2 Ethyl acetate NLMPC control performance indices for overhead impurity setpoint tracking.

Configuration	Overhead loop IAE	Bottoms loop IAE
[L/D,V] NLMPC	0.91	2.14
[L/D, V] PI	2.41	6.84

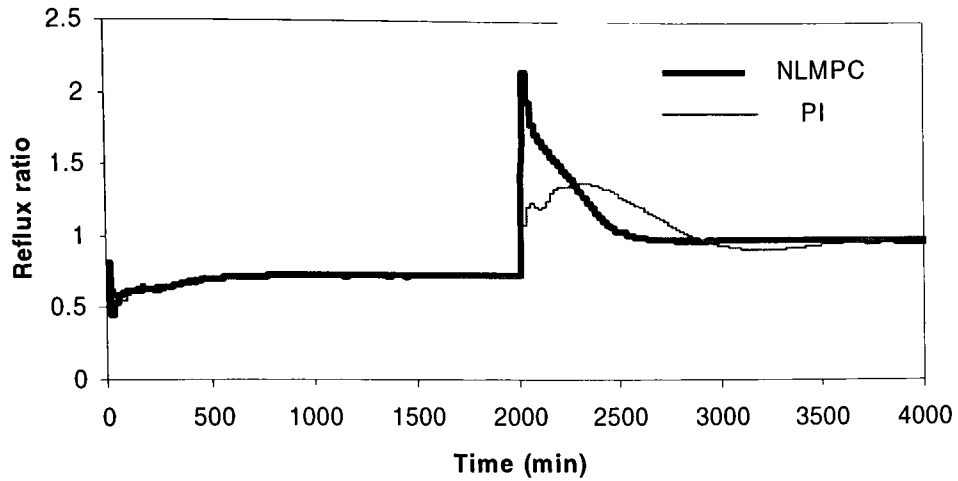


(a) Overhead acetic acid impurity

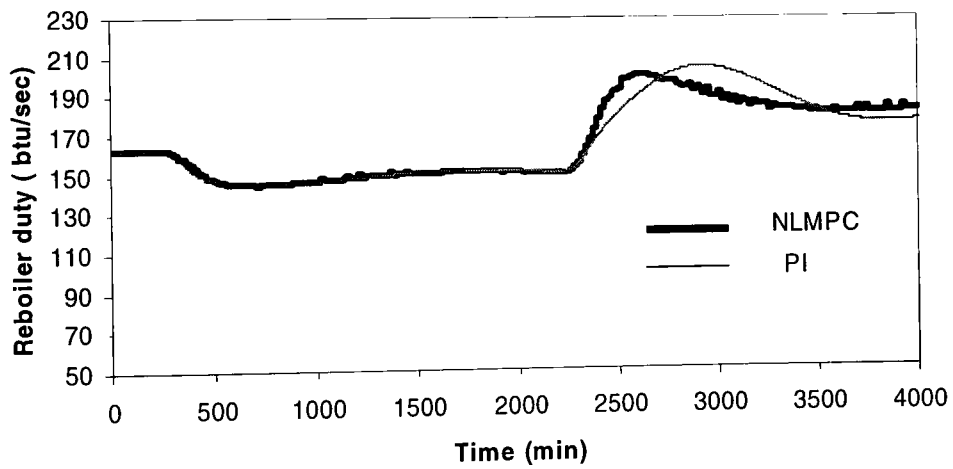


(b) Bottoms ethyl acetate impurity

Figure 5.8 Comparison of NLMPC and PI controller for dual-ended composition control for overhead impurity setpoint tracking.



(c) Manipulated variable for overhead composition loop



(d) Manipulated variable for bottoms composition loop

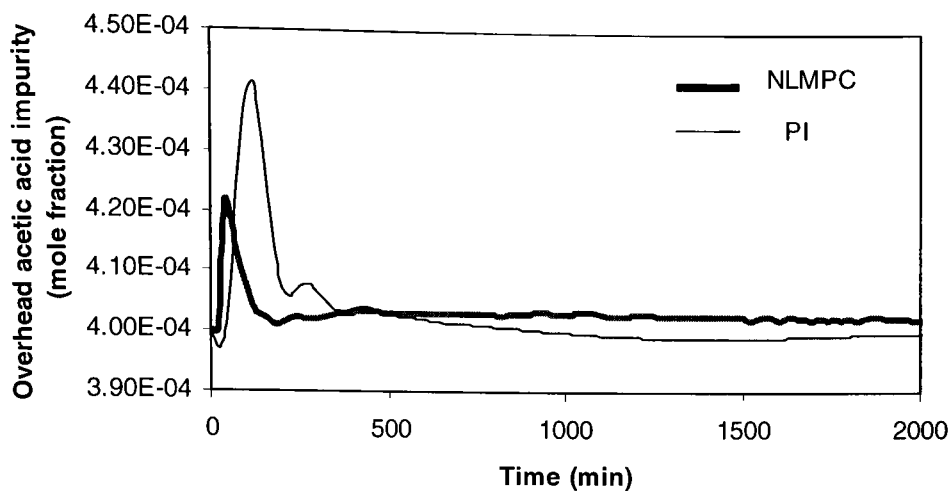
Figure 5.8 Comparison of NLMPC and PI controller for dual-ended composition control for overhead impurity setpoint tracking.

5.4.3 Unmeasured feed rate disturbance rejection

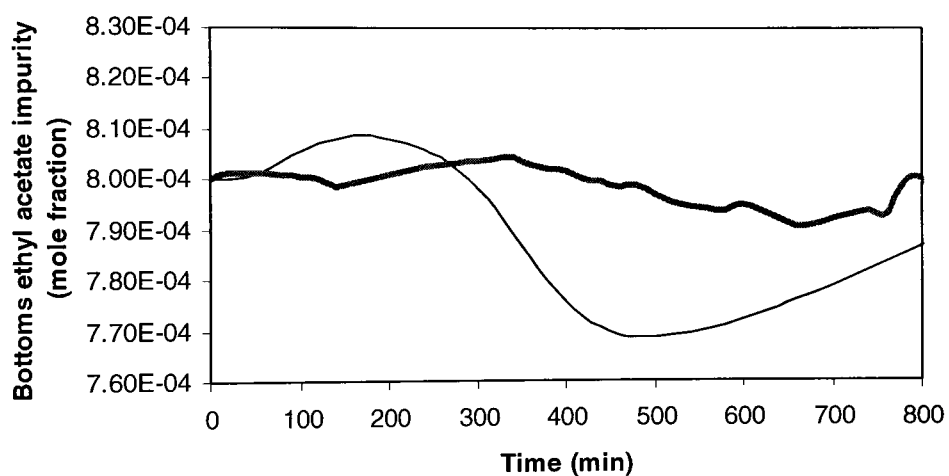
Feed disturbance rejection capabilities of NLMPC were tested by introducing a 25% step change in recycle feed flow. The test was the same used for PI feed rate step disturbance testing. The feed disturbance was considered unmeasured and not modeled in the NLMPC controller. The IAE control performance indices for ethyl acetate reactive column calculated over 2000 minutes of closed-loop response for unmeasured disturbance rejection test are given in the Table 4.2. Figure 4.6 (a) to (d) shows selected responses for controlled variables and manipulated variables for different control configurations.

Table 5.3 Ethyl acetate NLMPC control performance indices for unmeasured feed rate disturbance rejection

Configuration	Overhead loop IAE	Bottoms loop IAE
[L/D,V] NLMPC	0.188	0.462
[L/D, V] PI	0.422	1.271

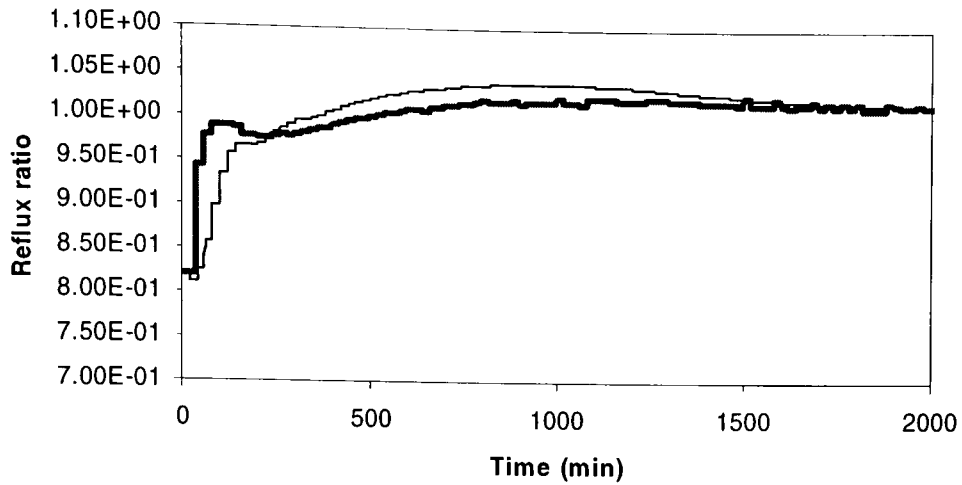


(a) Overhead acetic acid impurity

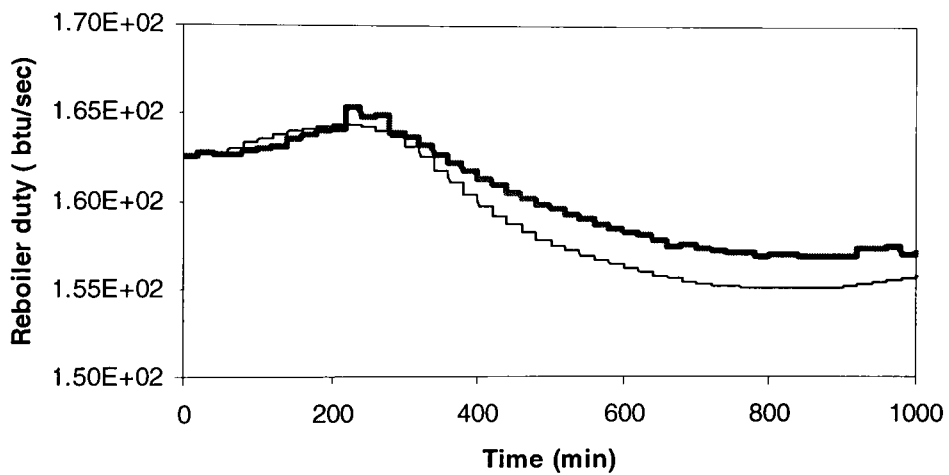


(b) Bottoms ethyl acetate impurity

Figure 5.9 Comparison between NLMPC and PI controllers for dual-ended composition control for unmeasured feed rate disturbance rejection



(c) Manipulated variable for overhead composition loop



(d) Manipulated variable for bottom composition loop

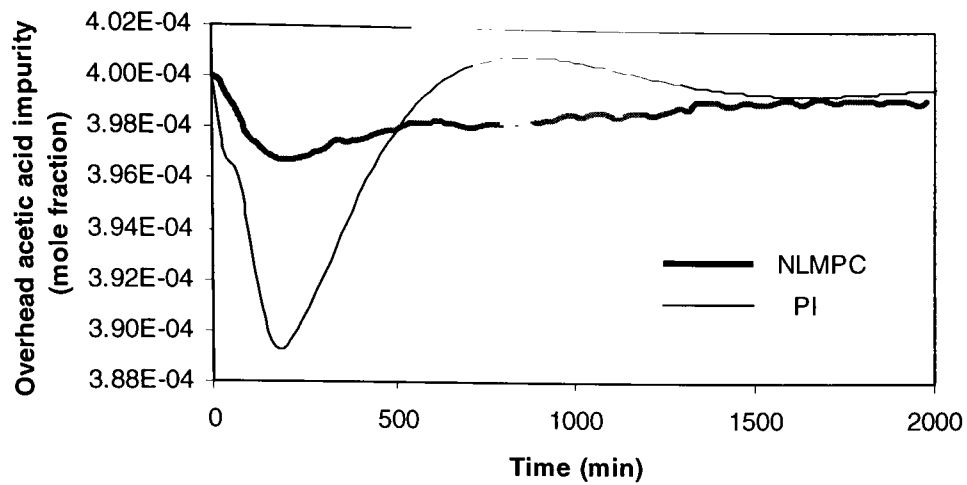
Figure 5.9 Comparison between NLMPC and PI controllers for dual ended composition control for unmeasured feed rate disturbance rejection

5.4.4. Unmeasured feed composition disturbance rejection

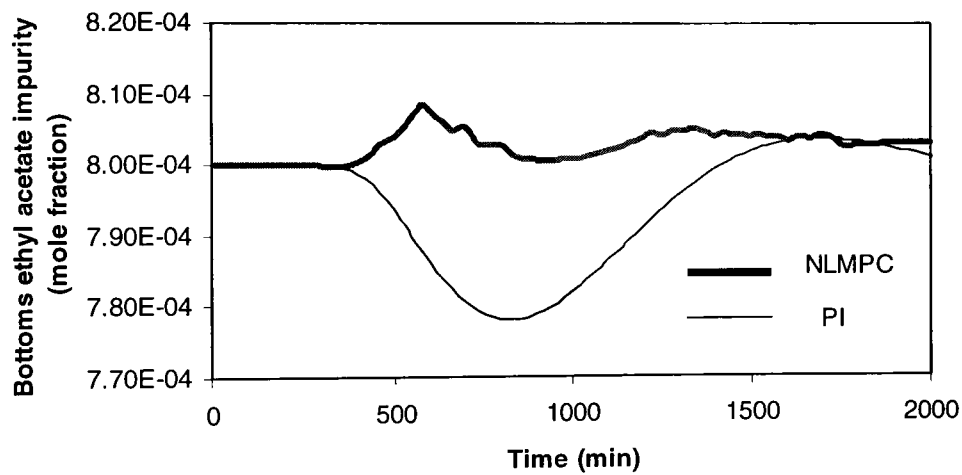
Feed composition disturbance rejection capabilities of NLMPC were tested using a composition step change of -10% in the acetic acid feed at $t=10$ minutes. The feed composition disturbance was considered unmeasured and not modeled in the NLMPC controller. The IAE control performance indices for ethyl acetate reactive column calculated over 2000 minutes of closed-loop response for unmeasured feed composition disturbance rejection tests are given in Table 5.4. Figure 5.10 (a) to (d) shows responses for controlled variable and manipulated variables.

Table 5.4 Ethyl acetate NLMPC control performance indices for unmeasured feed composition disturbance rejection

Configuration	Overhead loop IAE	Bottoms loop IAE
[L/D,V] NLMPC	0.117	0.331
[L/D, V] PI	0.247	0.866

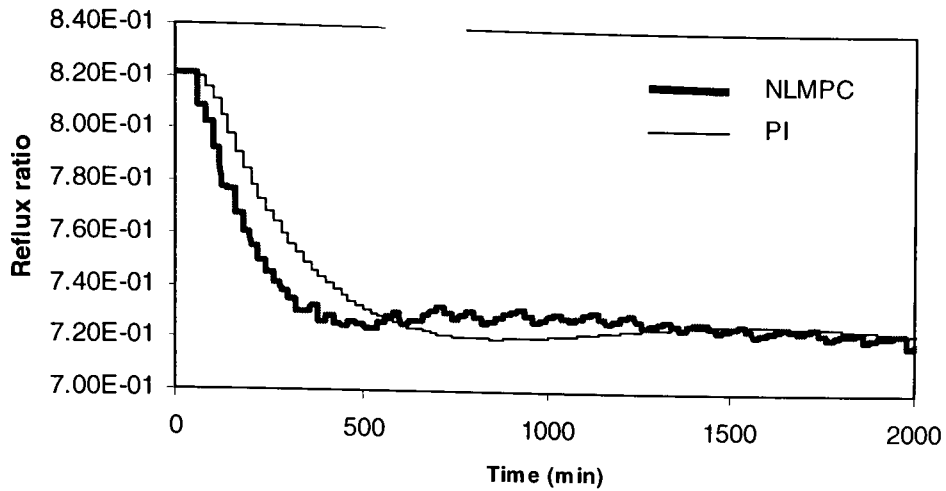


(a) Overhead acetic acid impurity

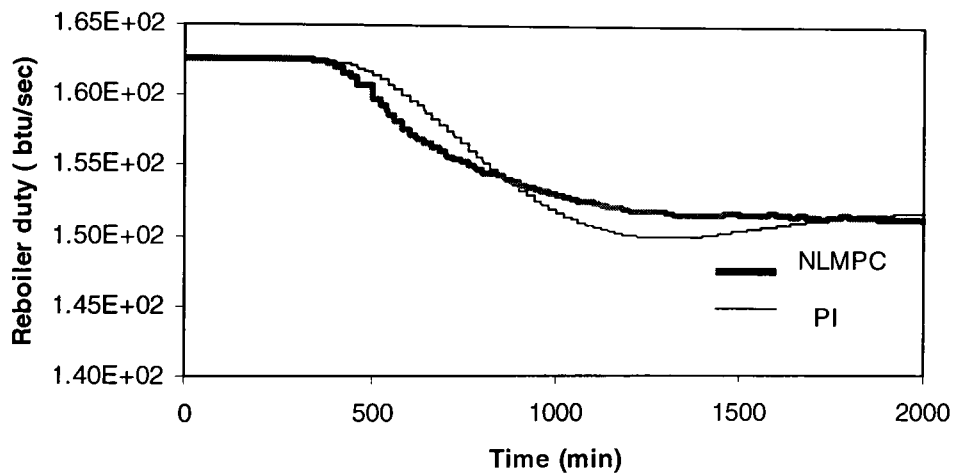


(b) Bottoms ethyl acetate impurity

Figure 5.10 Comparison between NLMPC and PI controllers for dual-ended composition control for unmeasured feed composition disturbance rejection



(c) Manipulated variable for overhead composition loop



(d) Manipulated variable for bottom composition loop

Figure 5.10 Comparison between NLMPC and PI controllers for dual-ended composition control for unmeasured feed composition disturbance rejection

5.4.5 Effect of model mismatch on NLMPC performance

The NLMPC algorithm incorporates the nonlinear mathematical model of the process. The mathematical model developed for the plant process never be perfectly accurate. For example, there is some level of uncertainty involved in the determination of kinetic or thermodynamic parameters used for the model development. Hence, these parameters like rate constants, equilibrium constants, and tray efficiency will be a source of model mismatch between model and actual plant. Secondly, the models might not be updated with respect to changes in certain characteristics of the plant. For example, catalyst deactivation over a time period can change some of the kinetic parameters of the system. This will cause the process-model mismatch.

The ability of NLMPC to handle the model mismatch was tested by using inaccurate model in terms of the reaction equilibrium rate constant. A 5% and 25% difference in the equilibrium constant values were used to test the effect of process / model mismatch.

5.4.5.1. Effect of process / model mismatch on tuning of NLMPC

An Ethyl acetate reactive distillation process is highly nonlinear. Hence, process/model mismatch causes larger deviations in the manipulated values in order to keep the plant controlled variables at their setpoint. This indicates that there may be a need for retune the NLMPC controller in presence of process/model mismatch. It is advisable to tune the controller for higher magnitude of model mismatch.

The introduction of error in equilibrium reaction constant caused no significant difference in open loop time constant for the system. Hence, the value of the prediction

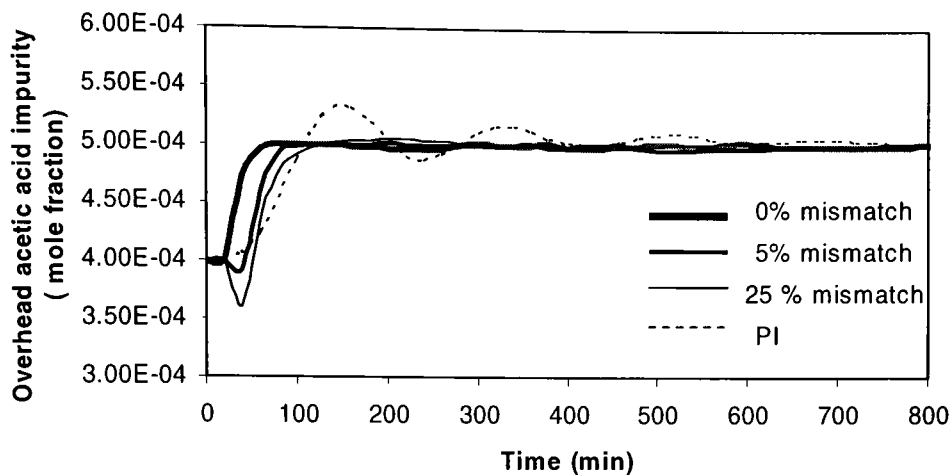
horizon was not expected to vary much. Closed loop simulations were carried out as discussed in 5.4.1 to determine the value of the prediction horizon. The prediction horizon of 80 sample times was selected for NLMPC in presence of process/model mismatch. In similar fashion the control horizon was selected as 15 sample interval. The equal concerned error (ECE) was kept 10:1 same as the case without any model mismatch. The model mismatch causes the changes in manipulated variables of the model from their corresponding values in the plant. This causes the deviation in the controlled variables from their desired setpoints. Move suppression factor adjusts the aggressive ness of the controller. Hence, for the reactive distillation control in presence of model mismatch, move suppression values were increased to 0.045 for overhead composition loop and 0.055 for bottom composition loop.

Table 5.5 Tuning parameters for NLMPC with 25% process/model mismatch

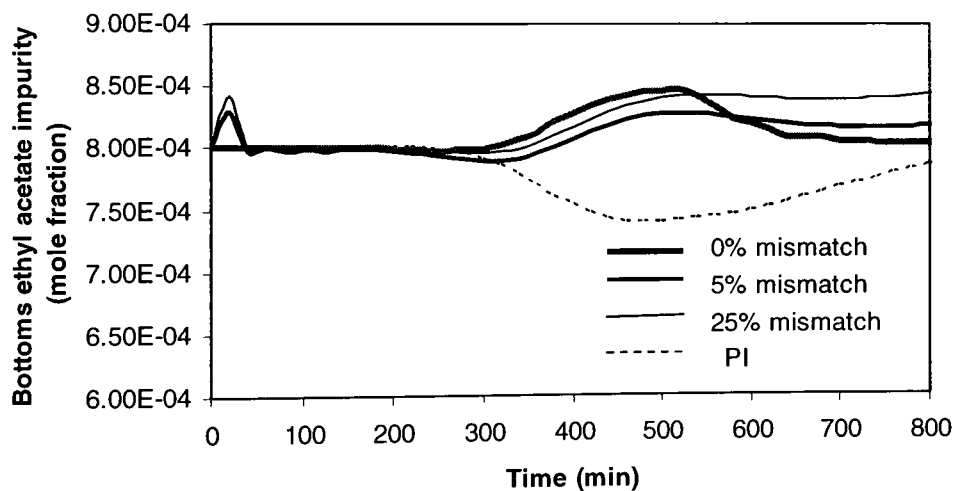
Prediction Horizon	80
Control Horizon	15
Equal concern error (Overhead Impurity: Bottom impurity)	10:1
Move suppression factor	
Overhead manipulated variable	0.045
Bottom manipulated variable	0.055

Figure 5.11 (a) to (d) shows the effect of model mismatch for overhead impurity setpoint tracking. Figure 5.12 (a) to (d) shows the effect of model mismatch for feed

composition disturbance rejection. Results of Figure 5.11, Figure 5.12 and Figure 5.13 show that the NLMPC can handle the process-model mismatch in satisfactory way.

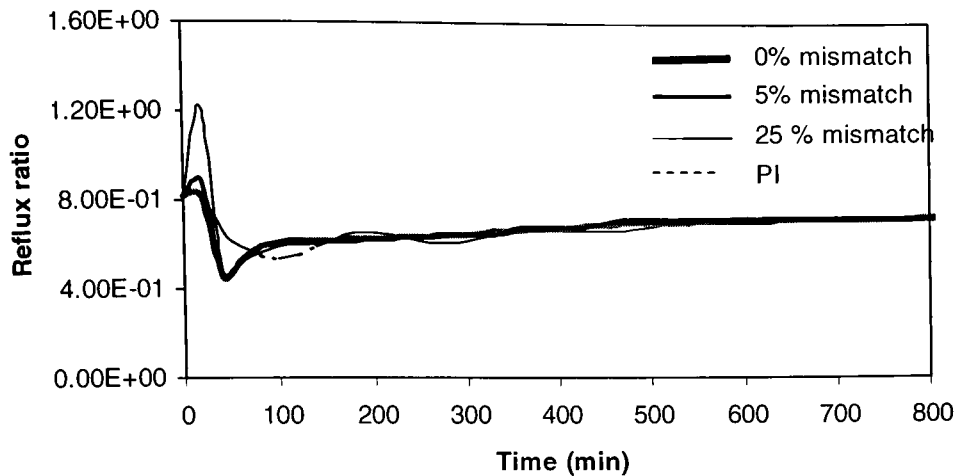


(a) Overhead acetic acid impurity

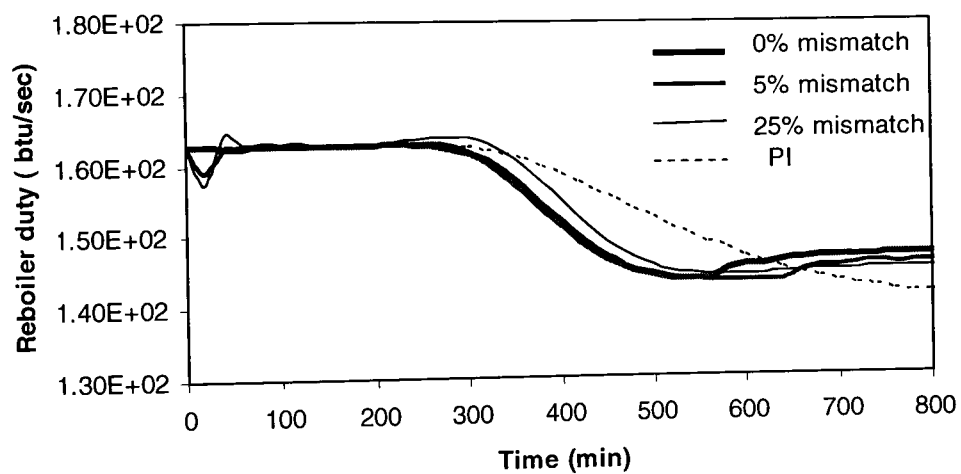


(b) Bottoms ethyl acetate impurity

Figure 5.11 Effect of model mismatch on the closed-loop performance of NLMPC for overhead impurity setpoint tracking (% mismatch correspond to % error in the value of equilibrium constant for esterification reaction for the model and the plant.)

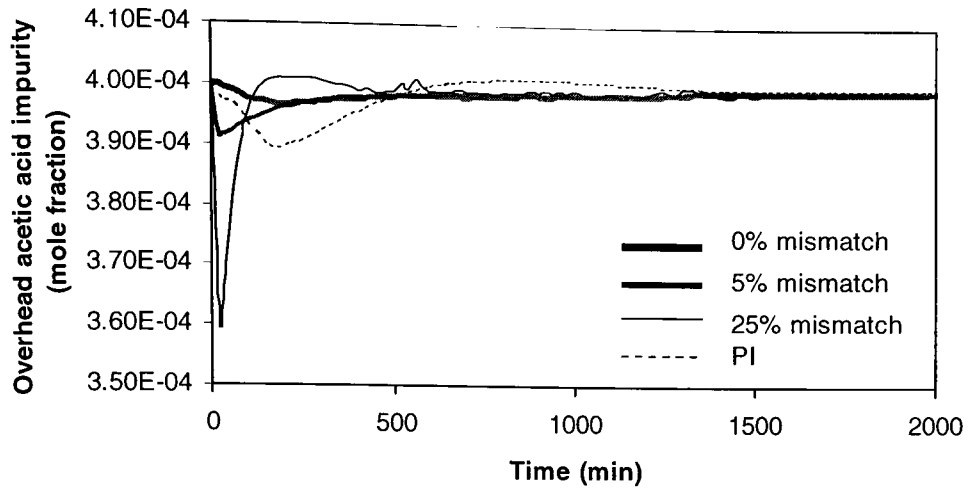


(c) Manipulated variable for overhead composition loop

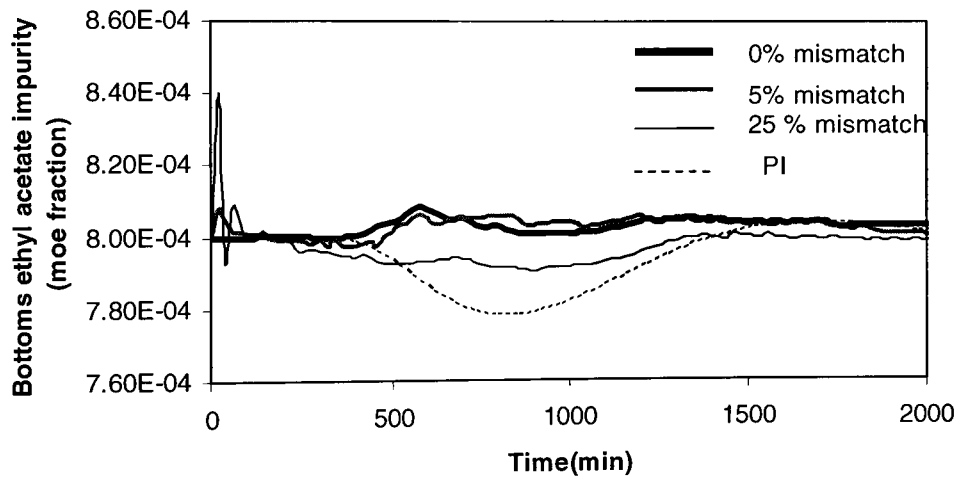


(d) Manipulated variable for bottom composition loop

Figure 5.11 Effect of model mismatch on the closed-loop performance of NLMPC for overhead impurity setpoint tracking

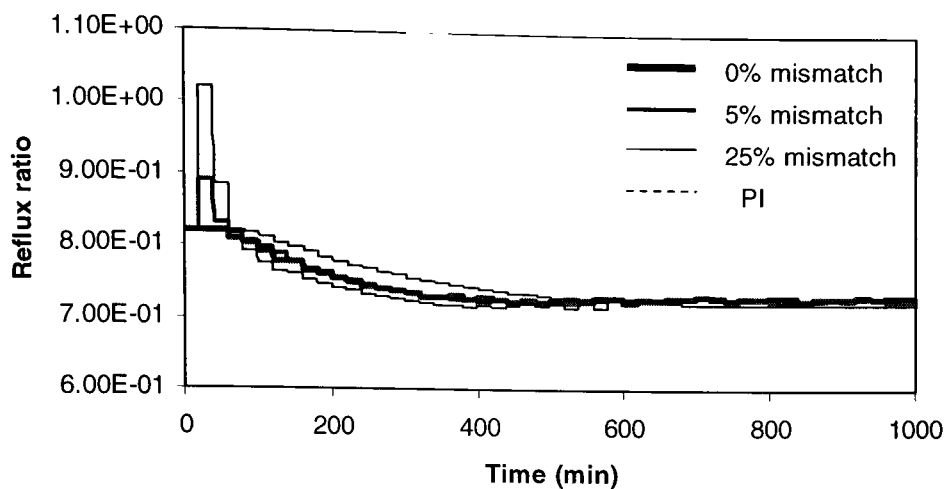


(a) Overhead acetic acid impurity

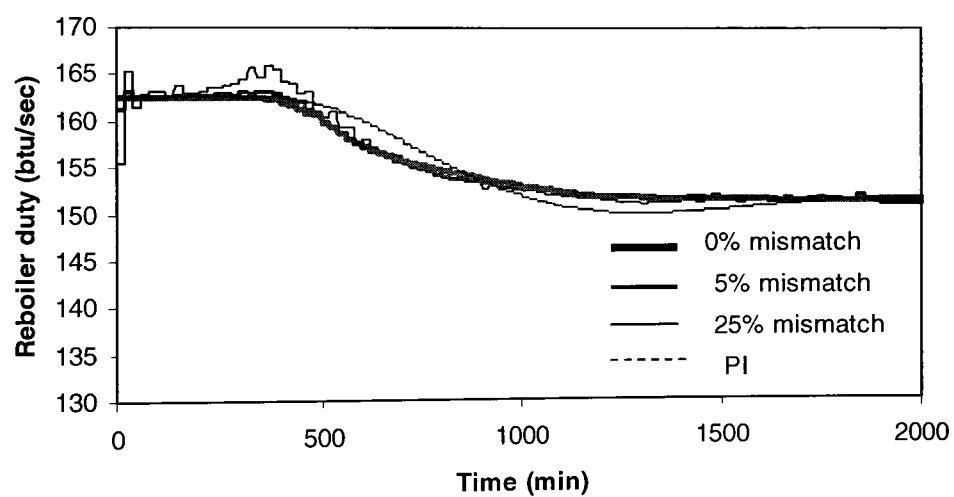


(b) Bottoms ethyl acetate impurity

Figure 5.12 Effect of model mismatch on closed-loop performance of NLMPC for unmeasured feed composition disturbance.

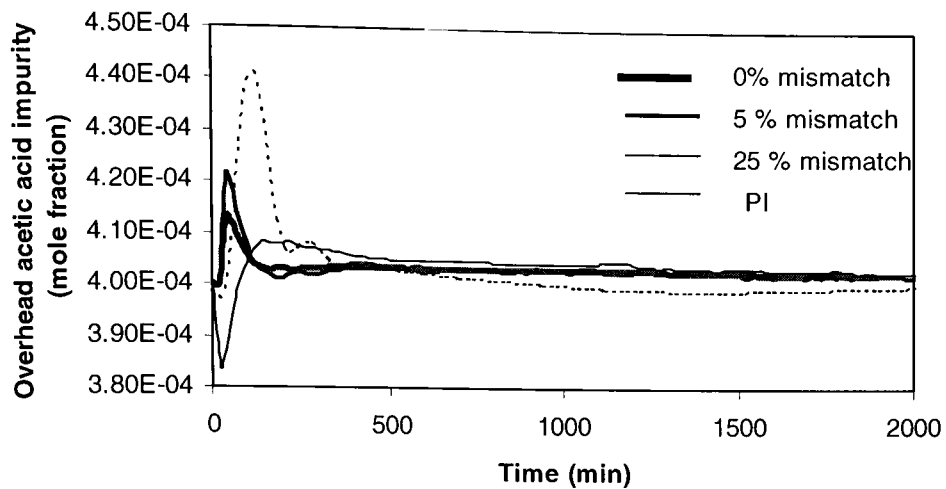


(c) Manipulated variable for overhead composition loop

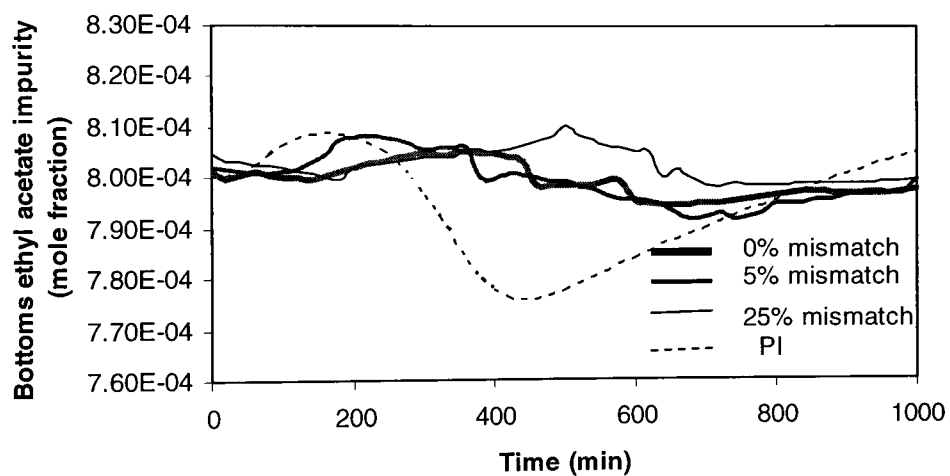


(d) Manipulated variable for bottom composition loop

Figure 5.12 Effect of model mismatch on closed-loop performance of NLMPC for unmeasured feed composition disturbance

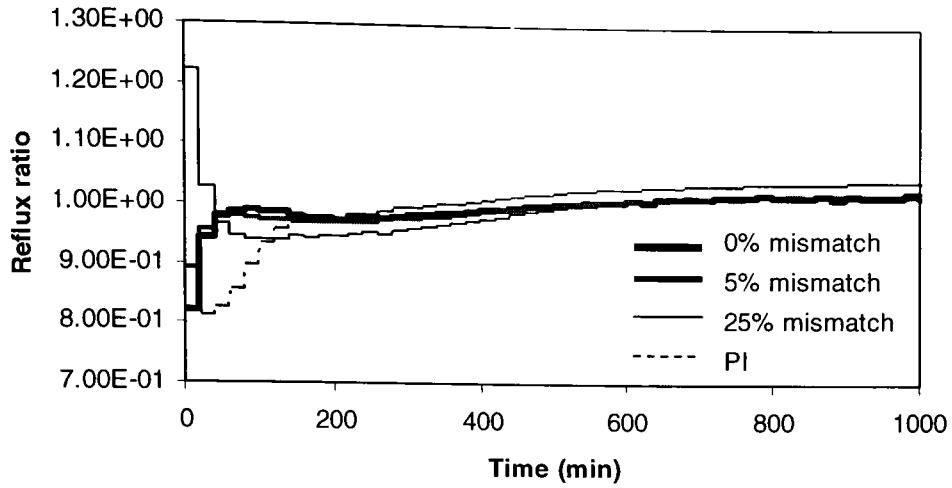


(a) Overhead acetic acid impurity

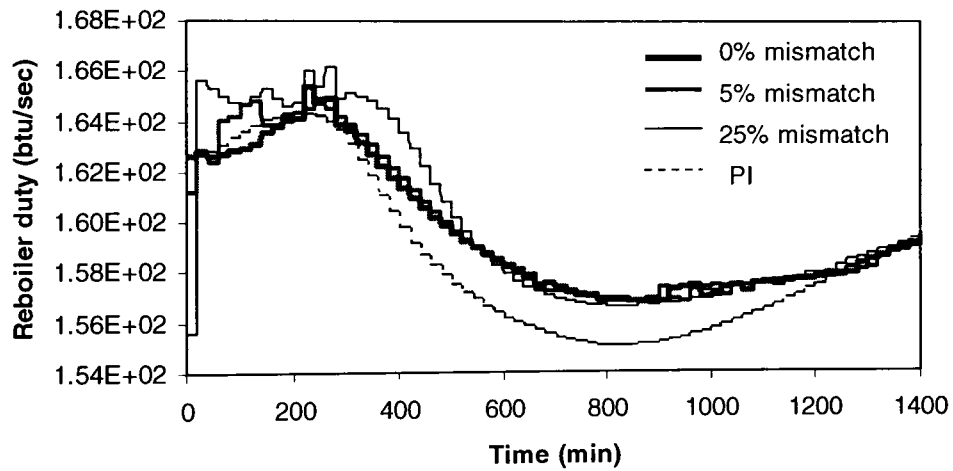


(b) Bottom ethyl acetate impurity

Figure 5.13 Effect of model mismatch on closed-loop performance of NLMPC for unmeasured feed rate disturbance



(c) Manipulated variable for overhead composition loop



(d) Manipulated variable for bottom composition loop

Figure 5.13 Effect of model mismatch on closed-loop performance of NLMPC for unmeasured feed rate disturbance

The IAE performance indices for overhead setpoint tracking, unmeasured feed rate disturbance rejection and unmeasured feed composition disturbance rejection are given in Table 5.6, Table 5.7, and Table 5.8, respectively. The IAE for overhead setpoint tracking is determined for closed loop simulation of 800 minutes and IAE for disturbance rejection tests are determined for closed-loop simulation of 2000 minutes.

Table 5.6 Effect of model mismatch on NLMPC control performance indices for overhead impurity setpoint tracking

Configuration	Overhead loop IAE	Bottoms loop IAE
[L/D,V] PI	0.855	1.248
[L/D, V] NLMPC- Perfect model	0.325	0.621
[L/D, V] NLMPC- 5% mismatch	0.468	0.6388
[L/D, V] NLMPC- 25% mismatch	0.588	1.0459

Table 5.7 Effect of model-mismatch on NLMPC control performance indices for unmeasured feed rate disturbance rejection

Configuration	Overhead loop IAE	Bottoms loop IAE
[L/D,V] PI	0.422	1.271
[L/D, V] NLMPC- Perfect model	0.188	0.462
[L/D, V] NLMPC- 5% mismatch	0.381	0.739
[L/D, V] NLMPC- 25% mismatch	0.541	1.104

Table 5.8 Effect of model-mismatch on NLMPC control performance indices for unmeasured feed composition disturbance rejection

Configuration	Overhead loop IAE	Bottoms loop IAE
[L/D,V] PI	0.247	0.866
[L/D, V] NLMPC- Perfect model	0.117	0.331
[L/D, V] NLMPC- 5% mismatch	0.213	0.393
[L/D, V] NLMPC- 25% mismatch	0.324	0.514

5.5 Discussion of results

The application of NLMPC using the [L/D, V] configuration for the control of the ethyl acetate reactive distillation column is discussed in this chapter. Section 5.4.1 describes the effect of the tuning parameters on the closed-loop performance of NLMPC. Figure 5.3 shows that using a longer prediction horizon was necessary for stability and performance of NLMPC. The control horizon determine the number of manipulated moves in the future to be calculated by the optimization algorithm at each control interval. Hence, the control horizon determines the number of degrees of freedom for the optimization problem. The choice of the control horizon was based on the closed loop performance and computational requirements for solving the optimization problem. The equal concern errors prioritize the controlled variable for the MIMO control system. For ethyl acetate reactive distillation, the primary control objective was to control the overhead acetic acid impurity. Hence, values of equal concern errors were determined such that the primary controlled objective is satisfied. The values of move suppression factors were determined by minimizing the IAE for overhead impurity setpoint changes.

The closed-loop performance of NLMPC was shown to be superior for overhead impurity setpoint tracking compared to dual-ended PI composition control. The feed rate disturbance as well as the feed composition disturbance were used to assess the performance of NLMPC in presence of unmeasured disturbances. Figure 5.9 and 5.10 show that NLMPC was able to handle the unmeasured disturbances with less deviation from the setpoint and faster settling time than the PI controller..

Each of the closed-loop dynamic responses for the NLMPC controller have shown small fluctuations over the duration of the simulation. This might be attributed to the accuracy tolerance for the nonlinear optimizer. Moreover, around 25% of the gradient information for the optimizer was obtained thorough finite difference approximations. Gill (1998) has pointed out that the accuracy and reliability of nonlinear optimization decreases with the use of finite difference approximations for gradient information.

The ability of NLMPC to handle the model mismatch was tested by introducing errors in the reaction equilibrium constant. The process-model mismatch of 5% and 25% difference in the equilibrium constant values were used. It was observed that the presence of process-model mismatch lead to retune the NLMPC controller. The NLMPC controller was tuned for 25 % model mismatch, case which ensures the tuning for a larger magnitude of process-model mismatch. As the presence of model mismatch caused no significant difference in the open-loop time constant for reactive distillation system, the value of prediction horizon used in case of perfect model case was not changed. However, a larger value of the control horizon was used for the application of

NLMPC with model mismatch case to obtain the satisfactory closed loop performance. Due to the highly nonlinear nature of the reactive distillation system, the model mismatch caused deviations in the manipulated variables in order to keep the plant at desired setpoints. It was observed that in the case of 25% model mismatch, the controlled variables show large deviation from setpoints before returning sluggishly to the desired setpoints as shown in the Figure 5.12 (d). The NLMPC control performance for overhead impurity setpoint tracking as well as unmeasured disturbance rejection has shown the ability of NLMPC to handle the process-model mismatch.

The improved control performance for NLMPC was obtained by using much more complicated algorithm and requiring more computational effort compared to a conventional PI controller. Efforts were made to reduce the computational burden of NLMPC algorithm. Some suggestions in this area are provided in Chapter 6.

CHAPTER 6

CONCLUSIONS AND RECOMMENDATIONS

6.1 Conclusions

Reactive distillation combines both separation and reaction in one unit. Control of reactive distillation is a challenging problem due to process nonlinearity, complex interactions between vapor-liquid equilibrium and chemical kinetics. The presence of multiple steady states and the highly nonlinear nature of reactive distillation may impose limitations on use of linear controllers. Hence, in this study the performance of nonlinear model predictive control (NLMPC) was assessed for the control of a reactive distillation column. The control of ethyl acetate reactive distillation column was selected for this study. A rigorous tray-to tray steady state as well as dynamic model was developed. The traditional decentralized PI controls with multiple SISO loops were compared with NLMPC via rigorous model based simulation for the ethyl acetate column.

The ethyl acetate reactive distillation system exhibits highly nonlinear nature. The steady state gain analysis was performed to analyze the effect of different manipulated variables on the control variables of the system.

The primary control objective of the ethyl acetate reactive distillation column was identified as the overhead acetic acid impurity composition. The during tuning of dual-PI composition controllers, the bottom composition loop was detuned. The dual-PI composition control of six different control configurations namely [L,B], [L,V], [L,V/B], [L/D,B], [L/D,V], and [L/D,V/B] were studied. All control configurations were tuned for

overhead impurity setpoint change and tested for control performance using feed composition and feed rate changes.

The overall results for dual-PI composition control shown satisfactory control performance for each configuration. Detuning of bottom composition loop provide the dynamic coupling between overhead and bottom composition loop. This enhances the control performance for overhead composition loop, which is the primary process objective for this system. Use of [L/D,V] and [L/D,V/B] provided best overall performance for overhead impurity setpoint tracking as well as for unmeasured disturbances in feed composition and feed flow.

An algorithm was developed for nonlinear model predictive control (NLMPC). The solution procedure for NLMPC involves setting up the control problem as a nonlinear programming (NLP) problem and solving it over prediction horizon. A simultaneous solution and optimization approach was selected for implementation of NLMPC. The orthogonal collocation on finite elements method was used to discretize the dynamic model equations. These discretized model equations were appended as constraints for nonlinear optimization problem. The discretization of model equations results in a large-scale sparse system of nonlinear algebraic equations. A sparse nonlinear optimization package (SNOPT) was used for solving nonlinear optimization problem at every sample interval.

The developed NLMPC algorithm was applied for dual-ended composition control of the ethyl acetate reactive distillation using [L/D,V] configuration. The closed loop simulations were used to determine the tuning parameters such as the prediction

horizon, control horizon, equal concerned error and move suppression factor. The effect of each tuning parameter on the closed loop control performance was analyzed before making the final selection of tuning parameters. The performance of NLMPC for dual ended composition control was tested for overhead impurity setpoint tracking and for unmeasured disturbances in feed composition and feed rate.

The control performance of NLMPC for overhead impurity setpoint tracking as well as for unmeasured disturbances in feed composition and feed flow was shown to be superior compared to dual-PI composition control. However, these results are pertaining to only [L/D,V] configuration.

The ability of NLMPC to handle the model mismatch was tested by introducing errors in the reaction equilibrium constant. The process-model mismatch of 5% and 25% difference in the equilibrium constant values were used. The effect of model mismatch on the tuning parameters for NLMPC was analyzed via closed loop simulations. The controller performance in presence of model mismatch was tested for overhead impurity setpoint tracking and for unmeasured disturbances in feed composition. It was shown a satisfactory performance of NLMPC in presence of process-model mismatch.

6.2 Recommendations

This study is an attempt to assess the performance of nonlinear model predictive control (NLMPC) for the control of reactive distillation column. An attempt is made to develop the algorithm for NLMPC which can be applied for nonlinear models of the processes. Following recommendations are made for further research in this area.

(1) NLMPC algorithm involves a large amount of computational efforts as it requires a solution of a large scale nonlinear optimization problem at each sample interval. This limits the efficient application of NLMPC in real time manner. Hence, improving the computational efficiency for NLMPC algorithm is one of the key future research directions in this area.

The nonlinear optimization approach and nonlinear modeling approach are major areas which can be considered for improving the computational efficiency of overall NLMPC algorithm. The current study uses the sparse nonlinear optimization package (SNOPT) for solving nonlinear optimization at each interval. SNOPT uses a sequential quadratic programming (SQP) algorithm that obtains search directions from sequence of quadratic programming subproblems. The user needs to provide the gradient information for the SNOPT and the missing gradients are calculated by means of finite difference approximations. In the current study, 75% of gradients are calculated analytically and remaining 25% of gradients are determined by means of finite difference approximation. For a large-scale optimization problem, calculation of gradients by means of difference approximation reduces the computational efficiency as well as decreases the reliability of optimization algorithm. (Gill, 1998). Use of analytical derivative calculation packages for fortran such as ADIFOR can improve the computational efficiency and reliability of nonlinear optimization problem. The use of modified SQP algorithms has shown improved performance for nonlinear optimization problems (Rao and Rawlings, 1998) Hence these optimization approaches should be considered for NLMPC algorithm.

(2) NLMPC incorporates nonlinear models of the process in the control algorithm. In the present study a detailed first principle model of reactive distillation was developed. This detailed dynamic model was discretized by means of orthogonal collocation on finite elements and appended as nonlinear constraints for optimization problem. A detailed model of reactive distillation column involves a large number of variables which results in increasing the size of optimization problem for simultaneous solution and optimization approach. The efficient use of nonlinear model reduction techniques such as use of orthogonal collocation along the length of column, (Srivastava and Joseph, 1987), wave propagation model approach (Chen, C.H., 1969) can decrease the size of nonlinear optimization problem, effectively improving performance of NLMPC algorithm.

(3) The present study considered [L/D,V] control configuration for comparison between NLMPC and decentralized PI control structure. It is advisable to consider the other control configurations and analyze the performance of NLMPC for dual composition control of reactive distillation column.

REFERENCES

- Abufares, A. A. and Douglas, P. L. Mathematical Modeling and Simulation of an MTBE Catalytic Distillation Process using SPEEDUP and AspenPlus. *Chem. Eng. Res. Des., Trans. Insti. Chem. Eng. Part A*, 73, 1995, 3-12.
- Al-Arfaj, M. A., Luyben, W. L. Comparative Control of Ideal and Methyl Acetate Reactive Distillation, *Chem. Eng. Sci.*, 57, 2002, 5039-5050.
- Al-Arfaj, M. A.; Luyben, W. L. Control Study of Ethyl tert-butyl Ether Reactive Distillation. *Ind. Eng. Chem. Res.*, 41, 2002, 3784-3796.
- Al-Arfaj, M. A.; Luyben, W. L., Control of Ethylene Glycol Reactive Distillation Control, *AIChE Journal*, 48(2), 2002, 905-908.
- Aljeski, K., Duprat, F., Dynamic Simulation of the Multicomponent Reactive Distillation, *Chem. Eng. Sci.*, 51, 1996, 4237-4252.
- Allgower, F.; Zheng, A., *Nonlinear Model Predictive Control*, Birkhauser Verlag, 1991
- Arnikar, H. J., Rao, T. S. and Bodhe, A. A. A Gas Chromatographic Study of the Kinetics of Uncatalyzed Esterification of Acetic Acid by Ethanol. *J. Chromatogr.*, 47, 1970, 265.
- Astrom, K. L., Hagglund, T. Automatic Tuning of Simple Regulators with Specifications on Phase and Amplitude Margins. *Automatica*, 20(2), 1984, 645-651.
- Badgwell, T. A., Qin, S. J. Review of Nonlinear Model Predictive Control Applications. in *Nonlinear Predictive Control: Theory and Practice*. Edited by Kouvaritakis, B. and Cannon, M., IEE, London, 2001.
- Barbosa, D., Doherty, M. F. The Influence of Equilibrium Chemical Reactions on Vapor Liquid-Phase Diagrams. *Chem. Eng. Sci.*, 43, 1988, 529-540.
- Barbosa, D.; Doherty, M. F. Design and Minimum Reflux Calculations for Double-Feed Multicomponent Reactive Distillation Columns, *Chem. Eng. Sci.*, 43, 1990, 2377-2389.
- Baur, R., Higler, A.P., Taylor, R. and Krishna, R. Comparison of Equilibrium Stage and Nonequilibrium Stage Models for Reactive Distillation. *Chem. Eng. Journal*, 76, 1999, 33-47.
- Biegler, L.T., Solution of dynamic optimization problems by successive quadratic programming and orthogonal collocation, *Comput. Chem. Eng.*, 8, 1984, 243-248.

- Bock, H., and Wozny, G. Analysis of Distillation and Reaction Rate in Reactive Distillation. Distillation and Absorption '97. *Inst. Chem. Eng. Sympo. Series*, 142, 1997, 553-564.
- Boston, J. F., Sullivan, S. L. A New Class of Solution Methods for Multicomponent, Multistage Separation Processes. *Canadian Journal of Chem. Eng.*, 52, 1974, 52-63.
- Box, G. E. P., Jenkins, G. M., Reinsel, G. C. *Time Series Analysis: Forecasting and Control*, 3rd ed, Prentice Hall, Eaglewood Cliffs, NJ, 1994.
- Chang, Y. A., Seader, J.D. Simulation of Continuous Reactive Distillation by Homotopy –Continuation Method, *Comput. Chem. Eng.*, 12(12), 1988, 1243-1255.
- Chen, C. H. M. Sc. Thesis, Polytechnic Institute of New York, 1969.
- Cuthrell J. E., Biegler, L.T. On the optimization of differential algebraic systems, *AIChE J.*, 33(8), 1987, 1257-1270.
- Cutler, C. R, Finlayson, S. G. Multivariable Control of a C₃-C₄ Splitter Column. Presented at the National Meeting of the AIChE, New Orleans, LA, 1988.
- Cutler, C. R., Ramaker, B. L., Dynamic matrix control – a computer algorithm. In *Proceedings of the Joint Automatic Control Conference*, 1980
- Deshpande, P. B. *Distillation Dynamics and Control*. Instrument Society of America, Research Triangle Park, NC, 1985.
- Doherty, M.F., Buzad, G. Reactive Distillation by Design, *Chem. Eng. Res. Des., Transactions of the Institute of Chemical Engineers*, Part A, 70, 1992, 448-458.
- Duvall, P. M. *On Control of High Relative Volatility Distillation Columns*. Ph. D Dissertation, Texas Tech University, Lubbock, Texas, 1999.
- Edger, T. F. and Himmelblau, D. H. *Optimization of Chemical Processes*. McGraw Hill, New York, 1988.
- Finlayson, B. A. *Nonlinear analysis in chemical engineering*. McGraw-Hill, New York, 1980.
- Franks, R. G. E. *Modeling and Simulation in Chemical Engineering*. John Wiley and Sons, New York, 1972.

- Ganguly, S., Saraf, D. N. A Comparative Experimental Study of the Performance of Non-Linear Model Predictive Controllers for Dual Composition Control of Distillation Columns. *Process Control and Quality*, 11(2), 1998, 97-117.
- Garcia, C.E., Morari, M. Internal model control. 1. A unifying review and some new results. *Ind. Eng. Chem. Proc. Des. Dev.*, 21, 1982, 308-323.
- Gill, P.E., Murray, W. and Saunders, M.A., User's Guide for SNOPT 5.3/6.0: A Fortran Package for Large Scale Nonlinear Programming, Systems Optimization Laboratory, Stanford University, 1998.
- Gokhale, V. B. *Control of a Propylene/Propane Splitter*. M. S. Thesis, Texas Tech University, Lubbock, TX, 1994.
- Grosser, J.H., Doherty, M.F., and Malone, M.F. Modeling of Reactive Distillation Systems. *Ind. Eng. Chem. Res.*, 26, 1987, 983-989.
- Hauan, S., Lien, K.M. A Phenomenon based design approach to reactive distillation. *Chem. Eng. Res. Design, Trans. of the Insti. of Chem. Eng.*, Part A, 76, 1998, 396-407.
- Hertzberg, T., Asbjornsen, O. A., Parameter Estimation in Nonlinear Differential Equations. In *Computer Applications in the Analysis of Data and Plants*. Science Press Princeton, 1977.
- Hicks, G. A., Ray, W. H. Approximation Methods for Optimal Control Synthesis. *Can. J. Chem. Eng.*, 49, 1971, 522.
- Holland, C.D. *Fundamentals of Multicomponent Distillation*, New York: McGraw-Hill 1981.
- Isla, M. A., Irazoqui, H. A. Modeling, analysis and simulation of a methyl tert-butyl ether reactive distillation column. *Ind. Eng. Chem. Res.*, 35, 1996, 2396-2408.
- Izzaraz, A., Bentzen, G. W., Anthony, R.G. and Holland, C.D. Solve More Distillation Problems, Part 9- when Reactions Occur. *Hydrocarbon Processing*, 59(4), 1980, 195-203.
- Jones, D. I., Finch, J. W. Comparison of Optimization Algorithms. *Int. J. Control*, 40, 1984, 747.
- Kister, H. J. *Distillation Design*. McGraw-Hill Inc., New York, 1992.

- Komatsu, H. Application of the Relaxation Method of Solving Reacting Distillation Problems. *J. Chem. Eng. Japan*, 10, 1977, 200-205.
- Komatsu, H., Holland, C. D. A New Method of Convergence for Solving Reacting Distillation Problems. *J. Chem. Eng. Japan*, 10, 1977, 292-297.
- Kreul, L. U., Gorak, A. and Barton, P. I., Modeling of Homogeneous Reactive Separation Processes in Packed Columns, *Chem. Eng. Sci.*, 54, 1999, 19-34.
- Krishnamurthy, R. and Taylor, R. A Nonequilibrium Stage Model of Multicomponent Separation Processes. *AIChE J.*, 32, 1985, 449-465.
- Kumar, A., Daoutidis, P., Modeling, Analysis and Control of Ethylene Glycol Reactive distillation column, *AIChE J.*, 32, 1999, 449-465.
- Lee, J. H., Dudukovic, M. P., A Comparison of the Equilibrium and Nonequilibrium Models for Multicomponent Reactive Distillation Column. *Comput. Chem. Eng.*, 23, 1988, 159-172.
- Luyben, W. L. *Practical Distillation Control*. Van Nostrand Reinhold, New York, 1992.
- Luyben, W. L.; *Process Modeling, Simulation, and Control for Chemical Engineers*, Second Edition, McGraw Hill International Edition, 1990.
- Marlin, T. E., *Process Control: Design Processes and Control Systems for Dynamic performance*, McGraw Hill, Inc., 1995.
- McDonald, K. A., McAvoy, T. J. Application of Dynamic Matrix Control to Moderate and High-Purity Towers. *Ind. Eng. Chem. Res.*, 26(5), 1987, 1011-1018.
- Meadows, E. S., Henson, M. A., Eaton, J. W. and Rawlings, J. B. Constrained State Estimation and Discontinuous Feedback in Model Predictive Control, *Proceedings of the 1993 European Control Conference*, 1993, 2308-2312.
- Meadows, E. S., Rawlings, J. B. Model Predictive Control, Nonlinear Process Control, edited by Henson, M., Seaborg, D. Prentice Hall PTR, 1997.
- Mommessin, P. E., Holland, C. D. Solve More Distillation Problems, Part 13- Multiple Columns with Reactions. *Hydrocarbon Processing*, 62(11), 1983, 195-200.
- Moore, C. F. Selection of Controlled and Manipulated Variables. in *Practical Distillation Control*, ed. Luyben, W. L., Van Nostrand Reinhold, New York, 1992.

- Muske, K. R., Rawlings, J. B. Model Predictive Control with Linear Models, *AIChE J.*, 39(2), 1993,262-287.
- Nelson, P. A. Countercurrent Equilibrium Stage Separation with Reaction. *AIChE J.*, 17, 1971, 1043-1049.
- Patwardhan, A. A., Rawlings, J. B. and Edger, T. F. Nonlinear Model Predictive Control,
- Renfro, J. G., Morshedi, A. M. and Asbjornsen, O. A. Simultaneous Optimization and Solution of Systems Described by Differential /Algebraic Equations. *Comput. Chem. Eng.*, 11(5),1987, 503-517.
- Riggs, J. B. *An Introduction to Numerical Methods for Chemical Engineers*, 2nd ed., Texas Tech University Press, Lubbock, Texas, 1994.
- Riggs, J. B. *Chemical Process Control*.2nd ed., Ferret Publications, Lubbock, Texas, 2001.
- Ruiz, C. A., Basualdo, M. S., Scenna, N. J. Reactive Distillation Dynamic Simulation. *Chem. Eng. Res. Des., Tran. Inst. Chem. Eng.*, Part A, 73,1995, 363-378.
- Sargent, R. W. H., Sullivan, G. R. The Development of an Efficient Optimal Control Package. In *Optimization Techniques, Proceedings of the 8th IFIP Conference on Optimization Techniques*, Wurzburg, 1977 (Stoer, J. ed.), Springer-Verlag, Berlin, 1978.
- Sawistowski, H., and Pilavakis, P. A. Distillation with Chemical Reaction in Packed Column. *Inst. Chem. Eng. Sympo. Ser.*, 56, 1979, 49-63.
- Sawistowski, H., and Pilavakis, P. A. Performance of Esterification in a Reaction-Distillation Column. *Chem. Eng. Sci.*, 43, 1988, 355-360.
- Scenna, N. J., Ruiz, C.A. and Benz, S. J. Dynamic Simulation of Startup Procedures of Reactive Distillation Columns. *Comp. Chem. Eng.*, 22, 1998, S719-S722.
- Seferlis, P., Grievink, J. Optimal Design and Sensitivity Analysis of Reactive Distillation Units Using Collocation Models, *Ind. Eng. Chem. Res.*, 40, 2001, 1673-1685.
- Sharma, M. M. Separations through Reactions. *Journal of Separations Process Technology*, 6, 1985, 9-16.
- Shinsky, F. G. Distillation Control for Productivity and Energy Conservation. 2nd ed., McGraw-Hill, New York, 1984.

- Sivasubramanian, M. S. and Boston, J. F., The Heat and Mass Transfer Approach for Modeling Multicomponent Separation Processes. In Bussemaker, H. Th. and Iedema, P. D. *Computer Applications in Chemical Engineering*, Amsterdam, Elsevier, 1990, 331-336.
- Sneesby, M. G., Tade, M. O. and Smith, T. N. Two-Point Control of a Reactive Distillation Column for Composition and Conversion, *Journal of Process Control*, 9, 1998, 19-31.
- Sneesby, M. G., Tade, M. O., Datta, R. and Smith, T. N., ETBE synthesis via reactive distillation. 1. Steady-state simulation and design aspects. *Ind. Eng. Chem. Res.*, 36, 1997a, 1855-1869.
- Sneesby, M. G., Tade, M. O., Datta, R. and Smith, T.N. ETBE Synthesis via Reactive Distillation. 2. Dynamic Simulation and Control Aspects. *Ind. Eng. Chem. Res.*, 36, 1997b, 1870-1881.
- Sneesby, M. G.; Tade, M. O.; Smith, T. N., Multiplicity and Pseudo-Multiplicity in MTBE and ETBE Reactive Distillation, *Chem. Eng. Res. Des., Transactions of the Institution of Chemical Engineers*, Part A, 76, 1998, 525-531.
- Sorensen, E. and Skogested, S. Control Strategies for Reactive Batch Distillation. *Journal of Process Control*, 4, 1994, 205-217.
- Suzuki, I., Yagi, H., Komatsu, H. and Hirata, M. Calculation of Multicomponent Distillation Accompanied by Chemical Reaction. *J. Chem. Eng., Japan*, 4, 1971, 26-33.
- Taylor, R.; Krishna, R., Modeling Reactive Distillation, *Chem. Eng. Sci.*, 55, 2000, 5183-5229.
- Tsang, T. H., Edger, T. F. and Himmelblau, D. M. Optimal Control via Collocation and Nonlinear Programming. *Int. J. Control*, 21, 1975, 763.
- Tyreus, B. D., Luyben, W. L. Tuning PI Controllers for Integrator/Deadtime Processes. *Ind. Eng. Chem. Res.*, 31(11), 1992, 2625-2628.
- Venkatraman, S, Chan, W. K., Boston, J. F., Reactive Distillation using Aspen Plus, *Chem. Eng. Prog.*, 86(8), 1990, 45-54.
- Villadson, J, Stewart, W. E., Solution of Boundary-Value Problems by Orthogonal Collocation, *Chem. Eng. Sci.*, 22, 1967, 1483-1501.

- Wang, J. C., and Henke, G. E. Tridiagonal Matrix for Distillation. *Hydrocarbon Processing*, 45 (8), 1966, 155-163.
- Zheng, Y., and Xu., X. Study of Catalytic Distillation Processes, Part I: Mass Transfer Characteristics in Catalyst Bed within Column. *Chem. Eng. Res. Des., Trans. Inst. Chem. Eng.*, Part A, 70, 1992, 459-546.